Aerospace Department

Group 5

AS5211: Subsonic Aircraft Design

Team Members-
Ganesh -AE17B006
Humaira -AE17B008
Abhijeet -AE17B016
Adarsh Kumar -AE17B017
Arnav -AE17B021
Jeeva -AE17B029
Krishnavamshi -AE17B036

Instructors:
Dr.Shankar Ghosh
Dr.Bharath M.Govindarajan

Contents

1 Project Overview **4**
- 1.1 Mission Statement . . . 4
- 1.2 Configuration . . . 4
  - 1.2.1 Fuselage . . . 4
  - 1.2.2 Wing . . . 5
  - 1.2.3 Empennage . . . 5
  - 1.2.4 Landing Gear . . . 6
  - 1.2.5 Power Plant . . . 6
  - 1.2.6 Auto Rotation . . . 6
- 1.3 Specifications . . . 7
- 1.4 Calculations and Data Collection . . . 9
  - 1.4.1 Data collection: . . . 9
  - 1.4.2 Calculations . . . 10
- 1.5 3-view drawing(initial) . . . 12

2 Weight Estimation **14**
- 2.1 Introduction . . . 14
- 2.2 Weight estimation . . . 14

3 Wing Loading and Thrust Loading **18**
- 3.1 Introduction . . . 18
- 3.2 Selection of wing loading based on prescribed flight velocity . . . 18
- 3.3 Selection of wing loading based on range (R) . . . 20
- 3.4 Selection of wing loading based on absolute ceiling (H_{max}) . . . 22
- 3.5 Selection of optimum wing loading . . . 24
- 3.6 Engine selection: . . . 25

4 Airfoil selection **26**
- 4.1 Introduction . . . 26
- 4.2 Aerodynamics characteristics of airfoils . . . 27
- 4.3 Geometrical characteristics of airfoils . . . 30
- 4.4 Effects of geometric parameters, Reynolds number and roughness on aerodynamic characteristics of airfoils . . . 31
- 4.5 Choice of airfoil camber . . . 31
- 4.6 Choice of airfoil thickness ratio . . . 32
- 4.7 Selection of wing parameters . . . 32
  - 4.7.1 Aspect ratio(A) . . . 32
  - 4.7.2 Sweep(Λ) . . . 32
  - 4.7.3 Taper ratio(λ) . . . 33
  - 4.7.4 Twist . . . 33
  - 4.7.5 Wing Incidence . . . 33
  - 4.7.6 Dihedral . . . 34
  - 4.7.7 Wing vertical location . . . 35
  - 4.7.8 Flaps . . . 36
  - 4.7.9 Aileron . . . 36

4.7.10 Slats . . . 37

5 Parachute deployment and Auto Rotation 38
5.1 Introduction . . . 38
5.1.1 Force exerted on the Parachute . . . 38
5.1.2 Force supported by Autorotation mechanism . . . 38

6 Fuselage and tail sizing 43
6.1 Fuselage sizing: . . . 43
6.1.1 Features of the fuselage: . . . 43
6.1.2 Seating arrangements: . . . 44
6.2 Preliminary horizontal and vertical tail sizing: . . . 47
6.2.1 Choice of aspect ratio for horizontal tail: . . . 47
6.2.2 Choice of taper ratio for horizontal tail . . . 47
6.2.3 Choice of sweep for horizontal tail . . . 48
6.2.4 Airfoil selection for horizontal tail . . . 48
6.2.5 Choice of aspect ratio for vertical tail . . . 48
6.2.6 Choice of taper ratio for vertical tail . . . 48
6.2.7 Choice of sweep for vertical tail . . . 48
6.2.8 Airfoil selection for vertical tail . . . 48
6.2.9 Other important parameters: . . . 49
6.3 Engine location . . . 50
6.3.1 Engine Selection . . . 50
6.3.2 Span-wise locations of wing mounted engines . . . 51
6.4 Fuel System . . . 51
6.5 Landing gear . . . 51

7 Weights and center of gravity 52
7.1 Estimation of airplane weight: . . . 52
7.1.1 Approximate group weights method: . . . 52
7.1.2 Statistical group weights method . . . 52
7.2 Estimation of the component weights and c.g. locations: . . . 53
7.2.1 Wing . . . 53
7.2.2 Horizontal Tail . . . 53
7.2.3 Vertical Tail . . . 54
7.2.4 Engine . . . 54
7.2.5 Landing Gear . . . 54
7.2.6 Fuselage and systems . . . 54
7.2.7 Fuel . . . 55
7.2.8 Payload and crew . . . 56
7.3 Determination of wing location and c.g. of the airplane . . . 56
7.4 Calculation of C.G. location and C.G. shift . . . 57
7.4.1 C.G. shift for different loading conditions . . . 58

8 Cross-checks on design of tail surfaces 60
8.1 Introduction . . . 60
8.2 Static longitudinal stability and control . . . 60
8.2.1 Specifications . . . 60
8.2.2 Revised estimate of the area of horizontal tail . . . 61
8.2.3 Remark . . . 62
8.3 Directional stability and control . . . 65
8.3.1 Specifications . . . 65
8.3.2 Equations for directional stability . . . 65
8.3.3 Revised estimate of area of vertical tail . . . 65
8.3.4 Area of rudder . . . 66
8.4 Lateral Stability and control . . . 67
8.4.1 Selection of dihedral angle . . . 67

9 Performance estimation **69**
9.1 Level flight performance 69
9.1.1 Stalling speed 69
9.1.2 Variations of V_{min} and V_{max} with altitude 70
9.1.3 Steady climb 74
9.1.4 Range and endurance 76
9.1.5 Turning performance 80
9.1.6 Take-off distance 83
9.1.7 Landing distance 83

10 Final Specifications: **85**
10.1 Specifications 85

11 Conclusions **88**

12 Bibliography **90**

A Matlab code for weight estimation **91**

B Matlab code for wing loading **92**

C Matlab code for Turn Performance **95**

Chapter 1

Project Overview

1.1 Mission Statement

Our main objective behind this project is to design "A passenger plane with additional security measures and better fuel efficiency". The goals we want to achieve are-

- A modular plane with detachable passenger compartment fitted with parachutes and air bags which can be deployed to safely land the compartment in case of emergency situations that can result in a tragedy saving a lot of human lives.
- The plane is going to be design in a way to maximize lift to drag ratio to achieve better fuel economy despite the additional weight of deployment mechanism.
- To make safer journey possible for very important person and also affordable for masses in future, we are also focusing on making it more economical.

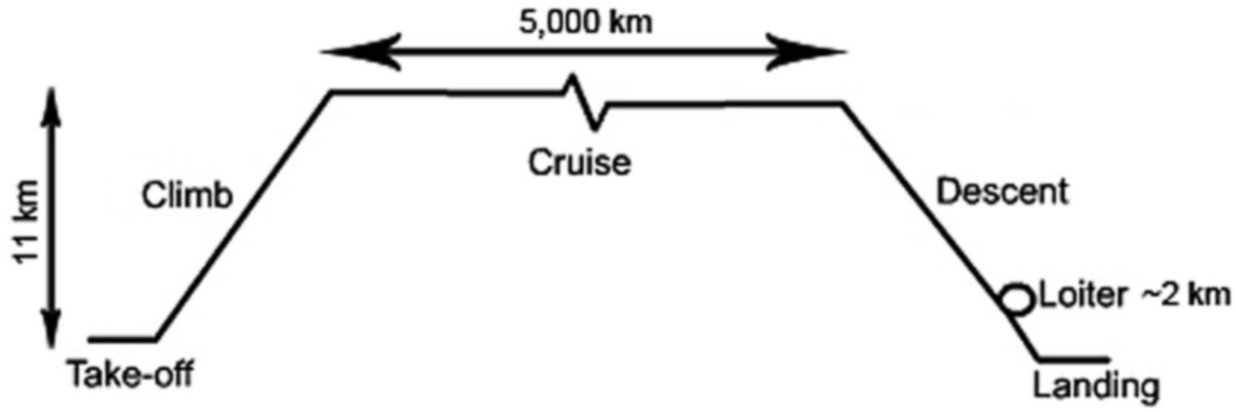

1.2 Configuration

1.2.1 Fuselage

The fuselage of the proposed aircraft has an odd internal structure. It is designed in such a way that parts of it can be rid off and the remaining structure can be ejected in case of emergency. This capsule(remaining part of the fuselage) is capable of safe landing by deploying a parachute and an auto rotation mechanism discussed later.

1.2.2 Wing

The safety factor has now increased at the cost of the weight fraction of the passengers. Hence, the wing must be designed to produce higher lift at lower speed(as a result of increased weight).

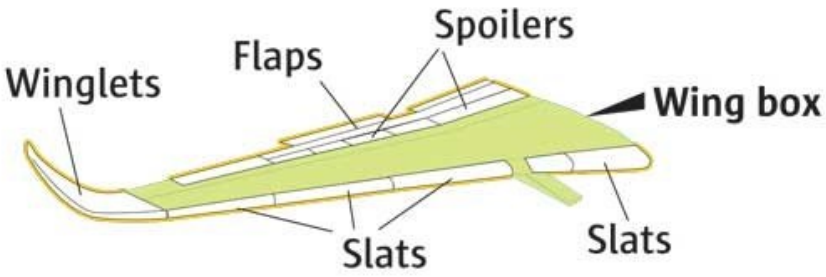

Figure 1.1: Front view

1.2.3 Empennage

A conventional tail design with modular mechanism has been used in order to reduce the structural stresses on the aircraft. This design also takes an advantage of making the aircraft controllable at low speeds as the thrust blown from the engines increases effectiveness of the control surfaces of the horizontal stabilizer.

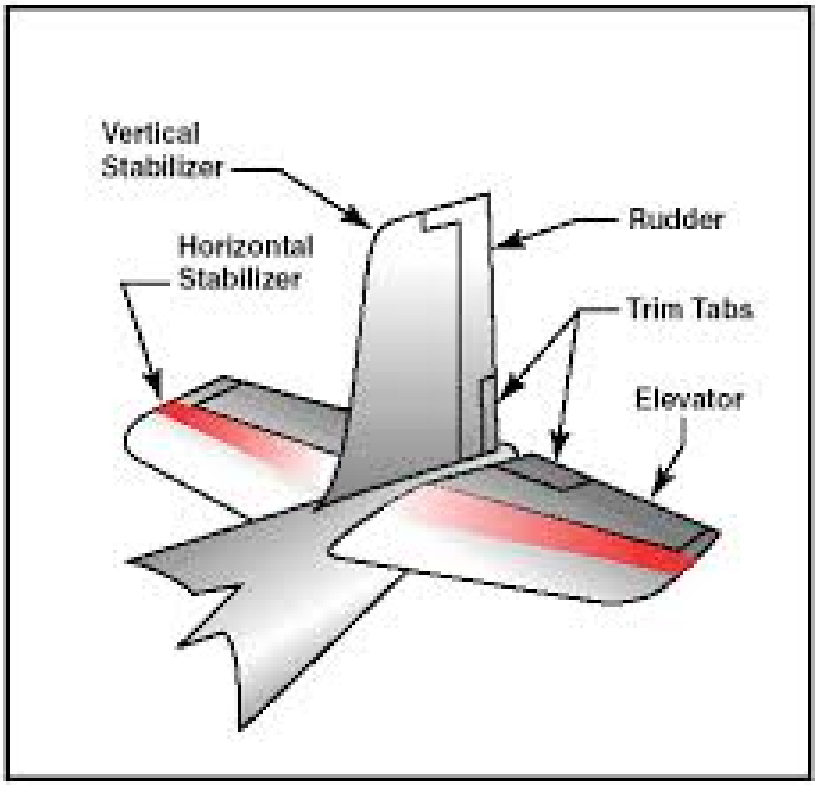

Figure 1.2: Front view

1.2.4 Landing Gear

Tricycle landing gear has been used in order to support the structural integrity of the plane during landing and as the centre of mass is expected to be in front of centre of lift as observed in conventional aircraft.

1.2.5 Power Plant

We use a Rolls Royce Trent 1000 high bypass turbofan engine which has sufficient thrust rating for the required payload carrying capability.

1.2.6 Auto Rotation

As a part of the mission statement, to provide an extra edge in safety, we added additional equipment of parachutes and imposed the concept of auto rotation into our plane. They are functional only in case of emergency. In case of an emergency where the plane is out of control, or there is a total engine failure case, passengers can be ensured safety by deploying parachutes from a special pod which will be ejected from the main fuselage structure in which the passengers are contained and a system of blades get exposed such that they glide in their plane of rotation(for Auto Rotation purpose).

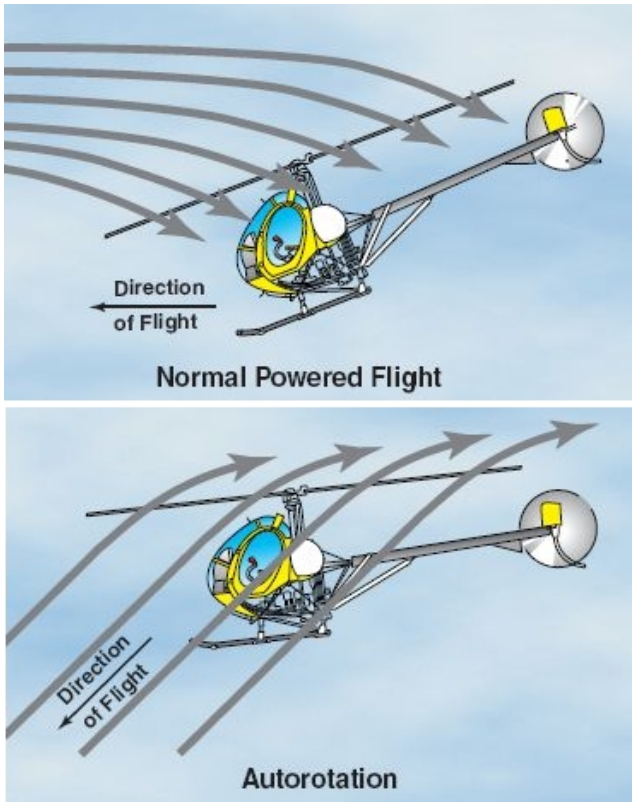

Figure 1.3: Front view

1.3 Specifications

Our specifications values are determined using existing airplanes data and our requirements.

1. **General description of airplane**
   Type of airplane: Modular commercial airplane

2. **Power plant**
   Type of power plant:Three shaft high bypass ratio turbofan
   Name: RR trent 1000
   Engine rating: 6.01
   Specific fuel consumption: 0.549 hr^{-1}
   Weight of power plant:12240 kg
   No. of engines: 2

3. **Wing**
   Span(m): 43
   Tip chord(m): 2
   Flap area(m^2): 34.43
   Flap area/wing area(S_{flap}/S):0.17
   Root chord(m): 7.5
   Area (S in m^2): 198.12
   Aileron area(m^2): 9.7
   Aspect ratio(A): 9.33
   Aileron area/wing area($S_{aileron}/S$): 0.049

4. **Horizontal tail**
   Span(m): 15.82
   Tip chord(m): 1.78
   Area(m^2): 39
   Sweep(in degree): 34
   Elevator area(m^2): 19.63
   Elevator area/Tail area: 0.35
   Tail area/Wing area(S_{ht}/S): 0.28

5. **Vertical tail surface**
   Type of vertical tail: Conventional
   Height(m): 8
   Root chord(m): 7.25
   Tip chord(m): 2.56
   Area(m^2): 39
   Rudder area(m^2): 18.6
   Aspect ratio(A_{vt}): 1
   Rudder area/tail area: 0.48
   Tail area/Wing area(S_{vt}/S): 0.19

6. **Fuselage**
   Length(m): 48
   Length of nose(l_{nose}): 1.7 m
   Length of cockpit($l_{cockpit}$): 4 m
   Length of tail cone($l_{tailcone}$): 14.3 m
   Length of payload compartment: 25 m

Number of seats in cockpit: 4
Length/wingspan: 1.045

7. **Landing gear**
   Type of landing gear: Tricycle configuration
   Number and size of wheels: 3×4
   Wheel base(m): 15.57
   Wheel tread(m): 9.82
   Location of landing gears: Refer 3-view diagram

8. **Overall dimensions of airplane**
   Length(m): 45
   Wing span(m): 43
   Height(m): 4
   Landing gear wheel tread(m): 9.82
   Landing gear wheel base(m): 15.57
   Length/wingspan: = 1.045
   Height/wingspan: 0.09
   Tread/wingspan: = 0.23

1.4 Calculations and Data Collection

1.4.1 Data collection:

	Boeing 737-800	**Airbus A310**	**Airbus A320**
W_o/W_{pay}	5.32	4.5	3.83
W_o/S	630.94	630.94	600.49
AR	9.44	8.8	9.39
λ(Taper ratio)	0.28	0.28	0.24
l_f/b	1.11	1.11	1.11
Crosssectional size of fuselage	3.73×3.73	5.64×5.64	4.14×3.95
l_{nose}/l_f	0.02	0.03	0.04
$l_{cockpit}/l_f$	0.06	0.11	0.09
$l_{tailcone}/l_f$	0.3	0.21	0.32
S_{ht}/S	0.26	0.29	0.25
S_{vt}/S	0.18	0.21	0.18
A_{ht}	5.54	4.13	5
A_{vt}	1.56	1.45	1.82
λ_{ht}	0.19	0.42	0.26
λ_{vt}	0.31	0.4	0.3
Sweep	25	28	25
S_{ele}/S_{ht}	0.25	0.45	0.23
S_{rud}/S_{vt}	0.24	0.59	0.33
$S_{aileron}/S$	0.09	0.07	0.03
S_{flap}/S	0.11	0.17	0.17
C_{ele}/C_{ht}	0.27	0.49	0.31
C_{rud}/C_{vt}	0.34	0.47	0.29
$C_{aileron}/C_{wing}$	0.17	0.08	0.13
C_{flap}/C_{wing}	0.24	0.16	1
T/W_o	0.28	0.31	0.31
W_o/P	1	324.68	330.49
Rating of engine	CFM56-7B24	P&W 4152	CFM56-5A3
Approximate dimension of engine	2.43×2×2.16	3.9×2.38×2.48	2.422×1.908×2.101
Wheel base/L_f	0.33	0.34	0.34
Wheel head/L_f	0.15	0.21	0.2

1.4.2 Calculations

Data inside brackets are known by having comparative analysis of similar aircraft's available data and after fixing on the mission profile we decided the number of passengers to be 150. The formulas and the sample calculations follows:
Let W_{pay} be the payload weight.

$$W_{pay} = 30000kg$$

From the data of similar aircraft(Boeing 737-800 for this sample) we get the ratios as mentioned above:

$$\frac{W_0}{W_{pay}} \times W_{pay} = W_0 \implies 5.32 \times 30000 = 159574.47 \ kg$$

$$W_0 / \frac{W_0}{S} = S \implies 159574.47/630.94 = 252.92 \ m^2$$

Similarly all the specifications are calculated using the formulae stated below:

1. $\sqrt{S \times A} = b$
2. $\lambda = \frac{C_{\mathrm{t}}}{C_{\mathrm{r}}}$; $\mathrm{S} = \frac{b}{2} \times (\mathrm{C_t} + \mathrm{C_r})$
   $\mathrm{C_r} = \frac{2 \times S}{b \times (1+\lambda)}$; $\mathrm{C_t} = \frac{2 \times S \times \lambda}{b * (1+\lambda)}$
3. $(\frac{l_f}{b}) \times \mathrm{b} = l_{\mathrm{f}}$
4. $l_{\mathrm{nose}} = (\frac{l_{nose}}{l_f}) \times l_{\mathrm{f}}$
   $l_{\mathrm{cockpit}} = (\frac{l_{cockpit}}{l_f}) \times l_{\mathrm{f}}$
   $l_{\mathrm{payload\ section}} = l_{\mathrm{f}} - l_{\mathrm{nose}} - l_{\mathrm{cockpit}} - l_{\mathrm{tailcone}}$
5. $S_{\mathrm{ht}} = (\frac{S_{ht}}{S}) \times S$
   $b_{\mathrm{ht}} = \sqrt{S_{\mathrm{ht}} \times A_{\mathrm{ht}}}$
   $C_{\mathrm{r,ht}} = \frac{2 \times S_{ht}}{b_{ht} \times (1+\lambda_{ht})}$
   $C_{\mathrm{t,ht}} = \lambda_{ht} \times C_{\mathrm{r,ht}}$
6. From data of similar aircraft's we estimated:
   $(\frac{S_{ele}}{S_{ht}}, \frac{S_{rud}}{S_{vt}}, \frac{S_{aileron}}{S}, \frac{S_{flap}}{S})$
   $(\frac{C_{ele}}{C_{ht}}, \frac{C_{rud}}{C_{vt}}, \frac{C_{aileron}}{C}, \frac{C_{flap}}{C})$

   Similarly we got the data for the rating of the engine, wheel base and wheel thread.

The specifications are found based on data from similar aircrafts and compiled in the table below:

	Boeing 737-800	**Airbus A310**	**Airbus A320**	**Final**
W_o	159574.47	135135.13	114903.6	125000
S	252.92	214.18	191.35	198.12
b	48.86	43.41	42.39	43
C_r	8.1	7.69	7.28	7.5
C_t	2.25	2.18	1.75	2
l_f	54.25	48.10	46.96	45
l_{nose}	1.27	1.42	1.77	1.7
$l_{cockpit}$	3.56	5.24	4.07	4
$l_{tailcone}$	16.24	10.27	15.04	17.3
$l_{payload}$	33.18	31.16	26.08	25
S_{ht}	65.77	62.54	48.41	55.48
S_{vt}	46.95	44.12	33.68	38.9
b_{ht}	19.09	16.07	15.56	15.81
b_{vt}	8.56	7.99	7.83	7.92
$C_{r,ht}$	5.81	5.49	4.95	5.22
$C_{t,ht}$	1.08	2.29	1.27	1.78
$C_{r,vt}$	8.37	7.91	6.60	7.26
$C_{t,vt}$	2.59	3.12	2.00	2.56
S_{ele}	16.28	28.34	10.92	19.63
S_{rud}	11.15	26.01	11.20	18.61
$S_{aileron}$	25.03	14.56	4.85	9.70
S_{flap}	29.29	35.87	32.98	34.43
T	44505.32	42432.43	35436.27	38934.35
P	159574.47	416.21	347.68	3.53
$Wheel\ base$	17.66	16.21	15.79	15.56
$Wheel\ head$	8.12	10.23	9.50	9.82

All specifications are in respective SI units.

1.5 3-view drawing(initial)

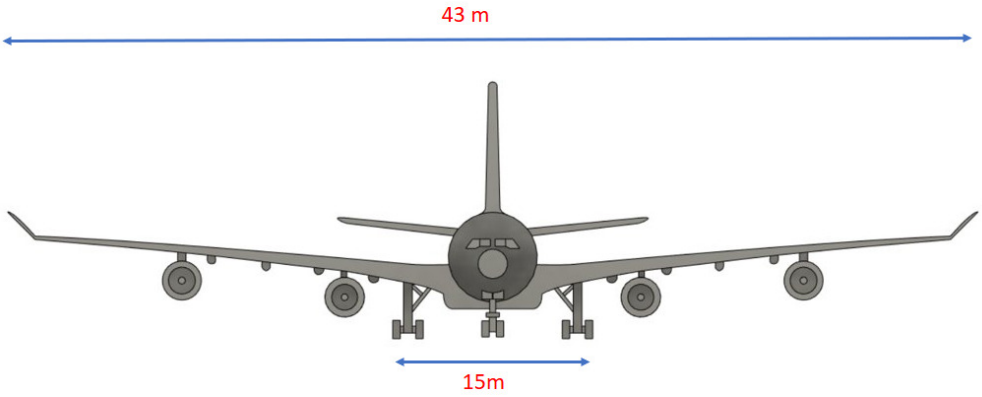

Figure 1.4: Front view

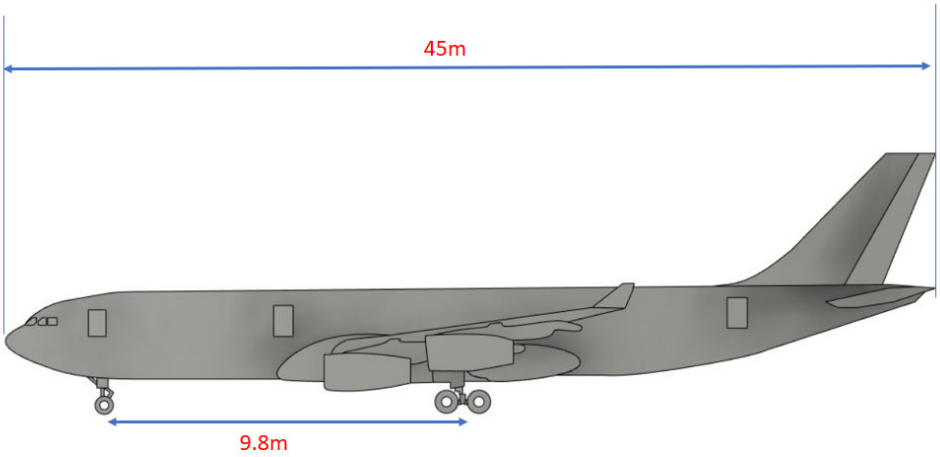

Figure 1.5: Side view

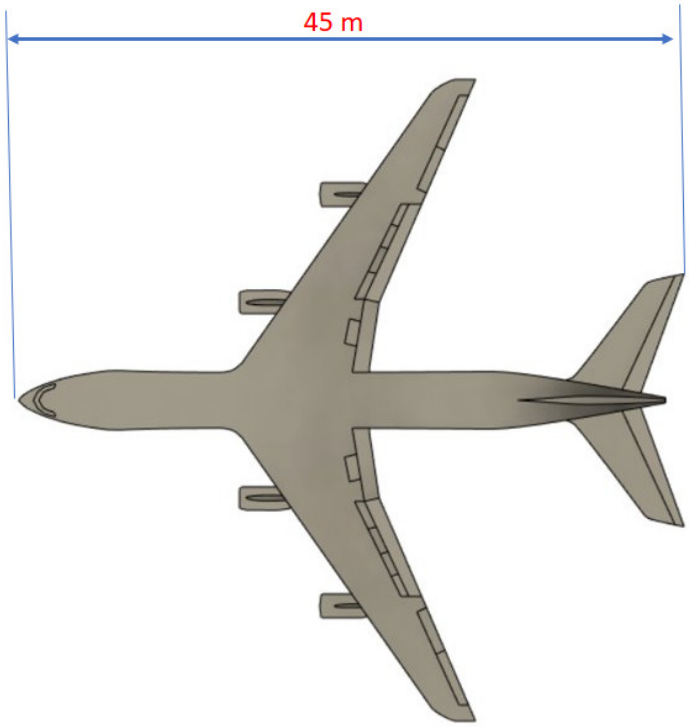

Figure 1.6: Top view

Chapter 2

Weight Estimation

2.1 Introduction

An accurate estimate of the weight of the airplane is required for the design of the airplane. This is arrived at in various stages. In the last chapter, the procedure to obtain the first estimate of the gross weight was indicated. This was based on the ratio of the payload to the gross weight of similar airplanes. This estimate of the gross weight is refined in this chapter, by estimating (a) the fuel fraction i.e. weight of fuel required for the proposed mission of the airplane, divided by gross weight and (b) empty weight fraction i.e. empty weight of airplane divided the gross weight.

2.2 Weight estimation

Weight of payload(W_{pay}) = 30,000 kg

$$W_0 = \frac{W_{payload}}{1 - \frac{W_e}{W_0} - \frac{W_f}{W_0}}$$

Empty weight fraction:

$$\frac{W_e}{W_0} = A(W_0)^c$$

From data of aircrafts' (Jet-transport)

$$\text{A} = 0.97\ (kgf)^{-c} \text{ and c = -0.06}$$

Valid for W_0 = 10 - 950 K kg

$$\frac{W_e}{W_0} = 0.97(W_0)^{-0.06} \tag{2.1}$$

Fuel-weight fraction:

$$\frac{W_f}{W_0} = K\left(1 - \frac{W_{0final}}{W_0}\right)$$

$$\frac{W_f}{W_0} = 1.06\left(1 - \frac{W_{0final}}{W_0}\right)$$

where 1.06 is the K_{th} factor.

$$\frac{W_{0final}}{W_0} = \frac{W_5}{W_1} = \frac{W_5}{W_4}.\frac{W_4}{W_3}.\frac{W_3}{W_2}.\frac{W_2}{W_1}.\frac{W_1}{W_0} \tag{2.2}$$

where W_0, W_1, W_2, W_3, W_4 and W_5 are weights of the aircraft before takeoff, during climb, cruise, loiter(descent) and after landing.

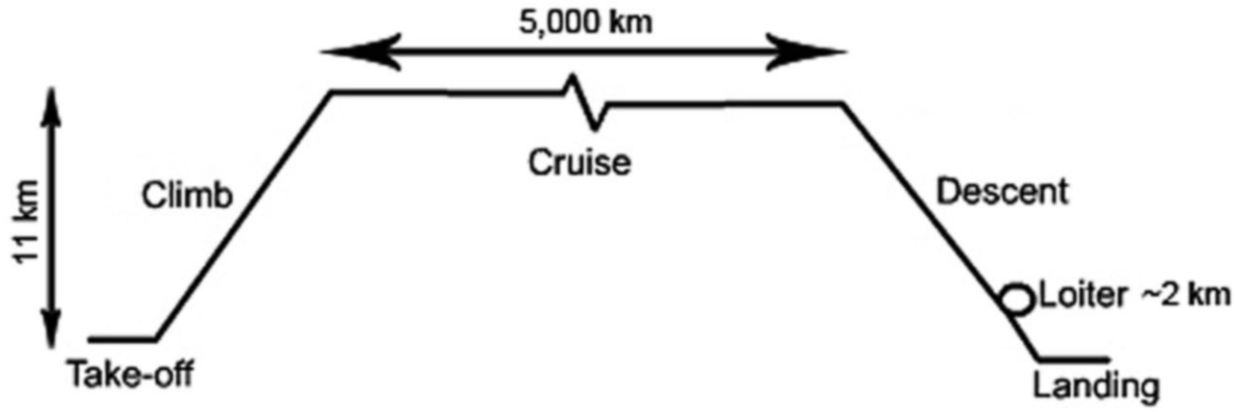

Figure 2.1: Phases of flight

$$\frac{W_1}{W_0} = 0.98 \quad \frac{W_2}{W_1} = 0.98 \quad \frac{W_5}{W_4} = 0.98$$

$$\frac{W_4}{W_3} = loiter\ \ phase \qquad \frac{W_3}{W_2} = cruise\ \ phase$$

$$\textbf{Cruise phase} - \frac{W_3}{W_2}$$

$$R = \frac{-3.6V(L/D)\ln\frac{W_2}{W_3}}{TSFC}$$

here the value 3.6 is a result of conversion of velocity from m/s to kmph; after manipulation, we get

$$\frac{W_3}{W_2} = exp\left(\frac{-R \times TSFC}{3.6 \times V(L/D)}\right)$$

$$\left(\frac{L}{D}\right)_{max} = \frac{1}{2\sqrt{C_{D0}K}}$$

$$C_{D0} = 0.005\tau W_f S^{-1}\left(1 - \frac{2C_{1f}}{R_w}\right) \times \left[1 - 0.2M + 0.12\left(\frac{M(\cos\Lambda^{0.5}}{A_f - (t/c)}\right)^{20}\right]$$

$$\tau = \left(\frac{R_w - 2}{R_w}\right) + \frac{1.9}{R_w}\left[1 + 0.526\left(\frac{t/c}{0.25}\right)^3\right] \tag{2.1}$$

$$R_w = \frac{S_{wet}}{S}$$

$$f(\lambda) = 0.005\left[1 + 1.5(\lambda - 0.6)^2\right] \tag{2.2}$$

High subsonic:

$$R_w = 5.5 \quad T_f = 1.1$$

$$\left(1 - \frac{2C_{1f}}{R_w}\right) = 1 \quad A_f - (t/c) = 0.93 - 0.14 = 0.79 \tag{2.3}$$

$$\tau = \left(\frac{5.5 - 2}{5.5}\right) + \frac{1.9}{5.5}\left[1 + 0.526\left(\frac{0.14}{0.25}\right)^3\right] = 1.013$$

for $\tau = 1.013$, t/c from eq(2.3):

$$t/c = 0.14 \tag{2.4}$$

$$\lambda = 0.25 \tag{2.5}$$

$$f(\lambda) = 0.005[1 + 1.5(0.25 - 0.6)^2] = 0.00592$$

$$considering \quad \Lambda_{1/4} = 30^o, \quad M = 0.778, \quad AR = 9.3, \quad A_f = 0.93.$$

$$\left[\frac{(M\cos\Lambda_{1/4})^{0.5}}{A_f - (t/c)}\right]^{20} = 0.175$$

Hence,

$$C_{D0} = 0.005 \times 1.013 \times 5.5 \times 1.1 \times S^{-0.1} \times 0.854$$

$$C_{D0} = 0.026S^{-0.1}$$

S = 198.12 m^2

$$\boxed{C_{D0} = 0.015}$$

$N_e = 0$

$$K = \left[\frac{1}{\pi AR}(1 + 012M^6)\left(1 + \frac{0.142 + f(\lambda)A(10t/c)^{0.33}}{(\cos\Lambda_{1/4})^2} + \frac{0.1(N_e+1)}{(4+AR)^{0.8}}\right)\right] = 0.035(1.012) + 0.013$$

$$\boxed{K = 0.048}$$

$$(L/D)_{max} = 16.13$$

Now,

$$\frac{W_3}{W_2} = exp\left(\frac{-R \times TSFC}{3.6V(L/D)_{max}}\right) \tag{2.6}$$

we need **TSFC**,
from reference[12],

$$TSFC = c(1 - 0.15\mu^{0.65})(1 + 0.28(1 + 0.063\mu^2) \times M)\sigma^{0.08}$$

$$c = 0.7 \quad \mu(Bypassratio) = 10 \quad M = 0.778 \quad \sigma = 0.34$$

$$TSFC = 0.549\ hrs^{-1}$$

put in eq(2.6)

$$\boxed{\frac{W_3}{W_2}} = 0.99$$

now,

$$\frac{W_4}{W_3} = loiter\ phase$$

$$\frac{W_4}{W_3} = exp\left(\frac{-E \times TSFC}{L/D}\right)$$

$$(L/D)_{max} = 16.13 \quad E_{jet} = 6hr \quad TSFC = 0.549$$

$$\boxed{\frac{W_4}{W_3} = 0.815}$$

$$\frac{W_5}{W_1} = \frac{W_5}{W_4}.\frac{W_4}{W_3}.\frac{W_3}{W_2}.\frac{W_2}{W_1}.\frac{W_1}{W_0}$$

$$\boxed{\frac{W_5}{W_1} = 0.759}$$

$$\frac{W_f}{W_0} = 1.06(1 - 0.759) = 0.255$$

where K_{tf} factor(1.06 in the above equation) is multiplied to the resultant weight fraction to account for trapped fuel

$$\boxed{\frac{W_f}{W_0} = 0.255}$$

put all the values in equation

$$W_0 = \frac{W_{payload}}{1 - \frac{W_e}{W_0} - \frac{W_f}{W_0}} = \frac{30000}{1 - 0.97 - (W_0)^{-0.06}}$$

When solved using iterative numerical methods[1], we get

$$\boxed{W_0 = 114,196kg}$$

$$\boxed{W_f = 29,120kg}$$

$$\boxed{W_e = 59,782kg}$$

[1] Appendix A for code

Chapter 3

Wing Loading and Thrust Loading

3.1 Introduction

The wing loading $\frac{W}{S}$ and the thrust loading $\frac{T}{W}$ or the power loading $\frac{W}{P}$ influence a number of performance considerations like take-off distance (S_{TO}), maximum speed (V_{max}), maximum rate of climb $(R/C)_{max}$, absolute ceiling (H_{max}) and maximum rate of turn (ψ_{max}). Thus, the wing loading and the thrust loading or power loading are the two most important parameters affecting the airplane performance. For airplanes with jet engines, the parameter characterising engine output is the thrust loading and for airplane with engine-propeller combination the parameter characterising the engine output is power loading.

3.2 Selection of wing loading based on prescribed flight velocity

We are optimising the wing loading with velocity Vp at a certain altitude Hp to get the lowest thrust requirement T_{Vp}. In order to obtain the relation between T_{Vp} and wing loading p,

In level flight, T=D Let,

$$\bar{t}_{Vp} = T_{Vp}/W; T_{Vp} = \frac{1}{2}\rho V_p^2 S C_D \tag{3.1}$$

Where ρ is atmospheric density at altitude H_p=11000 m

Hence,

$$\bar{t}_{Vp} = \frac{\rho V_p^2 S C_D}{2W} \tag{3.2}$$

Denoting $\frac{\rho V_p^2}{2}$ as q_p and $\frac{W}{S}$ as p yields,

$$\bar{t}_{Vp} = \frac{q_p}{p} C_D \tag{3.3}$$

And the Drag coefficient can be written as

$$C_D = C_{D0} + K C_L^2 \tag{3.4}$$

$$C_D = F_1 + F_2 p + F_3 p^2 \tag{3.5}$$

Where

$$F_1 = K_t C_{fe} W \frac{(S_{wet})_{wing}}{S_{old}} \;\; ; \;\; F_2 = \frac{C_{D0} - F_1}{\frac{W}{S}_{old}} \;\; ; \;\; F_3 = \frac{1}{\pi A e q^2}$$

$$K_t = 1 + \frac{S_{ht}}{S} + \frac{S_{vt}}{S} \tag{3.6}$$

Where, $(S_{wet})_{wing}$ = wetted area of wing $\approx 2S_{exposed\ wing}$ C_{fe} = equivalent skin friction drag coefficient, e = Oswald efficiency factor, A = Aspect ratio of wing, $(\frac{W}{S})_{old}$ = Wing loading from preliminary 3-view drawing stage, C_{D0} = Parasitic Drag coefficient.

Substituting $C_{D0} = F_1 + F_{2p} + F_{3p}^2$ we get,

$$\bar{t}_{Vp} = \frac{q_p}{p}(F_1 + F_2 p + F_3 p^2)$$

$$\bar{t}_{Vp} = q_p(F_1/p + F_2 + F_3 p) \tag{3.7}$$

Wing loading p which will minimise t_{Vp} for chosen Vp is obtained by differentiating the last equation with p and expanding it to 0

$$\frac{d\bar{t}_{Vp}}{dp} = 0 \tag{3.8}$$

$$\implies 0 = q_p(\frac{-F_1}{P^2} + F_3)$$

$$\implies p = \sqrt{\frac{F_1}{F_3}} = q_p\sqrt{F_1 \pi A e}$$

From the last 2 equations,

$$(\bar{t}_{Vp})_{min} = q_p(\frac{F_1}{p} + F_2 + F_3 p^2) \tag{3.9}$$

which is the minimum thrust loading considering Vp and p is the optimum wing loading considering Vp. Allowing 5% tolerance above maximum, we get a range for wing loading.
To find the optimum wing loading for cruise at M=0.778 at H_p=11000 m
Drag polar is $C_D = F_1 + F_2 p + F_3 p^2 = F_1 + F_2 p + \frac{k}{q^2}p^2$,
where $F_1 = 0.00939$; $F_2 = 9.91 \times 10^{-7} m^2 N^{-1}$; k=0.0483
At 11km altitude, sonic speed $a = \sqrt{\gamma RT} = 295.04$ m/s

$$V_c = V_p = M \times a = 0.778 \times 295.04\ m/s \implies V_p = 229.5\ m/s$$

$$q_p = \frac{1}{2}\rho V_p^2 \implies q_p = \frac{0.3648 \times 229.5^2}{2} = 9607.05\ N/m^2 \tag{3.10}$$

Hence,

$$F_3 = \frac{0.0483}{9607.05^2} = 5.23 \times 10^{-10} m^4/N^2 \tag{3.11}$$

And the optimum wing loading considering Vp is

$$P = \sqrt{\frac{F_1}{F_3}} = \sqrt{\frac{0.00939}{5.23 \times 10^{-10}}} = 4237.23\ N/m^2 \tag{3.12}$$

$$(\bar{t}_{Vp})_{min} = q_p(\frac{F_1}{p} + F_2 + F_3 p)$$

$$(\bar{t}_{Vp})_{min} = q_p(\frac{2F_1}{p} + F_2)$$

$$(\bar{t}_{Vp})_{min} = 9607.05(\times\frac{0.00939}{4237.23} + 9.91 \times 10^{-7}) = 0.0521$$

The wing loading range with 5% tolerance will be

$$\bar{t}_{Vp} = 0.0521 \times 1.05 = 0.0547 \tag{3.13}$$

Using this value,

$$0.0547 = q_p(\frac{F_1}{p} + F_2 + F_3 p)$$

$$0.0547 = 9607.05(\frac{0.00939}{p} + 9.91 \times 10^{-7} + 5.23 \times 10^{-10} p)$$

$$p^2 - 8991.84p + 17.95 \times 10^6 = 0$$

which is a quadratic equation with solution,

$$\text{p=2991.49 or 6000.34 } N/m^2$$

Thus the **wing loading is between 2991.49 to 6000.34** N/m^2, then $\bar{t}_{Vp}$ will be within 5% tolerance of $(t_{Vp})_{min}$
Substituting the values, we get the graph of $\bar{t}_{Vp}$ vs W/S.

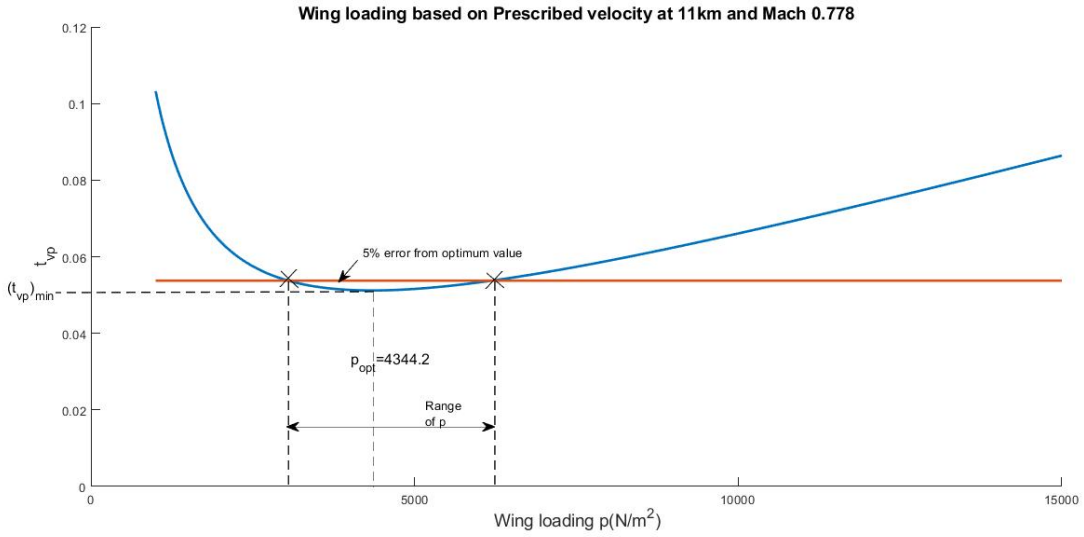

3.3 Selection of wing loading based on range (R)

Finding optimum wing loading based on range of the aircraft.
The expression for range R is

$$R = \frac{3.6}{TSFC}\sqrt{\frac{2}{\rho}}\frac{\sqrt{C_L}}{C_D}\sqrt{p}\ln\frac{W_1}{W_2} \tag{3.14}$$

Approximating,

$$\ln\frac{W_1}{W_2} \approx 2(\frac{W_1 - W_2}{W_1 + W_2})$$

Using this we get,

$$R = \frac{3.6}{TSFC}\sqrt{\frac{2}{\rho}}\frac{\sqrt{C_L}}{C_D}\sqrt{p}(\frac{W_1 - W_2}{W_1 + W_2}) \tag{3.15}$$

$$R = \frac{3.6}{TSFC}\sqrt{\frac{2}{\rho}}\frac{\sqrt{C_L}}{C_D}\sqrt{p}\frac{W_f}{W_{mean}}$$

where,

$$\bar{W}_f = W_1 - W_2 \ ; \ W_{mean} = \frac{W_1 + W_2}{2}$$

Noting, $C_L = \frac{2W}{\rho V^2 S} = \frac{p}{q}$ as $p = \frac{W}{S}$ and $q = \frac{\rho V^2}{2}$, yields:

$$\bar{W}_f = \frac{R}{3.6}\sqrt{\frac{\rho}{2}}TSFC\frac{C_D}{p}\sqrt{q} \tag{3.16}$$

$$\bar{W}_f = \frac{R}{3.6}\sqrt{\frac{\rho}{2}}TSFC\sqrt{q}(\frac{F_1}{p} + F_2 + F_3 p)$$

For optimum wing loading considering range,

$$\frac{d\bar{W}_f}{dp} = 0$$

This gives $P_{Rmax} = \sqrt{\frac{F_1}{F_3}}$; F_3 involves dynamic pressure

$$F_3 = \frac{k}{q^2} \ ; \ k = \frac{1}{\pi A e}$$

The optimum wing loading considering range is given by

$$p_{Rmax} = q\sqrt{\pi A e F_1} \tag{3.17}$$

Allowing 5% tolerance in W_f produces a range of wing loading which gives a near optimum result. From the data:

R=5000 km ; $\rho = 0.3648$; F_1=0.00939 ; $F_2 = 9.91 \times 10^{-7} m^2/N$
k=0.0483 ; TSFC=0.549 hr^{-1} ; $M_{cr} = 0.778$; $h_{cr} = 11km$

$$C_D = F_1 + F_2 p + F_3 p^2$$

Speed of sound a=295.04 m/s and density $\rho = 0.3648 \ \ kg/m^3$
Consequently,
$V_{cr} = 0.778 \times 295.1 = 229.5 \ m/s$
q=$0.5 \times \rho \times V^2$=9607.05 N/$m^2$
$F_3 = \frac{k}{q^2} = \frac{0.0483}{9607.05^2} = 5.23 \times 10^{-10} m^4/N^2$

Using these values,

$$P_{Rmax} = \sqrt{\frac{F_1}{F_3}} = 4237.23 \ N/m^2 \tag{3.18}$$

From Eq.(35)

$$(\bar{W}_f)_{min} = \frac{R}{3.6}\sqrt{\frac{\rho}{2}} TSFC \sqrt{q}\left(\frac{F_1}{p} + F_2 + F_3 p\right) \tag{3.19}$$

$$(\bar{W}_f)_{min} = \frac{5000}{3.6}\sqrt{\frac{0.3648}{2}} \times 0.55 \times \sqrt{9607.05}\left(\frac{2 \times 0.00939}{4237.23} + 9.91 \times 10^{-7}\right) \tag{3.20}$$

$$(\bar{W}_f)_{min} = 0.1731 \tag{3.21}$$

Allowing 5% tolerance,

$$(\bar{W}_f)_{min} = 0.1731 \times 1.05 = 0.1817 \tag{3.22}$$

From Eq.(35)

$$0.1817 = \frac{5000}{3.6}\sqrt{\frac{0.3648}{2}} \times 0.55 \times \sqrt{9607.05}\left(\frac{0.00939}{p} + 9.91 \times 10^{-7} + 5.23 \times 10^{-10} p\right) \tag{3.23}$$

which gives, p= 2991.78 and 6001.14 N/m^2

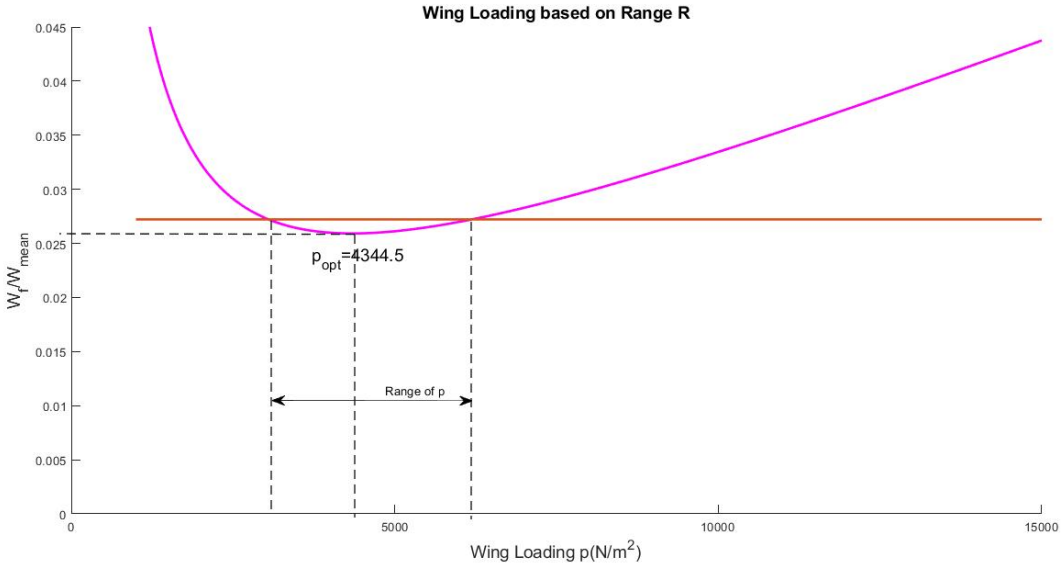

3.4 Selection of wing loading based on absolute ceiling (H_{max})

At absolute ceiling the flight is possible only at one speed at which,

$$T_{req} = T_{min} = D_{min}$$

Hence, for a jet airplane:

$$\bar{t}_{H_{max}} = \frac{D_{min}}{W} = \frac{1}{(L/D)_{max}}$$

For parabolic polar i.e. $C_D = C_{D0} + K(C_L)^2$, the following relations are already known at $(L/D)_{max}$.

$$(C_L)_{(L/D)max} = (C_{D0}/K)^{0.5}$$

and,

$$(C_D)_{(L/d)max} = 2C_{D0}$$

Hence,

$$\bar{t}_{Hmax} = \frac{1}{(L/D)_{max}} = \sqrt{4C_{D0}K} \tag{3.1}$$

substitute $C_{D0} = F_1 + F_2 p$

$$\bar{t}_{H_{max}} = \sqrt{4(F_1 + F_2 p)} \tag{3.2}$$

From the plot between $\bar{t}_{H_{max}}$ and p, it is seen that $\bar{t}_{H_{max}}$ increase as p increases. Sometimes, the flight

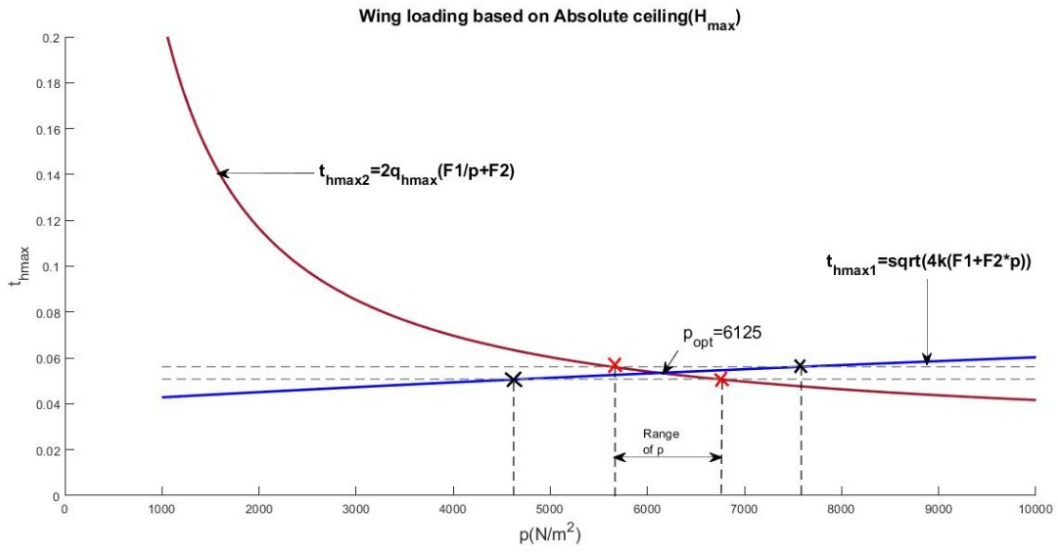

velocity($V_{h,max}$) may be prescribed at absolute ceiling. In this case, the optimisation of wing loading is carried out in the following manner.

$$\bar{t}_H = \frac{T_{req}}{W} = \frac{q_{H,max} S (C_D)_{(L/D)max}}{W} = \frac{q_{H,max} 2CD0}{P}$$

Substitute $C_{C0} = F_1 + F_2 p$, gives:

$$\bar{t}_H = 2q_{Hmax}\left(\frac{F_1}{p} + F_2\right) \tag{3.3}$$

Data- $F_1 = 0.00939$, $F_2 = 9.91\times10^{-7}$, $F_3 = k/q^2$, $k = 0.0483$

$$W = 1120267.175N \quad C_{D0} = 0.015 \quad S_{old} = 198m^2 \quad (W/S)_{old} = 5657.91N/m^2$$

q_{Hmax} corresponds to $V = V_{(L/D)max}$

$$(C_L)_{(L/D)max} = \sqrt{C_{D0}/K} = 0.5573$$

$$q_{Hmax} = \frac{(W/S)_{old}}{(C_L)_{(L/D)max}} = 10152.76\ N/m^2$$

Solving eq.(2) and eq.(3) we will get $p_{Hmax} = 5657.23\ N/m^2$
$\bar{t}_{Hmax}$ corresponds to p_{Hmax} is:

$$\sqrt{4 \times 0.0483 \times (0.00939 + 9.91 \times 10^{-7} \times 5657.23)} = 0.0538 \tag{3.4}$$

Allowing +-5% variation in $\bar{t}_{Hmax}$, the permissible limits on $\bar{t}_{Hmax}$ are:

$$\bar{t}_{max_{+5}} = 0.0565 \qquad and \qquad \bar{t}_{max_{-5}} = 0.0511$$

solving eq(2) with 5% variation of $\bar{t}_{Hmax}$, p_{Hmax} range is-

$$p_{Hmax(+5)} = 7197.81N/m^2 \quad and \quad p_{Hmax(-5)} = 4163.04N/m^2 \tag{3.5}$$

Solving eq(3) for the values of $\bar{t}_{max}$ variations gives:

$$p_{Hmax(+5)} = 5241.43N/m^2 \quad and \quad p_{Hmax(-5)} = 6155.13N/m^2 \tag{3.6}$$

Hence, to satisfy both the above criteria the range of permissible wing loading is given by:
a) Higher of the lower limits from the two considerations
b) Lower of the upper limits from the two considerations.
From Eq.(6) and (7) the range of values which satisfies these limitations are:

$$5241.43 < P < 6155.13\ N/m^2$$

3.5 Selection of optimum wing loading

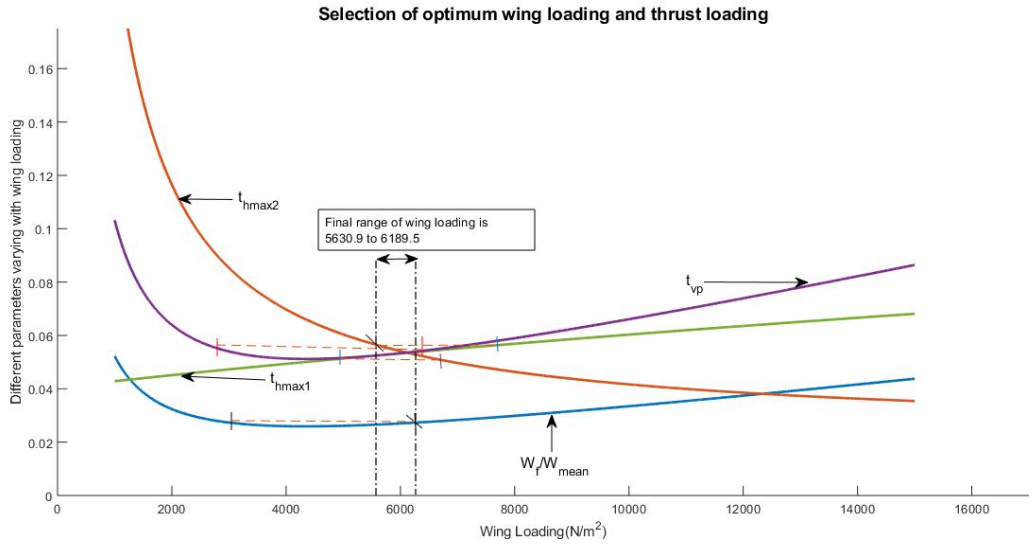

The range of wing loading was taken from intersection of all 4 graphs based on range, hmax(2) and prescribed velocity. The maximum value from this range i.e; $6189.5 N/m^2$ is selected as optimum value since the aircraft specified is a passenger aircraft and maximum wing loading is preferred from the calculated range considering the support safety regulations (Vp, range and hmax).

Thrust loading for each consideration is calculated for this optimum wing loading and the maximum value is our final thrust loading in order to perform all the parameters specified (Vp, range and hmax).

1. For this optimum wing loading, thrust loading based on prescribed velocity is 0.0537
2. Thrust loading based on absolute ceiling is 0.0536 for t_{hmax1} and 0.0532 for t_{hmax2}.
3. W_f/W_{mean} based on range is 0.0272
4. Maximum value among these is 0.0537 at 11km altitude. We have to normalize it to sea level with ratio of thrust at sea level to thrust at 11km for our engine Roll Royce Trent-1000. The ratio for our engine turns out to be 4.695(Ratio is obtained from the engine parameters available from the reference[6]).
5. So the thrust at sea level is $0.0537 \times 4.695 W_0 = 0.2523 \times 102569 \times 9.8 = 253.6$ KN

3.6 Engine selection:

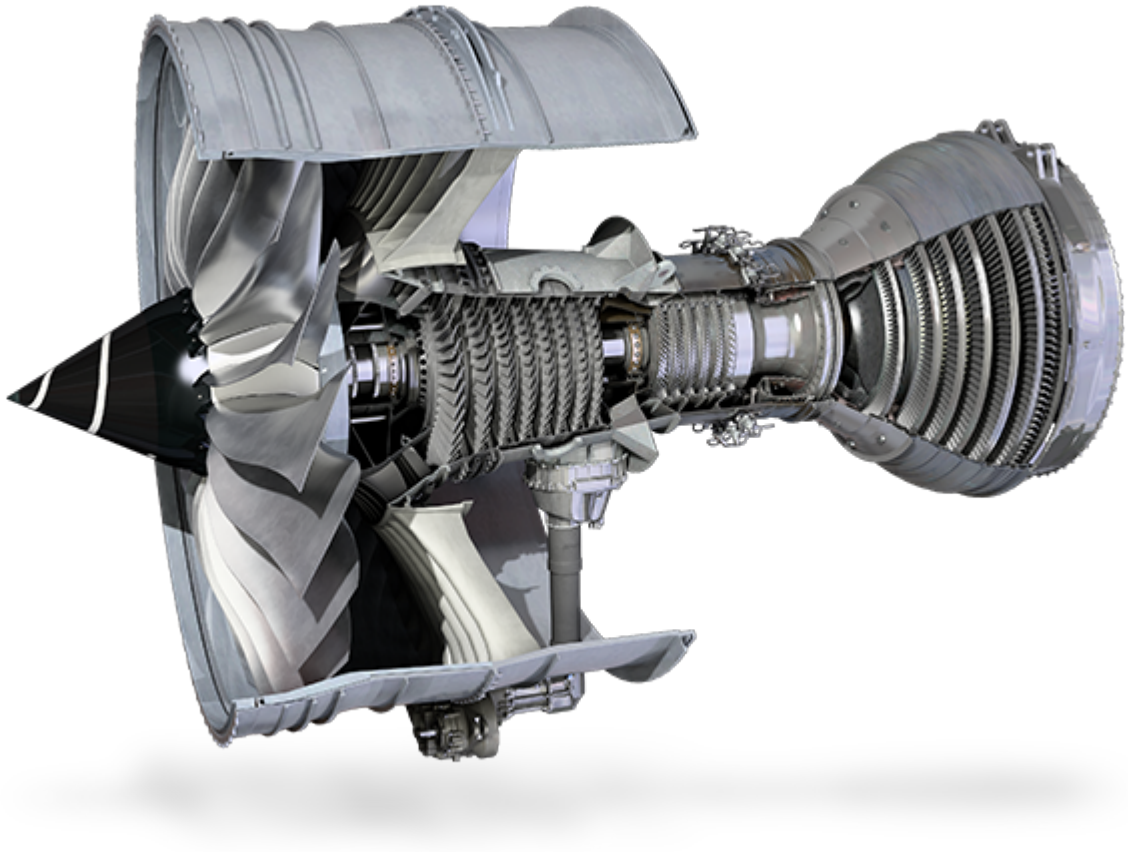

Figure 3.1: Rolls-Royce Trent-1000

This engine is a three-shaft high bypass(10:1) turbofan engine specially built for high subsonic aircraft. The weight of a single unit is approximately 5.3 tonnes, which produces a thrust of 265.4 - 360.4 KN with thrust loading of 6.01. The thrust loading calculated for our design is 0.579, the thrust to weight ratio from the wing loading considerations is 0.537 which indicates that this engine is suitable for our aircraft.

Chapter 4

Airfoil selection

4.1 Introduction

In the context of wing design the following aspects need consideration:

1. Wing area (S) : This is calculated from the wing loading and gross weight which have been already decided i.e. S= W / ($\frac{W}{S}$).
2. Location of the wing on fuselage : High-wing, low-wing or mid-wing.
3. Airfoil : Thickness ratio, camber and shape.
4. Sweep (Λ) : Whether swept forward, swept backward, angle of sweep, cranked wing, variable sweep.
5. Aspect ratio (A) : High or low.
6. Taper ratio (λ) : Straight taper or variable taper.
7. Twist (ϵ)
8. Wing incidence or setting (i_w)
9. High lift devices : Type of flaps and slats; values of $C_{L,max}$, $\frac{S_{flap}}{S}$
10. Aileron
11. Dihedral angle (Λ)

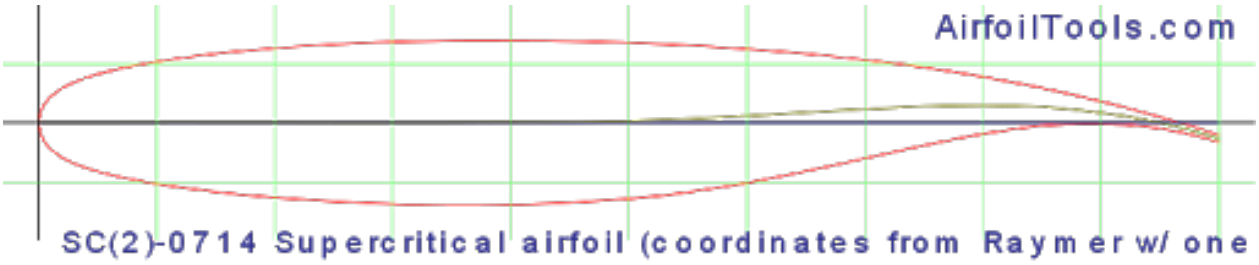

For airplanes flying at high subsonic speeds, the lift coefficient under cruising condition ($C_{L,cr}$) is around 0.5(0.63 for our design obtained from cruising condition). At this value of lift coefficient, the older NACA airfoils have drag divergence Mach number (MD) of around 0.68 for a thickness ratio (t/c) of around 15%. Advancements in computational fluid dynamics (CFD) enabled design of improved airfoils, called supercritical airfoils, which have drag divergence Mach number around 0.75 for thickness ratio of 15%. Divergence Mach number calculated for NASA SC(2) - 0714 came out to be 0.852, making it ideal for our design.

4.2 Aerodynamics characteristics of airfoils

The plots of Lift coefficient (C_l) vs angle of attack (α), Drag coefficient (C_d) vs C_l and pitching moment coefficient about quarter-chord $C_{m,c/4}$ vs α have been plotted using XFLR5 software. We did not incorporate transonic effects as the prescribed mach number of the plane is 0.778 ad it does not fall into transonic regime. The Reynolds number(Re) range for this plots has been calculated assuming cruise condition at 11km altitude:

Reynolds number calculation:

Reynolds number formula,

$$Re = \frac{v \times l}{\nu} \tag{4.1}$$

where, v is velocity of fluid
l is chord width
ν is kinematic viscosity

Re at wing root:

$$Re = \frac{229.5 \times 7.5}{3.8995 \times 10^{-5}} = 44,145,935 \tag{4.2}$$

Re at wing tip:

$$Re = \frac{229.5 \times 2}{3.8995 \times 10^{-5}} = 11,772,249 \tag{4.3}$$

For this range we get the following plots,

A) C_l **vs** α

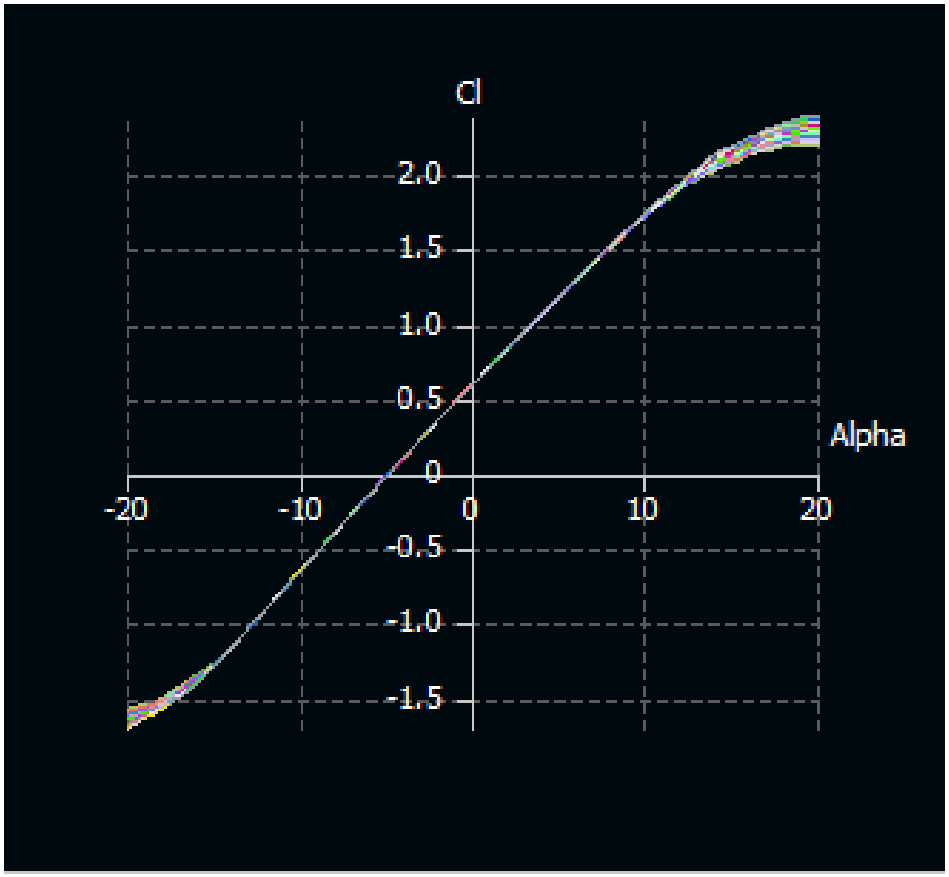

The first plot has four important features viz. (a) angle of zero lift (α_{0l}), (b) slope of the lift curve denoted by $\frac{dCl}{d\alpha}$ or a0 or $C_{l\alpha}$, (c) maximum lift coefficient ($C_{l,max}$) and (d) angle of attack (α_{stall}) corresponding to $C_{l,max}$.

$C_{l,max} = 2.09$, $\alpha_{stall} = 18^0$, $\alpha_{0L} = -4^0$ and $\frac{dCl}{d\alpha} = 0.1$ per degree

Stall pattern:
Variation of the lift coefficient with angle of attack near the stall is an indication of the stall pattern. We want a gradual change pattern of the lift coefficient which is displayed by airfoils with t/c ratios of greater than 14% which was one of the primary reasons for choosing NASA SC(2) - 0714 airfoil with a thickness ratio of 14 %.

B) C_l **vs** C_d
Plot 2 has two important features viz. (a) minimum drag coefficient ($C_{d,min}$) and (b) lift coefficient ($C_{l,opt}$) corresponding to $C_{d,min}$.

$$C_{d,min} = 0.006 \text{ and } C_{l,opt} = 0.0 \text{ - } 1.0$$

We see the Drag bucket feature in our plot.The extent of this drag bucket and the lift coefficient at the middle of this region are also characteristic features of the airfoil. The camber decides $C_{l,opt}$ and thickness ratio(t/c) decides the extent of the drag bucket.

C) C_m **vs** α

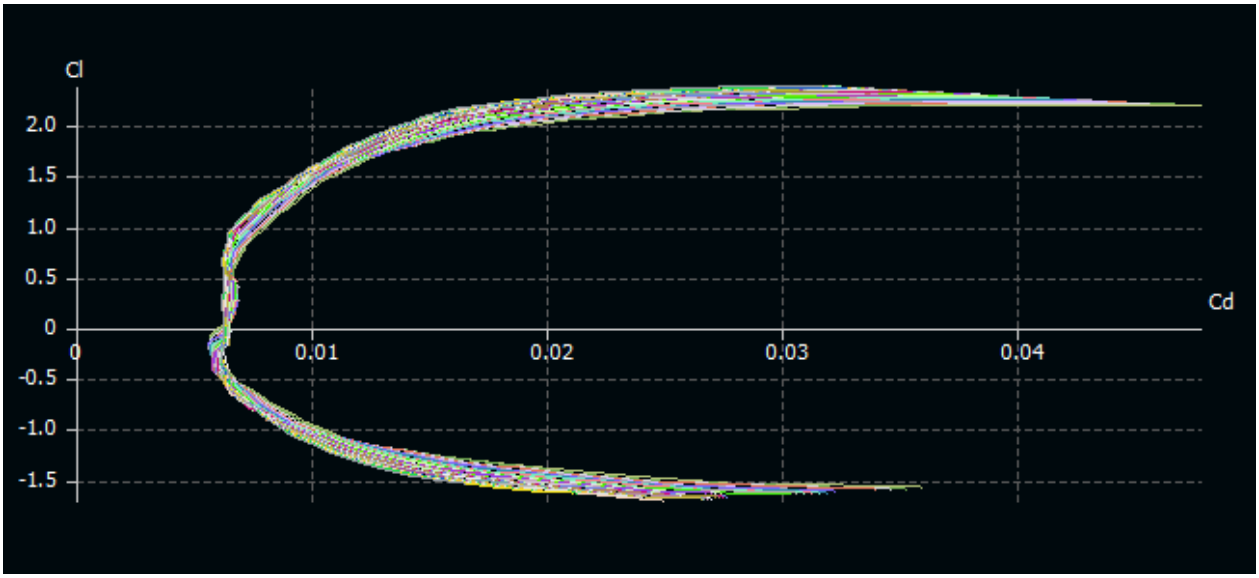

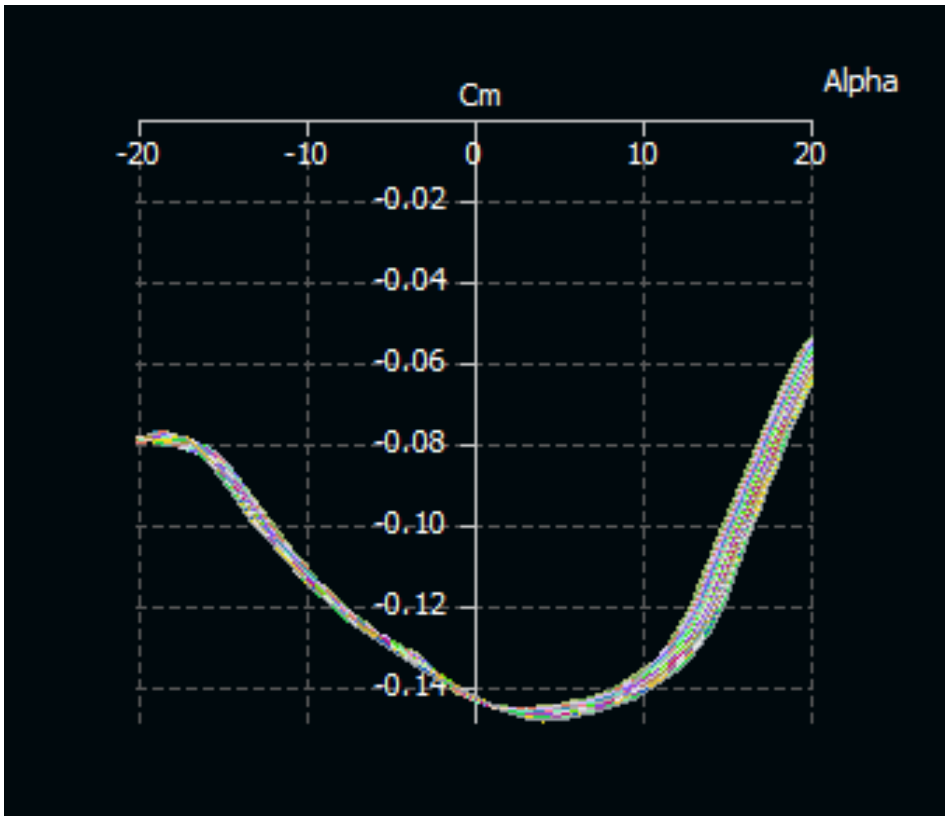

This plot is used to work out the location of the aerodynamic center of the airfoil. We have plotted C_m vs α at the quarter chord location of the airfoil.

4.3 Geometrical characteristics of airfoils

Camber line:
The line joining the extremities of the camber line is the chord. The leading and trailing edges are defined as the forward and rearward extremities, respectively, of the mean line.
The maximum camber as a fraction of the chord length ($y_{c,max}$/c) and its location as a fraction of chord ($x_{yc,max}$/c) are the important parameters of the camber line. The maximum ordinate of the thickness distribution as fraction of chord ($y_{t,max}$/c) and its location as fraction of chord ($x_{yt,max}$/c) are the important parameters of the thickness distribution.

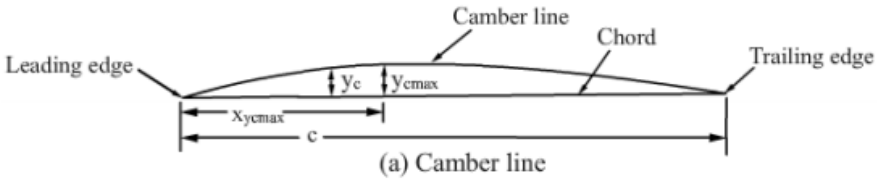

(a) Camber line

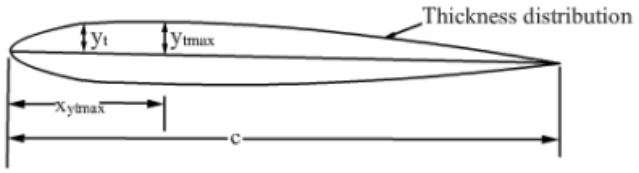

(b) Thickness distribution
(symmetric about chord line)

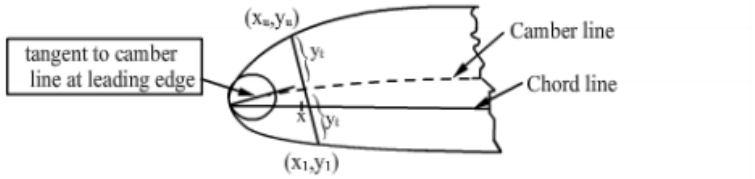

(c) Airfoil coordinates superposition of thickness distribution over camber line

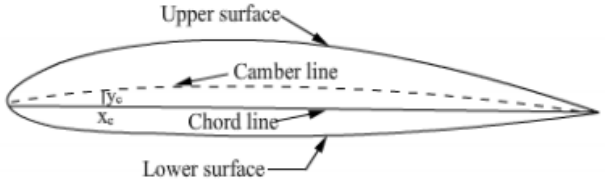

(d) Airfoil shape

Similar airfoils considered:

1. NASA Supercritical Airfoil SC(2)-0706 Remark: t/c ratio is 6% so exhibits abrupt stall

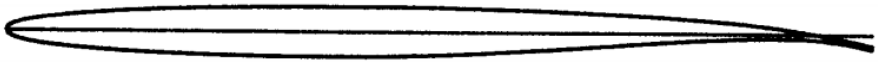

2. NASA Supercritical Airfoil SC(2)-0610 Remark: $C_{l,opt}$ is 0.6 which is less than the $C_{l,design}$(calculated

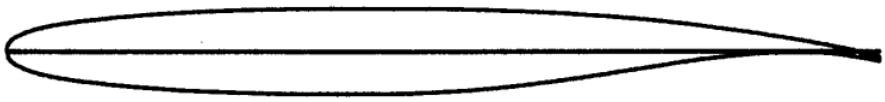

to be 0.63)

4.4 Effects of geometric parameters, Reynolds number and roughness on aerodynamic characteristics of airfoils

1. The camber decides α_{0l} , $C_{l,opt}$ and $C_{m,ac}$. For a given family of airfoils, with an increase of camber, α_{0l} and $C_{m,ac}$ becomes more negative whereas $C_{l,opt}$ increases.

2. The thickness ratio influences $C_{d,min}$ and $C_{l,max}$. For a given family of airfoils, the minimum drag coefficient ($C_{d,min}$) increases with (t/c). The maximum lift coefficient ($C_{l,max}$) is highest for (t/c) between 12 to 16%. The stall pattern is also gradual for these thickness ratios as described before.

3. The Reynolds number (Re) mainly influences $C_{l,max}$ and $C_{d,min}$. The former ($C_{l,max}$) increases with Re and the latter generally decreases with Re.

4. The surface roughness influences $C_{l,max}$ and $C_{d,min}$. With increase of roughness $C_{l,max}$ decreases and $C_{d,min}$ increases.

5. The critical Mach number, in connection with the airfoil, is defined as the Free stream Mach number at which the maximum Mach number on the airfoil is unity. This quantity can be obtained theoretically by calculating the pressure distribution on the airfoil, but cannot be determined experimentally. However, when the critical Mach number is exceeded, the drag coefficient starts to increase. Making use of this behavior, the term Drag divergence Mach number (M_D) is defined as the Mach number at which the drag coefficient shows an increase of 0.002 over the subsonic drag value.The drag divergence Mach number (M_D) depends on airfoil shape, thickness ratio, and lift coefficient. For a given airfoil MD is highest near $C_{l,opt}$. It decreases with thickness ratio.

4.5 Choice of airfoil camber

The camber and the thickness ratio decides the characteristics like $C_{l,opt}$, $C_{l,max}$, $C_{d,min}$, drag divergence Mach number (MD), weight of the wing and the stall pattern. For a good design, the camber should be chosen such that $C_{l,opt}$ of the airfoil is close to the lift coefficient of the aircraft (C_L) in the flight corresponding to the mission of the airplane. This lift coefficient is called design lift coefficient ($C_{L,design}$). This would correspond to the cruise flight condition.

$$C_{L,design} = \frac{2W}{\rho v^2 S} \tag{4.4}$$

We choose the camber of the airfoil such that $C_{l,opt}$ approximately equals $C_{L,design}$.

4.6 Choice of airfoil thickness ratio

At the preliminary design stage the guidelines are obtained from the airfoils used on similar airplanes. Low speed airplanes have a thickness ratio between 15 to 18%. NASA LS(1)0417 is being used on low speed airplanes. NASA MS (01)-031 is being used on medium speed airplanes with turboprop engines. The high subsonic airplanes use super critical airfoils of camber which would give $C_{l,opt} = C_{L,design}$ and (t/c) around 14%. At supersonic speeds, $C_{d,min}$ is proportional to $(t/c)^2$. These airplanes have t/c between 3 to 5%. Concorde airplane had biconvex airfoil of t/c = 0.035. For our high subsonic airplane we choose the t/c ratio to be 14% which is consistent with the above discussion.

4.7 Selection of wing parameters

4.7.1 Aspect ratio(A)

From the data of similar air crafts we choose aspect ratio to be 9.33. We calculate the $C_{l,\alpha}$ for $A > 4$ using the formula,

$$C_{L\alpha} = \frac{2\pi A}{2 + \sqrt{4 + \frac{A^2\beta^2}{\eta^2}(1 + \frac{\tan^2 \Lambda_{1/2}}{\beta^2})}} \tag{4.5}$$

The above equation states that $C_{l\alpha}$ decreases as A decreases. Also the induced drag for a subsonic aircraft is given by:

$$C_{Di} = (1 + \delta)\frac{C_L^2}{\pi A} \tag{4.6}$$

Weight of the wing can be determined using the formula:

$$W_w = CS_w^a A^b (t/c)^c (1 + \lambda)^d (\cos \Lambda)^e \tag{4.7}$$

Low speed airplanes of earlier designs had aspect ratio between 6 to 7.5, but the current trend is to choose between 7.5 to 8.5. The medium speed airplane, using turboprop engines, of earlier design had an aspect ratio between 9 to 11. The current trend is the aspect ratio between 11 to 13. The high subsonic jet transport of earlier designs had an aspect ratio between 7 to 8. The current trend is between 8.5 to 10.0 which justifies our selection.

4.7.2 Sweep(Λ)

The wing sweep affects the slope of the lift curve ($C_{L\alpha}$), the maximum lift coefficient $C_{L,max}$, the induced drag coefficient (C_{Di}), the drag divergence Mach number (MD), the wing weight and the tip stalling.

A. Effect on $C_{L\alpha}$

$$C_{L\alpha} = \frac{2\pi A}{2 + \sqrt{4 + \frac{A^2\beta^2}{\eta^2}(1 + \frac{\tan^2 \Lambda_{1/2}}{\beta^2})}}$$

$C_{L\alpha}$ decreases as sweep increases as can be seen from the above equation.

B. Effect on $C_{L,max}$

$C_{L,max}$ of a swept wing decreases in proportion to $\cos \Lambda$

C. Effect on C_{Di}

The induced drag coefficient of a typical jet airplane is formulated to be:

$$C_{Di} = (1+\delta)\frac{C_L^2}{\pi A}$$

From this equation one can infer that induced drag coefficient increases as angle of sweep increases.

D. Effect on MD

For a swept wing the change in drag divergence Mach number due to sweep angle, is given approximately by the following equation

$$\frac{1-(M_D)_\Lambda}{1-(M_D)_{\Lambda=0}} = 1 - \frac{\Lambda}{90} \tag{4.8}$$

A typical unswept wing employing a super critical airfoil will be 0.78, but when the sweep is increased to 30 we get an increased MD of 0.853 which is what is in our case.

E. Effect on wing weight

The weight of the wing is proportional to $\frac{1}{\cos\Lambda}$. Thus it increases as sweep increases. We choose sweep as 30 from data of similar aircrafts.

4.7.3 Taper ratio(λ)

The taper ratio influences the following quantities
a) Induced drag
b) Structural weight
c) Ease of fabrication
Instead of an elliptic wing which is difficult to manufacture, we go for rectangular wing with a taper ratio of typically 0.3 to 0.5. This comprises the trade-off of induced drag which is higher than in the elliptical case. However it helps in reducing the wing structural weight.

4.7.4 Twist

A wing is said to have a twist when the chord lines of airfoils at different span-wise stations are not parallel to each other. The difference between the angles of attack of the airfoil sections at the root and near the tip is called geometric twist. Whereas, the aerodynamic twist is the intentional variation zero lift angle of airfoils at root and near the tip. In aircraft twist is given to prevent tip stalling.

Tip Stalling: It is a phenomenon in which the stalling on the wing begins in the region near the wing tip.

For our wing we chose 3° twisting as an initial estimate, so that the tip has has lesser angle of incidence compared to that at root.

4.7.5 Wing Incidence

The angle between fuselage reference line and the wing reference line is called wing incidence and denoted by i_w.The mean aerodynamic chord is the reference line of the wing. Fuselage reference line (FRL) is the reference line for the entire airplane. The reason for providing the wing incidence is given below

1. Setting the wing at an incidence helps to increase the effective angle of attack of the overall wing. Higher angle of attack helps for keeping take off and approach speed low. To see this lets denote i_w the incidence of the wing. For moderate values of the angle of attack of the airplane AoA, the lift coefficient of the wing has a linear behavior :

$$C_{l,wing} = \frac{dC_{lwing}}{d\alpha}(\alpha + i_w - \alpha_0) \tag{4.9}$$

Where α_0 is the value of $\alpha+i_w$ for which the lift coefficient is zero. α_0 is a constant. From the expression above it can be seen that the incidence of the wing increases the effective angle of attack of the overall wing.

2. On transport airplanes, setting wings at some angle becomes essential to have a horizontal floor during cruise so the flight attendants don't have to push their carts uphill. This will result in a slightly positive incidence angle.

3. For the economy in fuel consumption, the drag should be minimum during cruise. The fuselage has a minimum drag when its angle of attack is zero. However, during cruise, the wing should produce sufficient lift to support the weight of the airplane. Keeping these factors in view, the wing is mounted on the fuselage in such a manner that it produces the required amount of lift in cruise while the fuselage is at zero angle of attack.

During the preliminary design phase, i_w is obtained as follows.

$$C_{L,design} = \frac{W}{\frac{1}{2}\rho V^2 S} \tag{4.10}$$

Where rho and V corresponds to design flight conditions. Values of rho and V taken from the similar aircraft data. ρ=0.3648; V = 229.5 m/s. For an untwisted wing $\alpha_{0L} = \alpha_{0lr}$. Where α_{0L} = zero lift angle of attack at the root. From lift curve zero lift angle of attack(α_{0lr}) was obtained to be -4°. Now, wing with aerodynamic twist of :

$$\alpha_{0L} = \alpha_{0lr} + J\epsilon \tag{4.11}$$

where, ϵ is positive when the airfoil at the tip is at an angle of attack higher than at root. We took $\epsilon = 3^0$. The quantity J has a weak dependence on aspect ratio and taper ratio of the wing. However, a value of -0.4 can be taken for the first estimate of α_{0L}. Now wing incidence can be calculated from the expression below:

$$C_{L,design} = C_{L\alpha}(i_w - \alpha_{0L}) \tag{4.12}$$

$$\alpha_{0L} = \alpha_{0lr} + J\epsilon \tag{4.13}$$

where, $\epsilon = 3^\circ$; $\alpha_{0lr} = -4$; J=-0.4(Initial estimate)

Now, $\alpha_{0L} = -5.2^\circ$
Obtaining $C_{L\alpha}$ for wing:

$$C_{L\alpha} = \frac{2\pi A}{2 + \sqrt{4 + \frac{A^2\beta^2}{\eta^2}(1 + \frac{\tan^2 \Lambda_{1/2}}{\beta^2})}} \tag{4.14}$$

where $\beta^2 = 1 - M^2$, $\eta = C_{l\alpha}/2\pi$, $\Lambda_{\frac{1}{2}}$ is sweep of the half chord line, $C_{l\alpha}$ is the slope of lift curve for the wing airfoil.

$$C_{L\alpha} = 0.125 \; ; \; C_{L,design} = 0.63$$

Using these in $C_{L,design}$, $C_{L\alpha}$ relation, we get i_w as -0.16°. Negative sign means that the angle of attack at the tip is lower than that at the root.

4.7.6 Dihedral

For this preliminary design stage we take $\Gamma = 3^\circ$.

4.7.7 Wing vertical location

The wing configuration of a fixed-wing aircraft, including both gliders and powered aeroplanes, is its arrangement of lifting and related surfaces.
There are three choices for the location of the wing on the fuselage namely,high-wing, mid-wing and low-wing. High wing aircraft place the wing above the fuselage, the main body of the aircraft, while low wing aircraft place the wing below the fuselage, and mid wing aircraft at the center.

Comparison between high wing and low wing aircraft

Aerodynamics Stability Aerodynamic stability of the two designs differs a bit; the center of lift can be higher in a high-wing design, often offset with dihedral in low-wing aircraft.

Roll Characteristics
Considering lateral stability, For the high wing aircraft, the center of gravity sits below the wing, meaning the fuselage of the aircraft acts as a pendulum to increase roll stability relative to the low wing aircraft, whose center of gravity is balanced above the wing.
For the high wing aircraft, there will be relatively less tendency to enter an unstable spiral descent, but the aileron forces will be higher to complete a rolling maneuver.

Visibility

1. High-wing aircraft offer better visibility below the aircraft, especially for passengers in 4-seat or larger aircraft, as the wing doesn't block it.

2. Low-wing aircraft can offer better visibility above the aircraft, as the wing remains mostly out of the field of view.

3. a lot of midair collisions involve mixed types; low-wing aircraft descend into high-wing, or high-wing aircraft climb into low-wing.

Landing Characteristics
During the landing flare, the low wing aircraft will enter ground effect slightly before the high wing aircraft and will experience a larger reduction in drag for the same height above the ground.
The stronger ground effect during the flare will cause the low wing aircraft to float more readily than the high wing aircraft, which, a characteristic that, when used skillfully, helps to soften the touchdown. But this same ground effect can encourage ballooning during the flare, and may make precise landings more difficult to accomplish.
The high wing aircraft will still experience ground effect, but because the wing is several feet farther from the runway, the total effect on the aircraft is greatly reduced, as ground effect decreases exponentially with difference from the runway surface. The high wing aircraft thus may be capable of shorter landing distances, as it punches through ground effect more easily. so it is concluded that low-wing aircraft can incur more ground effect than high-wing.

Ground clearance
Ground clearance, specifically in multi engine aircraft, is going to be greater when engine are mounted on a high wing rather than low wing.This is true of both propeller and jet engines, although propellers tend to have a larger radius for a given aircraft size.

Cruise Characteristics
The lower drag profile of the low wing aircraft yields greater cruise performance relative to the high wing design; the result is higher true airspeed and or lower cruise fuel burns.

Takeoff Performance
The low wing configuration results in longer landing air distances, where air distance is the horizontal distance traveled between 50 feet above touch down to the touchdown point.

Mid-wing Configuration

Advantages:

1. Lower drag
2. No blockage of visibility. Hence,used on some military airplanes.
3. Advantages of ground clearance as in the case of high wing configuration

Disadvantages: Wing root structure passing through the fuselage is not possible, which leads to higher weight. However,in HFB Hansa airplane, a swept forward mid-wing is located behind the passenger cabin.This permits wing root structure passing through the fuselage.

After considering all the factors above we chose high wing configuration for our design.

4.7.8 Flaps

The flaps are high lift devices. These devices are deployed to increase the maximum lift coefficient ($C_{L,max}$) during take-off and landing.The flaps are located near the trailing edge. Common types of flaps are : plain flap, split flap, zap flap, single slotted flap, double slotted flap, triple slotted flap and fowler flap. Typical values of $C_{L,max}$ are different for different types of high lift devices. The plain flap and split flap are simple to fabricate.
The complexity of fabrication and the weight of the wing increase progressively for zap flap, single slotted flap, double slotted flap, triple slotted flap and fowler flap. The airplanes flying at high subsonic speed need high wing loading from the consideration of cruise. Hence, complicated high lift devices are employed to reduce take-off and landing distances.

Considering these factors, the flaps used on different types of airplane are as follows

1. The home-built and general aviation aircraft use plain flap.
2. Single slotted flaps are used on general aviation aircraft and some transport airplanes with turboprop engines e.g. SAAB 2000.
3. Double slotted flaps are used on some turbo-prop airplanes (e.g. ATR 72 -200) and on some jet airplanes.(e.g. Boeing 767).
4. Triple slotted flaps are employed on large jet airplanes. Some airplane companies have perfected the design of such flaps and use them.
5. Fowler flaps are used on some turboprop airplanes (e.g. IPTN M 250 100 and Dash 8 Q 300) and on many Boeing airplanes. The jet airplanes generally have leading edge slats in combination with Fowler flap to increase C_{Lmax} further.

After considering multiple factors, we reached to the conclusion that Double-slotted flaps are most suitable for our aircraft in terms of both weight and cruise velocity.

4.7.9 Aileron

Ailerons are a primary flight control surface which control movement about the longitudinal axis of an aircraft. This movement is referred to as "roll". They are used in pairs to control the aircraft in roll, which normally results in a change in flight path due to the tilting of the lift vector. The ailerons are attached to the outboard trailing edge of each wing and, when a manual or autopilot control input is given, they move in opposite directions from one another. For our design, two ailerons are mounted on each wing. At this stage of preliminary design, guideline from similar aircraft was taken.
From similar aircraft data,
the ratio of aileron area to wing area = 0.049.

4.7.10 Slats

Slats are extendable, high lift devices on the leading edge of the wings of some fixed wing aircraft. Their purpose is to increase lift during low speed operations such as takeoff, initial climb, approach and landing. They accomplish this by increasing both the surface area and the camber of the wing by deploying outwards and drooping downwards from the leading edge.Slats normally have several possible positions and extend progressively in concert with flap extension.

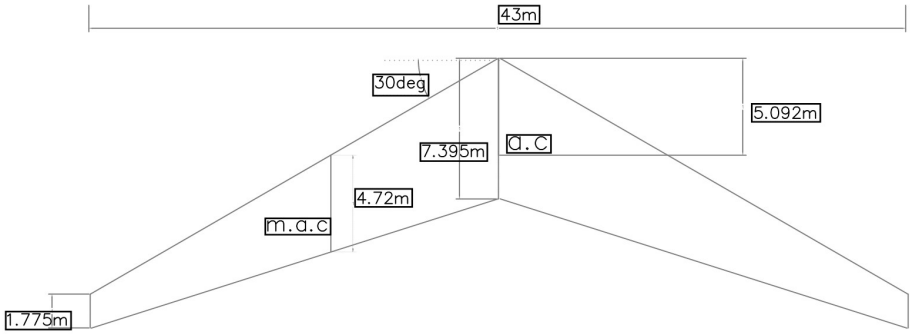

Figure 4.1: Top view of the designed wing

Chapter 5

Parachute deployment and Auto Rotation

5.1 Introduction

We now consider the emergency case where our special internal structure a.k.a. the pod is now ejected from the main fuselage structure and the parachute and auto rotation systems are deployed. We assume that the load of the aircraft is split between the parachute system and auto rotation system in the ratio of 1:1, which can be optimised later depending on the feasibility and the economy of the systems deployed for safety management.

5.1.1 Force exerted on the Parachute

We calculate the drag force on the parachute assuming that half of the weight of the plane is carried bu the parachutes(ratio of lift from parachute system and Auto rotation system is 1:1);

$$D = \frac{\rho v^2 S C_D}{2} \tag{5.1}$$

Assuming that the forward velocity of the plane after the parachutes are deployed in case of emergency is 150 m/s, at an altitude of atmospheric density of 1.2 kg/m^3 as the plane is about to reach its terminal velocity of 6 m/s, and C_D of parachute is assumed 0.75 for large parachutes(from references). Also, the structural weight of the pod ejected is 30 tonnes.

$$(15,000)(9.8) = \frac{(1.2)(6^2)(S)(0.75)}{2} \tag{5.2}$$

We end up with an area of 18,148 m^2 for the parachute system, which can be deployed as a system of three parachutes whose diameter turns out be 62.05 m for each one.

5.1.2 Force supported by Autorotation mechanism

Now for the auto rotation part, the remaining weight of the pod i.e, 15 tonnes of lift is produced by the auto rotation system. This system of blades now has a wing loading based on half of the weight of the deployed pod.

When the pod is ejected, Some force must be used to sustain rotor RPM(for the system of blades) so controlled flight can be continued to the ground. This force is generated by adjusting the collective pitch to allow a controlled descent. Airflow during descent provides the energy to overcome blade drag and turn the rotor. When the aircraft is descending in this manner, it is said to be in a state of autorotation. In effect the aircraft gives up altitude at a controlled rate in return for energy to turn the rotor at an RPM which provides aircraft control. Stated another way, the airplane has potential energy by virtue of its altitude. As altitude decreases, potential energy is converted to kinetic energy and stored in the turning rotor. This kinetic energy is used to cushion the touchdown when near the ground. Most autorotations are performed with forward airspeed. For simplicity, the following aerodynamic explanation is based on a vertical autorotative descent

(no forward airspeed) in still air. Under these conditions, the forces that cause the blades to turn are similar for all blades regardless of their position in the plane of rotation. Dissymmetry of lift resulting from helicopter airspeed is therefore not a factor, but will be discussed later.

During vertical autorotation, the rotor disk is divided into three regions: driven, driving and stall regions.

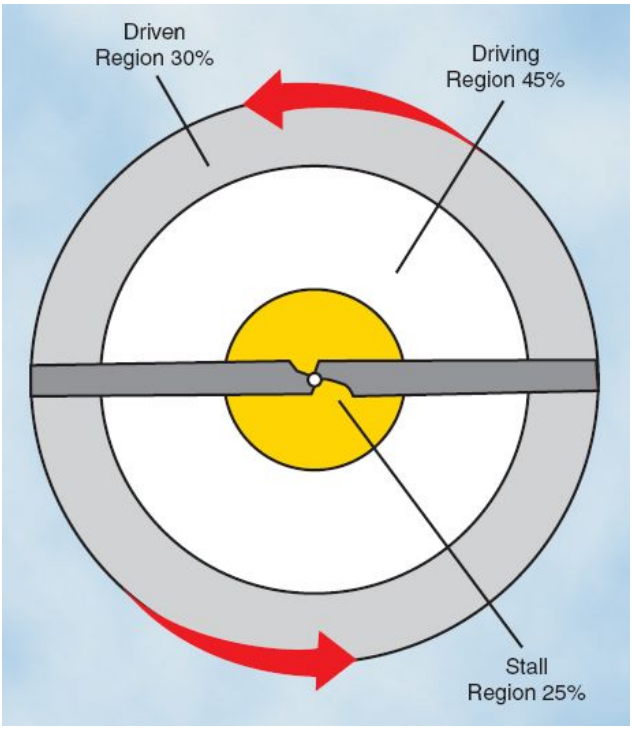

Figure 5.1: Front view

- The driven region, also called the propeller region, is nearest to the blade tips and normally consists of about 30 percent of the radius. The total aerodynamic force in this region is inclined slightly behind the rotating axis. This results in a drag force which tends to slow the rotation for the blade.
- The driving region or autorotative region, normally lies between about 25 to 70 percent of the blade radius. Total aerodynamic force in this region is inclined slightly forward of the axis of rotation. This inclination supplies thrust which tends to accelerate the rotation of the blade.
- The stall region includes the inboard 25 percent of the blade radius. It operates above the stall angle of attack and causes drag which tends to slow the rotation of the blade.

For our case, we remove the stalling region as it is of no use in our case(explicit use of blades for Auto rotation). The parameters and further calculations for the blade system will be included later.

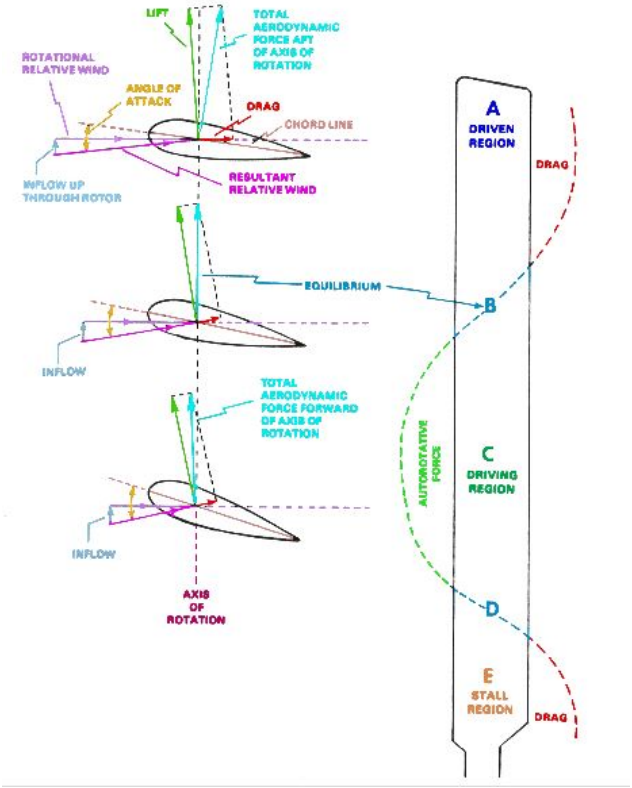

Figure 5.2: Force vectors in a vertical Auto rotative descent

The force vectors are different in each region, because the rotational relative wind is slower near the blade root and increases continually toward the blade tip. When the inflow up through the rotor combines with rotational relative wind, it produces different combinations of aerodynamic force at every point along the blade.

A constant rotor RPM is achieved by adjusting the collective pitch control so blade acceleration forces from the driving region are balanced with the deceleration forces from the driven and stall regions.

Vertical Autorotation

Autorotative force in forward flight is produced in exactly the same manner as when the helicopter is descending vertically in still air. However, because forward speed changes the inflow of air up through the rotor disk, the driving region and stall region move toward the retreating side of the disk where angle of attack is larger:

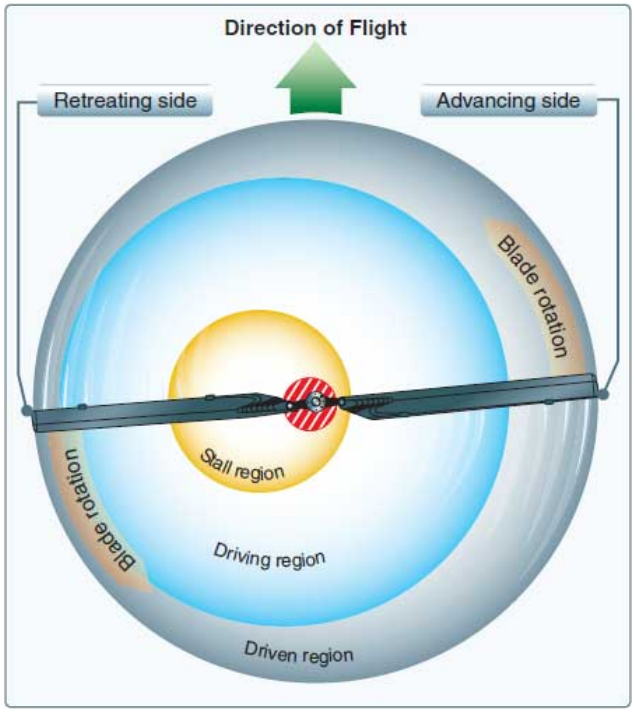

Figure 5.3: Aerodynamic regions of the Auto rotation system

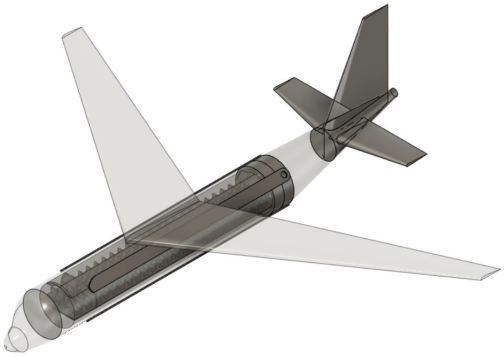

Figure 5.4: Three dimensional view highlighting the active aeroplane parts of the Auto-rotation mechanism

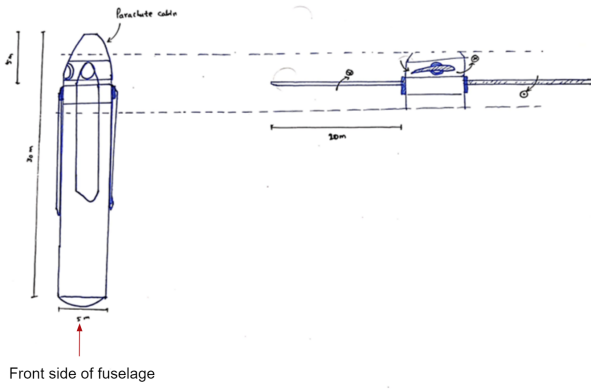

Figure 5.5: Side view depicting the pre deployment and post deployment stages

Chapter 6

Fuselage and tail sizing

In this section, we present the design features of the fuselage, preliminary sizing of the horizontal and vertical tails i.e. choice of aspect ratio, taper ratio, sweep and airfoil selection and the engine location with details on the landing gear system.

6.1 Fuselage sizing:

The main role of the fuselage is to hold the payload and provide structural integrity to the aircraft. As our aircraft is a passenger airliner, our main payload is live payload i.e. people.
Along with this payload, the fuselage also has accommodates the following:

1. The flight crew and the cabin crew in the transport airplane and the specialist crew members in airplanes used for reconnaissance, patrol and remote sensing.
2. Fuel, engine and landing gear when they are housed inside the fuselage.
3. Systems like air conditioning system, pressurization system, hydraulic system, electrical system, pneumatic system, electronic systems, emergency oxygen, flotations vests and auxiliary power units.

6.1.1 Features of the fuselage:

The following designs have been done based on the data of similar airplanes and the ideal design restrictions given in references. The major portion of the cabin is in the mid-fuselage which has a constant cross section(including the blades width that are inserted into the mid-fuselage section). The cruising altitude for our aircraft is 10.5 km. To account for the low pressure at such a high altitude we maintain a pressure corresponding to 8000 ft(2438 m) in ISA in these portion of the fuselage. The auxiliary power unit(APU) supplies power to start the main engine and will power the initial rotation of the blades in the auto-rotation system. All the air conditioning, pressurization, electrical, electronic, hydraulic, pneumatic and other systems are placed under the floor of the cabin.
Now, as shown in fig 6.1, the blades of the auto-rotation part is designed so as to get inserted into the mid-fuselage. The length of these blades as shown in the design is 20m. The calculations on how did we get this length is shown in a later chapter.
The Top view is designed to accommodate two classes of passengers: Economy and First class. Economy class has around 132 seats divided into 22 sets of 6 seats each, with aisle dividing this 6 seats. The First class sets are 8 in number and design in the fashion shown in the figure.

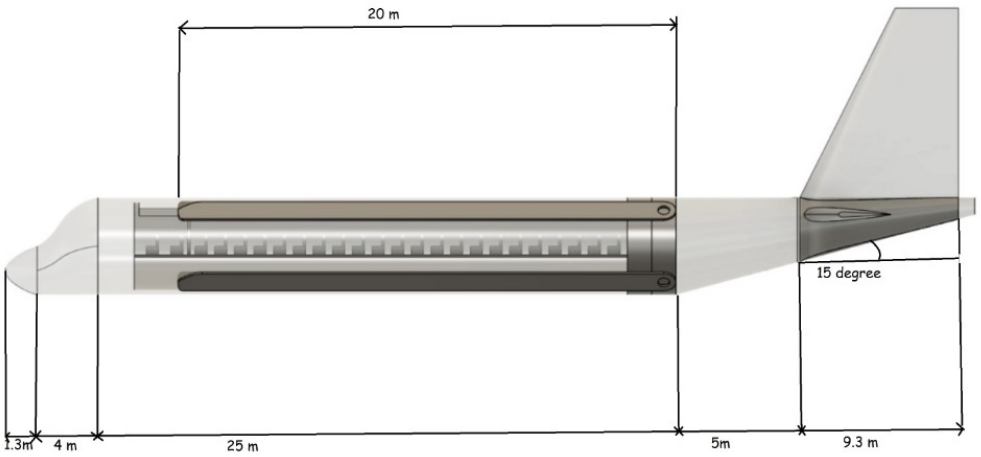

Figure 6.1: Side view of the fuselage

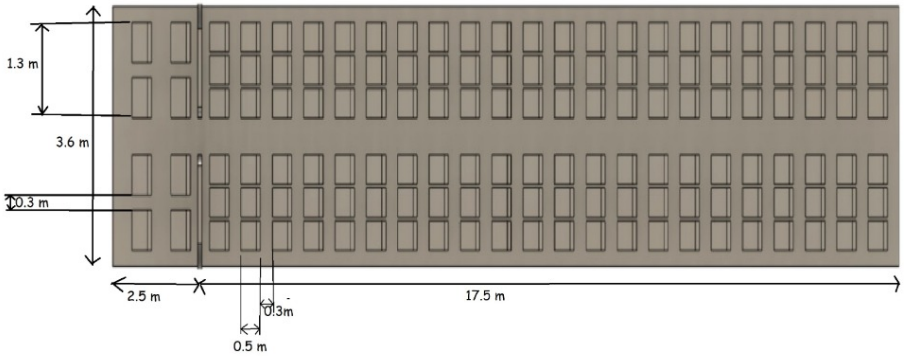

Figure 6.2: Top view of the fuselage

6.1.2 Seating arrangements:

The cross section designed based on designs of similar aircrafts is shown below in fig 6.4.
Seat pitch: It is the distance between the back of one seat to the back of the next seat. It includes the seat length and the leg room. From fig 6.2 we can see this length to be 0.3 m. The terms swat width, aisle width, elbow gap, gap between seat and wall of cabin, head room, aisle height, cabin width and fuselage width are shown in the figure 6.3
The cross sections designed for the aircraft are shown in fig 6.4

As mentioned before, we are having two types of seating arrangement first class and economy class. The dimensions of seat width, seat pitch and aisle width are higher for the first class than the economy.The maximum seating capacity for the aircraft is:
Total = (pilots + crew) + first class + economy class

$$\Rightarrow Total = (2 + 4) + 8 + 132 \tag{6.1}$$

$$\Rightarrow Total = 146$$

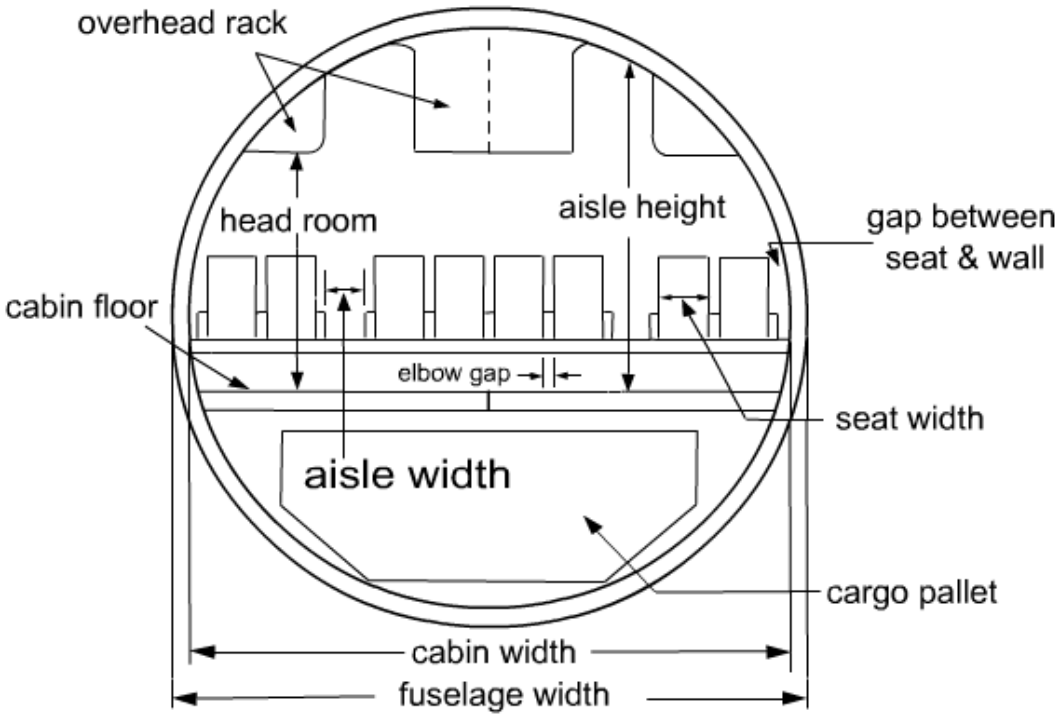

Figure 6.3: Terminology

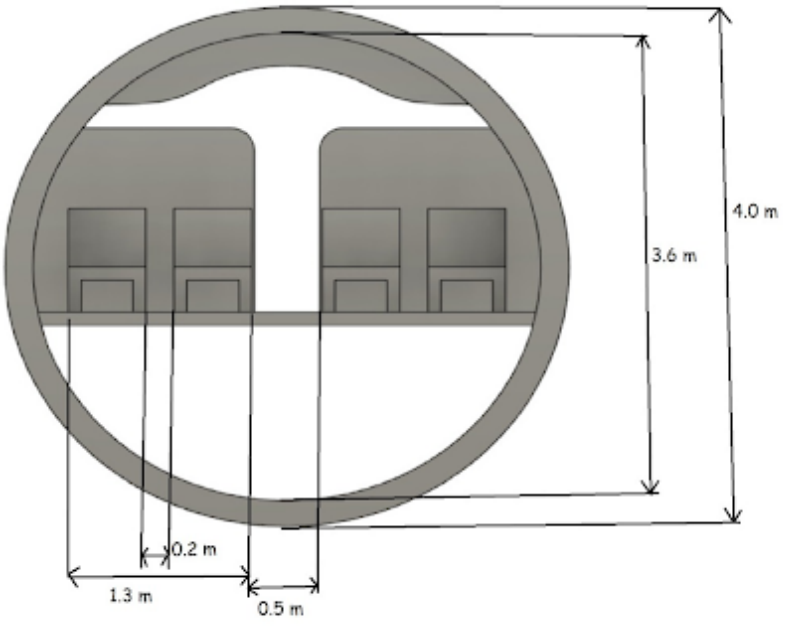

Figure 6.4: First Class

The pitch of seats typically lie between 0.76 m to 0.81 m for economy and 0.97 to 1.02 m for first class seating arrangement. This aircraft has economy pitch length equal to 0.8 m and first class pitch length equal to 1.0 m. The aisle width should be greater than 0.3 m for economy class; between 0.46 to 0.51 m for business class and between 0.51 to 0.71 m for first class seating arrangement. Our aircraft has aisle width equal to

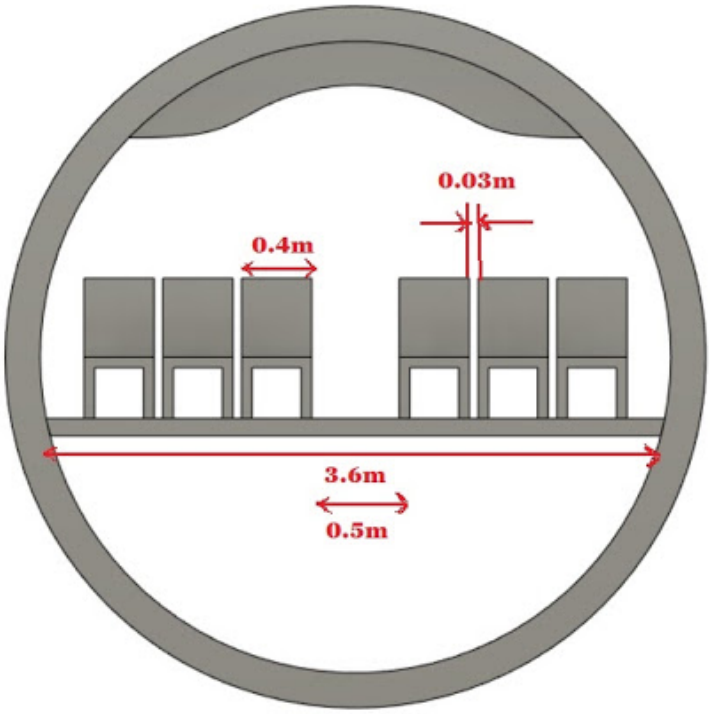

Figure 6.5: Economy class

0.5 m for both first class and economy class. The aisle height should be between 1.5 - 1.93 m. The value for this aircraft is 1.8 m as the cabin floor is placed symmetrically along the horizontal diameter of the cabin. The elbow rest is of length 0.03 m and 0.2 m respectively for economy and first, as shown in the figure 6.4 and 6.5.
The cabin width is arrived at considering W_{cer}(width of the cabin a the level of elbow rest), head room, aisle height, height of seat above cabin floor and shape of cabin.
Cargo volume: From reference[12], we get that the cargo colume should be approximately 0.442 m^3(15.6 ft^3) for long range airplanes.

$$\Rightarrow 0.442 \times 140 = 61.88m^3$$

Thickness of cabin: The thickness is between 6.2 to 10 cm (2.5 to 4 inches) for the fuselage with the two and three abreast seating arrangement respectively. We take the thickness to be 0.2 m to account for the additional insertion of the blades of autorotation system. This number is an initial guess.
Tail cones/ rear fuselages: Further, in the case of a passenger airplane the mid fuselage has a cylindrical shape and is followed by the tail cone or rear fuselage of a tapering shape.In passenger airplanes the tail cone is of substantial length and the cabin layout extends into the rear fuselage.The rear fuselage also supports the horizontal and vertical tail surfaces and the engine installation for rear mounted engines. The lower side of the rear fuselage should provide adequate clearance (about 0.15 m) for airplane during take-off and landing attitudes. Typically the ratio of the length of the rear fuselage to the equivalent diameter of the mid-fuselage is in between 2.5 - 3.6[1].Also the upsweep angle of the rear fuselage is between 15 to 20^o[2]

$$length_{rear} = ratio \times diameter_{(mid-fuselage)}$$

$$\Rightarrow length_{rear} = 3.6 \times 4m = 14.4m$$

[1]reference [11],chapter 6
[2]reference [11] chapter 6

6.2 Preliminary horizontal and vertical tail sizing:

The horizontal and vertical tails are designed to provide stability; the movable surfaces on tails namely elevator and rudder provide control. The complete design of tail surfaces requires information on location of the centre of gravity (c.g.)of airplane, shift in c.g. location during flight and the desirable level of stability. However, to obtain the c.g. location, the weights of horizontal and vertical tails are needed which depend on their size.A conventional tail arrangement is chosen.

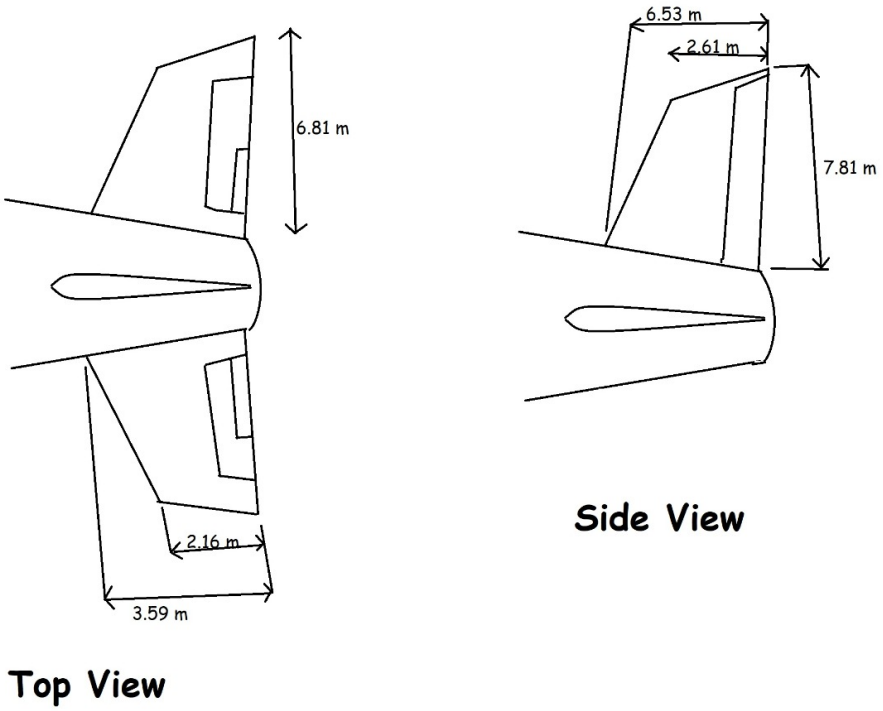

Figure 6.6: Tail layout

6.2.1 Choice of aspect ratio for horizontal tail:

The aspect ratio affects lift curve slope ($C_{L\alpha}$), induced drag coefficient (C_{Di}) and the structural weight.The purpose of the horizontal tail is to provide stability about Y-axis and the elevator provides control about the Y-axis. The lift and drag produced by the horizontal tail are much smaller than those produced by the wing. Consequently, while choosing aspect ratio of the horizontal tail, the reduction of structural weight is accorded more importance than the reduction of drag. Further, the structural weight decreases as aspect ratio decreases. Hence, the aspect ratio of the horizontal tail is lower than that of the wing. A value of aspect ratio between 3 to 5 is commonly used for subsonic airplanes.[3] The actual value of the aspect ratio would be a compromise between effects of aspect ratios on $C_{L\alpha}$, C_{Di} and the structural weight. The value of aspect ratio from data of similar aircrafts is 4.737 which is between the given range.

6.2.2 Choice of taper ratio for horizontal tail

the taper ratio influences induced drag, structural weight and ease of fabrication.For the high subsonic airplanes with swept wings having around 0.2, the horizontal tail has a taper ratio between 0.3 to 0.6[4]. From data of similar aircrafts the chosen value of taper ratio is 0.6.

[3] references[2]
[4] reference [2]

6.2.3 Choice of sweep for horizontal tail

In the case of high subsonic airplanes the tail should have a value of drag divergence Mach number(M_D) equal to higher than that of the wing. Hence, the sweep angle of the horizontal tail is equal to that of the wing or slightly higher($+ 5^o$)[5]. The chosen value from data of similar aircraft is 35^o

6.2.4 Airfoil selection for horizontal tail

For airplane flying at high subsonic Mach numbers, the drag divergence Mach number of the tail should be higher than that of the wing. A symmetrical airfoil with (t/c) of 90 % of the (t/c) of the wing can be a rough guideline for preliminary design purpose. So we choose NACA 0012 which is symmetrical and has t/c $0.12 \approx 90\%$ of 0.14 (wings thickness ratio)

6.2.5 Choice of aspect ratio for vertical tail

The aspect ratio of the vertical tail is defined as:

$$AR_{vt} = \frac{h_{vt}^2}{S_{vt}}$$

where, h_{vt} and S_{vt} are the height and area of the vertical tail respectively.
The subsonic airplanes with conventional tails have AR_{vt} between 1 to 2 from ref[6]. With this restriction and referring data of similar aircrafts we have AR_{vt} equal to 1.71.

6.2.6 Choice of taper ratio for vertical tail

A low value of λ reduces structural weight, a value of λ between 0.3 and 0.6 results in low value of induced drag and $\lambda = 1$ results in lower cost of fabrication. As a compromise a $\lambda = 0.3$ to 0.6 is chosen for subsonic airplanes with conventional tails[7]. The λ we get from data of similar aircrafts is 0.303.

6.2.7 Choice of sweep for vertical tail

In case of high subsonic airplanes the vertical tail should have a drag divergence Mach number equal to or higher than that of the wing. In case of high subsonic airplanes the sweep angle of vertical tail would be equal to or more than that of the wing. So our value of 35^o holds fine.

6.2.8 Airfoil selection for vertical tail

As discussed earlier horizontal and vertical tails employ a symmetrical airfoil.The same arguments stand for vertical tail as given earlier for horizontal one, hence NACA 0012 is the airfoil chosen here as well.

[5]reference[2]
[6]reference[11
[7]reference[11]

6.2.9 Other important parameters:

Some of the important parameters that decide the aerodynamic characteristics of the tail are area ratios $\frac{S_h}{S}$ and $\frac{S_v}{S}$, tail volume ratios(V_H and V_V), tail arm and tail span. All these parameters need to be decide for both the horizontal and vertical tails.
From the data of similar airplanes, the following values are chosen.

Parameter	Horizontal tail	Vertical tail
Area ratio($\frac{S_h}{S}$ and $\frac{S_v}{S}$)	0.253	0.176
Aspect ratio	5	1.82
Taper ratio	0.256	0.303

The areas of the horizontal and vertical tails($\frac{S_h}{S}$ and $\frac{S_v}{S}$) are:

$$S_h = 0.253 \times 185 = 46.805m^2$$
$$S_v = 0.176 \times 185 = 32.56m^2$$

The spans of the horizontal and vertical tails(b_h and b_v) are:

$$b_h = \sqrt{AR_h S_h} = \sqrt{5 \times 46.805} = 15.3m$$
$$b_v = \sqrt{AR_v S_v} = \sqrt{1.82 \times 32.56} = 7.7m$$

The chord lengths of the horizontal and vertical tails are:

$$c_{rh} = \frac{2S_h}{b_h(1+\lambda_h} = \frac{2 \times 46.805}{15.3 \times (1+0.256)} = 4.871m$$

$$c_{rv} = \frac{2S_v}{b_v(1+\lambda_v} = \frac{2 \times 32.56}{7.7 \times (1+0.303)} = 6.49m$$
$$c_{th} = \lambda_h c_{rh} = 0.256 \times 4.871 = 1.247m$$
$$c_{tv} = \lambda_v c_{rv} = 0.303 \times 6.49 = 1.966m$$

Tail arm:
Tail arm is the distance between the aerodynamic center of the wing and the aerodynamic center of horizontal tail (l_h) or vertical tail(l_v). The values of the tail arm are chosen based on the data collection[8] as :
$l_h = 0.5 \times l_h$ and $l_v = 0.45 \times l_h$ i.e.

$$l_h = 0.5 \times 44.6 = 22.3m$$
$$l_v = 0.45 \times 44.6 = 20.07m$$
$$V_h = \frac{S_h l_h}{S\bar{c}} = \frac{46.805 \times 22.3}{185 \times 4.29} = 1.315$$
$$V_v = \frac{S_v l_v}{Sb} = \frac{32.56 \times 20.07}{185 \times 43} = 0.082$$

[8] Reference[2]

6.3 Engine location

The number of engines and their location need to be chosen.The following considerations decide the number of engines used in the airplane.
(a) The ratings of the available engines.
(b) Cost of the engine.
(c) Ease of maintenance
(d) Performance and stability of the airplane with one engine being inoperative.

6.3.1 Engine Selection

The transport airplanes have two or more engines from the considerations of safety in the event of failure of one engine. Since our aircraft is transport airplane where range of passengers aircraft is able to carry is 100-200, **Twin engine** and from data of similar airplanes **Rolls Royce Trent 1000 Turbofan engine** is suitable choice for our airplane.
In the twin engine passenger airplanes with jet engines, the engines are located on **pylons on the wings**.

Figure 6.7: Engines held by pylons on wing

The advantages are as follows:

1. The engines act as a relieving load on the wing and the weight of the wing structure could be decreased by about 15 percent.
2. The space inside the wing can be fully utilized for fuel.
3. Easy access for maintenance, inspection and replacement of engines.

The disadvantages are as follows:

1. Smaller ground clearance increases the possibility of foreign objects being ingested in the engines.
2. Failure of outboard engine creates a large yawing moment. To counteract this moment requires larger vertical tail area and rudder deflection as compared to other locations of engines. These result in higher structural weight and drag.

6.3.2 Span-wise locations of wing mounted engines

A wing mounted engine acts as a relieving load. The reason for this is as follows.The structural design of wing is carried out considering mainly the load due to lift produced. In normal configuration the lift acts upwards. The weights of (a) fuel in the wing, (b) the engines attached to wing.
Thus, the bending moment produced due to the lift is reduced due to weights of fuel, engines etc. Hence, the weights of these items are called relieving weights. This also indicates that an engine located near the wing tip would cause maximum reduction in bending moment. However, there is another consideration for the spanwise location of the engine. This is due to effect on directional control when one engine fails. When all the engines (2 or 4) are operating, they do not produce any yawing moment. When one of the engines fails, the operating engine on the other wing half produces a yawing moment. This moment is balanced by a suitable deflection of rudder. In this situation, an engine located far outboard would require a large vertical tail and rudder deflection. This would increase overall weight and drag of the airplane. Hence, there is an optimum spanwise location for the engines which will minimise the overall weight and drag.
From the data on twin engined turboprop airplanes in Table 6.2, it is observed that the wing has constant chord upto 25 percent to 35 percent of the semispan. The engine nacelle is located such that it either starts or ends at this location.
Length of the engine = 4.738m
Width of the engine = 2.85m
Weight of the engine = 6,120kg
The engine nacelle is located such that its spanwise extent ends at 35 percent of wing semispan.**Spanwise location of the engine is 15.05 m from the fuselage reference line**

6.4 Fuel System

The fuel system includes fuel tanks, fuel pumps, fuel lines, vents and fuel flow controls. The fuel tanks are of three types.They are:
(a) Discrete (b) bladder and (c) integral.
Bladder tanks consist of rubber bags inserted into the space available for storage of fuel. They are also self sealing if a bullet pierces the tank; the rubber fills in the hole and prevents large loss of fuel and fire hazard. Because of these advantages of bladder tanks **We are using Bladder tanks as fuel tank for our aircraft**.

Calculation of fuel required for fuel.
for endurance of 6 hours with constant speed, fuel weight required = 29120 kg
Density of fuel = 800 kg/m^2
Volume of fuel = 23.296 m^3
Total volume for fuel system in wing is 30.25m(considering space available for fuel is 77 percent of available space in wing)

6.5 Landing gear

The following three types of landing gears are mainly used on airplanes:

1. Tricycle or nose wheel type
2. Tail wheel type
3. Bicycle with out trigger wheels on wings

Tricycle type or nose wheel landing gear are being used in our aircraft.This is the most commonly used landing gear. The nose wheel is near the nose of the fuselage and the two wheels located on the wings, in this case, form the tricycle arrangement.The main wheels and nose wheel are located such that they share roughly 90% and 10% of the airplane weight. The nose wheel is generally steerable.
b = 43m and l_f = 45m
From data of similar aircrafts,
(wheel track/b) = 0.15 and
(wheel base/l_f) = 0.39 $\Rightarrow$ Hence, wheel base = 15.57m, wheel track = 9.82m

Chapter 7

Weights and center of gravity

The weight of an airplane changes due to consumption of fuel and dropping off / release of armament or supplies. The payload and amount of fuel carried by the plane may vary from flight to flight. such factors lead to change the location of the center of gravity(c.g.) of the airplane. Stability and controllability of the airplane is affected by the shift in the c.g. location of the airplane. Hence, in this chapter we will deals with the methods to obtain the weights of various components of the airplane and calculation of the c.g location under various operating conditions. The weight of entire airplane can be sub divided into empty weight and useful load. The empty weight can be further subdivided into weights of :

1. Structures group
2. Propulsion group and
3. Equipment group

7.1 Estimation of airplane weight:

These are the two following methods of estimating the weight of an airplane:

1. Approximate group weight method.
2. Statistical group weights method

7.1.1 Approximate group weights method:

Based on trends in the data of weights of major components Ref.12, chapter 15 gives the weights of wing, fuselage, tails, landing gear, engine and other items in terms of the parameters relevant to the component(Table 7.1). The approximate location of c.g of each of these items is also given in Table 7.1.
A rough e.g. estimate is done with a crude statistical approach as provided in Table 7.1.
The wing and tail weights are determined from historical values for the weight per square foot of exposed planform area. The fuselage is similarly based upon its wetted area. The landing gear is estimated as a fraction of the takeoff gross weight. The installed engine weight is a multiple of the uninstalled engine weight. Finally, a catch-all weight for the remaining items of the empty weight is estimated as a fraction of the takeoff gross weight. This technique also applies the approximate locations of the component e.g. as given in Table 7.1. The resulting e.g. estimate can then be compared to the desired e.g. location with respect to the wing aerodynamic center. Also, these approximate component weights can be used as a check of the more detailed statistical equations provided below

7.1.2 Statistical group weights method

Deals with the estimation of weights of individual components. An expression for the weight of a specific airplane component is obtained, based on statistical data on similar airplanes. The expression involves the geometrical parameters and other features of the component.

Item	General Aviation	Multiplier	Approximate c.g. location
Wing	12*	$S_{exposed}$ m^2	40% MAC
Horizontal tail	10*	$S_{exposed}$ m^2	40% MAC
Vertical tail	10*	$S_{exposed}$ m^2	40% MAC
Fuselage	7*	S_{wetted} m^2	40-50% length
Landing gear	0.057	TOGW	-
Installed Engine	1.4	engine weight	-
All-else empty	0.10	TOGW	40-50% length

Table 7.1: For different type of Aircrafts approximate location of c.g. of each items
*The value is in kgf/m^2, when multiplied by the appropriate area in m^2, the weight of the component is obtained in kgf.
$ 15% of this weight is allocated to the nose gear and 85% to the main gear.

7.2 Estimation of the component weights and c.g. locations:

The aim of estimating the weights of individual components and their c.g. is to obtain the location of the c.g. of the airplane. Then, the shift in the airplane c.g. is examined under various conditions like (a) with full fuel and full payload (b) with full payload and reserve fuel (c) with partial payload and full or reserve fuel etc. We will be using approximate group weights method for the estimation of the weight of each component of the airplane. The weights and c.g. locations of various components are estimated below:

7.2.1 Wing

from similar aircraft data:
Wing area = 185.11 m^2
Root chord of wing = 7.5 m
Tip chord of wing = 2 m
Wing span = 43 m
semispan = 21.5 m
Mean aerodynamic chord = 4.72 m(calculated by using the formula for mac)
wing area(exposed) = 185.11
Location of the leading edge of mean aerodynamic chord(m.a.c.) from the leading edge of wing = 5.092 m (from known distances and geometry)
Location at the a.c. of the wing from the wing root chord = 6.272

Using Table 7.1, the estimated weight of the wing is : 185.107*12 = 2221.32 Kgf

Or
W_{Wing}/W_g = 0.019 = 1.9 % of W_g

From Table 7.1, the c.g. of wing is at 40 % of m.a.c.
Hence, the location of the c.g. of wing from the leading edge of the root chord of the wing is at: 5.092 + 0.4 x 4.720859 = 6.98 m

7.2.2 Horizontal Tail

The horizontal tail is mounted on V.tail. Hence, its exposed area is taken roughly equal to planform area which equals 46.805 m^2.
Hence, weight of h.tail = 46.805 x 10 = 468.05 kgf = 0.41 % of W_g
Mean aerodynamic chord of Horizontal tail = 3.417 m.(calculated by using the formula for mac)
The distance between the leading edge of the root and the leading edge of m.a.c. is 2.149 m(from known distances and geometry)
From Table 7.1, the c.g. of the h.tail is at 40 % of its m.a.c. Consequently, the distance between the leading

edge of the root chord of h.tail and the c.g. of h.tail is : 2.149 + 0.4 x 3.4168 = 3.516 m

7.2.3 Vertical Tail

Area of Vertical tail = 32.56 m^2
Hence, weight of v.tail = 32.56 x 10 = 325.6 kgf = 0.28 % of W_g.
Data required to arrive at the location of the c.g. of the vertical tail:
Mean aerodynamic chord of vertical tail = 4.631 m.(calculated by using the formula for mac)
The distance between leading edge of the root chord of v.tail and leading edge of m.a.c. = 2.215 m(from known distances and geometry).
From Table 7.1 the c.g. of vertical tail is at 40 % of its m.a.c. Consequently, the distance between the root chord of vertical tail and c.g. of vertical tail is : 2.215 + 0.4 x 4.6315 = 4.068 m.

7.2.4 Engine

From similar aircraft data, the weight of each engine is 6120 kgf.
Hence, from Table 7.1, the installed weight of the two engines is : 2 x 1.3 x 6120 = 17136 kgf = 15 % of W_g
Engine length = 4.738 m.
distance between the inlet of the engine and the leading edge of the root chord = 0.903 m.(from similar aircraft data)
Taking c.g. of engine to be at 40 % of engine length, the location of engine c.g. from the leading edge of the wing is : -0.903 + 0.4 x 4.738 = 0.992 m.
c.g. of the engine is 0.992 m behind of the leading edge of the root chord of the wing.

7.2.5 Landing Gear

From Table 7.1 the weight of the nose wheel plus the main landing gear is 5.7 % of W_g i.e. 0.057 x 114196.5 = 6509.198 kgf.
Out of this total weight, the nose wheel and main wheel account for 15 % and 85 % respectively. Hence, nose wheel weighs 0.15 x 6509.198 = 976.379 kgf and the main wheels weigh 0.85 x 6509.198 = 5532.82kgf.
Wheel base = 15.57 m.
As regards the locations of the C.G.s of nose wheel and main wheels, it is recalled that the nose wheel and main wheels share respectively 10 % and 90 % of the airplane weight.
From similar aircraft data the Wheel base is 15.57 m, Hence, the c.g. of the nose wheel is 0.9*15.57 = 14.013 m ahead of the C.G. of the airplane.
The C.G. of the main wheels, as a group, is = 0.1×15.57 = 1.557 m behind the c.g. of the airplane.

7.2.6 Fuselage and systems

Different section of fuselage are analysed separately in order to get the wetted are of the fuselage.

Nose portion

Length of nose = 1.3 m.
Diameter at the end of nose = 2 m.
average diameter = 1 m.
Wetted area or surface are of nose ≈

$$\pi \times 1 \times 1.3 = 4.084 m^2.$$

Cockpit portion

Length of cockpit = 4 m.
Diameter at the end of cockpit = 4 m.
Hence, wetted are of cockpit portion

$$\approx \pi \times (\frac{1+4}{2}) * 4 = 37.7m^2.$$

Midfuselage portion

Length of midfuselage = 25 m
Diameter of midfuselage = 4 m
Hence, wetted area of midfuselage = $\pi \times 4 \times 25 = 314.160\ m^2$

Tail cone

Average diameter = 4/2 = 2 m
Length of tail cone = 14.3 m
Hence, wetted area of tail cone ≈

$$\pi \times 2 \times 14.3 = 89.849m^2.$$

Consequently, wetted area of fuselage is : 4.084+37.7+314.107+89.849 = 445.792 m^2
Using value in Table 7.1, the weight of fuselage is : 445.792× 7 = 3120.544 kgf = 2.73 % of W_g.

Computation of the Weight of fuselage, along with furnishing etc., and the systems :

$$\frac{W_{fuselage} + W_{System}}{W_g} = \frac{W_{empty}}{W_g} - \left(\frac{W_{wing}}{W_g} + \frac{W_{H.tail}}{W_g} + \frac{W_{V.tail}}{W_g} + \frac{W_{Engine}}{W_g} + \frac{W_{LandingGear}}{W_g}\right)$$

$W_{empty}/w_g = 0.5147$

Hence,

$$\frac{W_{fuselage} + W_{System}}{W_g} = 0.5147 - (0.019 + 0.004 + 0.003 + 0.15) = 0.281$$

Now,

$W_{fuselage} + W_{system}$ = 114196.5×0.281 = 32122.19912 kgf

From Table 7.1, the c.g. of the fuselage and systems can be taken to be at 0.45 l_f or 0.45 x 48 = 21.6 m from the nose of the fuselage.

7.2.7 Fuel

W_{fuel}/W_g= 0.255
Mass of the fuel = 114196.5×0.255 = 29120 kgf
Density of the fuel = 0.8 kg/m^3
Volume of the fuel = 36400 m^3

Fuel is stored in the wing, so the c.g. of fuel can be taken at the same location as the c.g. of the wing. As

mentioned earlier, the c.g. of the wing is at 6.980 m behind the leading edge of the root chord of the wing. c.g. of the fuel is at 6.980 m behind the leading edge of the root chord of the wing.

7.2.8 Payload and crew

Payload and crew are generally clubbed together fro passenger airplanes.In general aviation aircraft flight crew is separately considered.
The weight of the crew and payload is 30000 kgf. The c.g. of these items is taken in the middle of the passenger cabin.
From figure 6.1 this location is :
$1.3 + 4 + (\frac{25+2.5}{2}) = 19.05$ m from the nose of the fuselage.

7.3 Determination of wing location and c.g. of the airplane

The position the wing is chosen such that the c.g. of the entire airplane with the gross weight is at 25 % of the mean aerodynamic chord of the wing. Before arriving at the location of wing which satisfies this condition, the following points are noted :

- The distance of the leading edge of the root chord of the wing from the nose of the fuselage is denoted by x.
- The 25 % of the mean aerodynamic chord (m.a.c.) of wing is 6.272 m behind x. Hence, the chosen location of the c.g. of the entire airplane is at (x + 6.272) m from the nose of fuselage.
- The c.g. of the wing, as calculated in section 7.2.1 is at : (x + 6.980) m
- The c.g. of the two engines as mounted on the wings, and as calculated in section 7.2.4 is at : (x + 0.992) m.
- The c.g. of the fuel, as mentioned in section 7.2.7 is at : (x + 6.980) m.
- The tail arm of the horizontal tail i.e. the distance between the aerodynamic center(a.c.) of the wing and the a.c. of Horizontal tail is 18.78 m.
  Further the c.g. of the Horizontal tail is at 40 % of its mean aerodynamic center(m.a.c.) and the m.a.c. being 3.4168 m. Hence, the location of the c.g. of the h.tail is at : x + 6.272 + 18.78 + (0.4 0.25) x 3.416 = (x + 25.564) m.

  In a similar manner, noting that the tail arm of vertical tail is 17.6 m and it's m.a.c. is 4.631 m, the location of the c.g. of vertical tail is at : x + 6.272 + 17.6 + (0.4 0.25) x 4.631 = (x + 24.567) m.
- The nose wheel and main wheels, as mentioned in section 7.2.5, are respectively 14.013 m ahead and 1.557 m behind the c.g.
  Hence, the c.g. of nose wheel is at : x + 6.272 14.013 = (x 7.741) m
  The c.g. of the main wheels, taken together is at : x + 6.272 + 1.557 = (x + 7.829) m.
- The fuselage plus the systems as a unit have the c.g. at 21.6 m from the nose of fuselage (section 7.2.6). The full payload plus the crew together have the c.g. at 19.05 m from the nose of the fuselage (section 7.2.8).

The weights of various items and their c.g. locations are presented in Table E 8.1a

To satisfy the choice, that the c.g. of the entire airplane is at 0.25 $\bar{c_w}$, leads to the following equation : 114196.5(x + 6.272) = 55780.13 x + 1556839)

item	**W (kgf)**	**X (m)**	**W.x (kgf-m)**
Wing	2221.283	x + 6.980	2221.283 x + 15505.32
Engines	17136	x + 0.992	17136 x + 17002.339
Fuel	29120	x + 6.980	29120 x + 203267.617
H.tail	468.05	x + 25.565	468.05 x + 11965.574
V.tail	325.6	x + 24.567	325.6 x + 7998.996
Nose wheel	976.379	x 7.741	976.379 x - 7557.945
Main wheel	5532.818	x + 7.829	5532.818 x + 43317.622
Fuselage+System	32122.2	21.6	693839.5
Payload + crew	30000	19.05	571500
			$\Sigma W_i x_i$ = 55780.13 x + 1556839
Airplane with c.g. at 0.25 $\bar{c_w}$	114196.5	x + 6.272	

Table 7.2: c.g. locations and weights of various components of airplane
X = location of c.g. of various components from nose

Or

$$x = \frac{155689 - 6.272 \times 114196.5}{114196.5 - 55780.13} = 14.389m.$$

Hence, the C.G. of the airplane is at : 14.389 + 6.272 = 20.662 m from the nose of the fuselage.

7.4 Calculation of C.G. location and C.G. shift

At this stage of the preliminary design, the lay-outs of fuselage with tail surfaces, payload and equipment are approximately known. The weights of these items has been calculated already using Table 7.1. Subsequently, the c.g locations of these items are also assigned. This group may be called fuselage group. Similarly the weights of items mounted on the wing (e.g. engines, fuel and landing gear) are already known.The C.G. locations of these items can also be assigned. This group may be called wing group.
Based on these data a balance table as shown in Table 7.3 is prepared :

item	W (kgf)	X (m)	W.x (kgf-m)
Wing	2221.283	21.370	47468.254
Engines	17136	15.382	263579.098
Fuel	29120	21.370	622286.945
H.tail	468.05	39.954	18700.533
V.tail	325.6	38.956	12684.184
Nose wheel	976.379	6.649	6491.572
Main wheel	5532.818	22.219	122931.553
Fuselage+Sys	32122.2	21.6	693839.520
Payload + crew	30000	19.05	571500
			$\Sigma W_i x_i$ = 2359481.659

Table 7.3: Weights and C.G. locations of each component(Balance Table)

X = location of C.G. of various components from nose

7.4.1 C.G. shift for different loading conditions

To carry out these calculations, the balance table with x = 14.389 m is presented as table 7.3. number of crew members(including pilots) = 6
number of total passengers = 140
Weight of 140 passengers = 30000-480 = 29520 kgf
weight of crew members + pilots = 480 kgf

Case (a) Full payload, but no fuel

In this case, the values from Table 7.3 are : W = 114196.5 29120 = 85076.5 kgf It may be added that the weight and moment due to trapped fuel is ignored. $\Sigma W.x = 2359481.659 - 622286.945 = 1737194.714 kgf - m$
Hence, C.G. location in this case is at : 1737194.714 / 85076.5 = 20.419 m
Hence, C.G. shift as fraction of $\bar{c}_W = (20.419 - 20.662)/4.721 = -5.14$ % of $\bar{c}_W$
Or the C.G. is at $0.198\bar{c}_W$

Case(b) No payload and no fuel

It may be noted that, while calculating C.G. location with W = Wg, the weights of passangers and crew were clubbed togather. However, for no payload case only the weight of passangers is considered as payload. In this case :
$W = 114196.5 - 29120 - 29520 = 55556.5 kgf$
$\Sigma W_i x_i = 2359481.659 - 622286.945 - (19.05 x 29520) = 1174838.714 kgf - m$
Hence, C.G. is at = 1174838.714 / 55556.5 = 21.147 m
Or C.G. shift as fraction of $\bar{c}_W = (21.147 - 20.662)/4.721 = +10.268$ % of $\bar{c}_W$
Or the C.G. is at $0.353\bar{c}_W$

Case (c) No payload but full fuel

In this case :
$W = 114196.5 - 29520 = 84676.5 kgf$
$\Sigma W_i x_i = 2359481.659 - (19.05 \times 29520) = 1797125.659 kgf - m$
Hence, C.G. is at = 1797125.659 / 84676.5 = 21.223 m
Or C.G. shift as fraction of $\bar{c}_W = (21.223 - 20.662)/4.721 = +11.89$ % of $\bar{c}_W$
Or the C.G. is at $0.369\bar{c}_W$

Case (d) Full fuel but with half of passengers in front half of passenger cabin

The weight of passengers is 29520 kgf
Half of this would be 14760 kgf
To obtain the C.G. of the airplane in this case, it is considered that the rear half of the passenger cabin is empty. The C.G. of this (rear half of passenger cabin) is at 1.3 + 4 + (25 + 2.5) x 0.75 = 25.925 m
Hence, in this case,
$W = 114196.5 - 14760 = 99436.5 kgf$
$\Sigma W_i x_i = 2359481.659 - (14760 \times 25.925) = 1976828.659 kgf - m$
Hence, C.G. is at = 1976828.659 / 99436.5 = 19.880 m
Or C.G. shift as fraction of $\bar{c}_W = (19.880 - 20.662)/4.721 = -16.56$ % of $\bar{c}_W$
Or the C.G. is at $0.084\bar{c}_W$

Case (e) Full fuel but with half of passengers in rear half of passenger cabin

In this case W = 99436.5 kgf
It is considered that the front half of passenger cabin is empty.
The C.G. of the front half of passengers cabin is at : 1.3 + 4 + (25 + 2.5) x 0.25 = 12.175 m
Consequently,
$\Sigma W_i x_i$= 2359481.659 14760 x 12.175 = 2179778.659 $kgf - m$

Hence, $x_{cg} = 2179778.659 \ / \ 99436.5 = 21.921$ m Or C.G. shift as fraction of $\bar{c}_W = (21.921 - 20.662)/4.721 = +26.67$ % of $\bar{c}_W$
Or the C.G. is at $0.517\bar{c}_W$

The cases (d) and (e) result in large shift of C.G. They are hypothetical cases. These are avoided by alloting the window seats first, then aisle seat and later the rest.
The first three cases cause C.G. travel between $0.198\bar{c}_W$ and $0.369\bar{c}_W$ or C.G. shift ΔC.G. $= 0.171\bar{c}_W$

Chapter 8

Cross-checks on design of tail surfaces

8.1 Introduction

The ability of a vehicle to maintain its equilibrium is termed stability and the influence which the pilot or control system can exert on the equilibrium is termed its controllability. The basic requirement for static longitudinal stability of any airplane is a negative value of dC_{mcg}/dC_L. Dynamic stability requires that the vehicle be not only statically, but also that the motions following a disturbance from equilibrium be such as to restore the equilibrium. Even though the vehicle might be statically stable, it is possible that the oscillations following a disturbance might increase in magnitude with each oscillation, thereby making it impossible to restore the equilibrium.
The topics dealt within this chapter are based on the following two observations:

1. For conventional subsonic airplanes, if the airplane has adequate level of static stability, then it would have reasonable dynamic stability.

2. If the area of the control surfaces are adequate to trim the airplane(i.e. bring the moments about the three airplane axes to zero) in certain critical conditions, then the airplane would have reasonable level of controllability.

Configuration of the airplane arrived at so far is checked for the following cases.

1. Longitudinal static stability and control.
   (a) At the rear-most location of C.G., the airplane should be at least neutrally stable for stick-free condition.
   (b) At the foremost C.G. location, the elevator must be able to provide control(i.e. trim), at C_{Lmax} in landing configuration.
   (c) There should be adequate control for nose wheel lift-off at $V = 0.85V_{T0}$

2. Directional static stability and control.
   (a) The vertical tail should provide desirable level of directional control in (1) cross wind take-off and landing, (2) one engine inoperative condition for multi-engine airplanes, (3) adverse yaw during roll

3. Adequacy of dihedral effect and aileron area
   (a) The dihedral angle of wing should be such as to give adequate level of dihedral effect.
   (b) The aileron area should give desired rate of roll.

8.2 Static longitudinal stability and control

8.2.1 Specifications

The horizontal tail must be large enough to ensure that the static longitudinal stability criterion, dC_{mcg}/dC_L is negative for all anticipated center of gravity positions.
An elevator should be provided so that the pilot is able to trim the airplane(maintain $C_m = 0$) at all anticipated values of C_L.

The horizontal tail should be large enough and the elevator powerful enough to enable the pilot to rotate the airplane during the take-off run, to the required angle of attack. This condition is termed as the nose wheel lift-off condition.

8.2.2 Revised estimate of the area of horizontal tail

Following simpler approach is used to obtain the area of horizontal tail(h.tail).

1. From chapter 4, C_m vs alpha curve, value of $C_{m\alpha}$ is obtained. From this value of $C_{m\alpha}$, the static margin stick-free is calculated.

2. The contribution of wing, fuselage, power and h.tail are worked out for cruise flight condition with airplane weight equal to the design gross weight. It may be pointed out that (a) the contribution of wing is zero int this case as the c.g. is at the a.c. of the wing (b) the contribution of h.tail should provide the required value of static margin. This gives the required value of tail volume ratio V_H. Subsequently the area of h.tail can be calculated.

The steps are as follows.

$$\frac{dC_m}{dC_L} = \left(\frac{dC_m}{dC_L}\right)_{wing} + \left(\frac{dC_m}{dC_L}\right)_{fuselage} + \left(\frac{dC_m}{dC_L}\right)_{nacelle} + \left(\frac{dC_m}{dC_L}\right)_{power} + \left(\frac{dC_m}{dC_L}\right)_{h.tail} \tag{8.1}$$

Contribution of fuselage $\left(\frac{dC_m}{dC_L}\right)_{fuselage}$:

Approximate expression for this contribution is:

$$\left(\frac{dC_m}{dC_L}\right)_{fuselage} = \frac{K_f W_f^2 l_f}{S c a_w} \tag{8.2}$$

where,
W_f = width of fuselage = 4 m
l_f = length of fuselage= 43 m
S = wing area = 185.11 m
c = mean aerodynamic chord of wing = 4.7 m
a_w = slope of lift curve of a wing = 5.53 per radian
K_f from ref [12] is 0.02.
Hence, $\left(\frac{dC_m}{dC_L}\right)_{fuselage} = 0.00295$
The contribution of $\left(\frac{dC_m}{dC_L}\right)_{nacelle}$ to $\left(\frac{dC_m}{dC_L}\right)$ is neglected.

Contribution of power $\left(\frac{dC_m}{dC_L}\right)_{power}$:

The contribution of the powerplant is given by the formula[12]:

$$\left(\frac{dC_m}{dC_L}\right)_{power} = \frac{T t_p}{W c} \tag{8.3}$$

where,
$\frac{T}{W}$ = Thrust loading
t_p = Distance of the thrust line from c.g.
For the airplane under design, t_p is estimated as 0.19m. At the cruise altitude, (T/W) is 0.0537
Hence,
$\left(\frac{dC_m}{dC_L}\right)_{power,cruise} = 0.002161$

Contribution of h.tail in stick-free case $\left(\frac{dC_m}{dC_L}\right)_{h.tail}$:

$$\left(\frac{dC_m}{dC_L}\right)_{h.tail} = -\frac{a_t}{a_w} V_H \eta_t \left(1 - \frac{d\epsilon}{d\alpha}\right)\left(1 - \tau \frac{C_{hot}}{C_{hce}}\right) \tag{8.4}$$

where,
a_t = Slope of lift curve of h.tail = 5.712 per radian, calculated using eq. no.(4.6)
a_w = Slope of lift curve of wing
η_t = Tail efficiency = 0.95
V_H = Tail volume ratio
ϵ = Down wash angle
$\tau = (dC_{Lt}/d\delta_e)/(dC_{Lt}/d\alpha)$
C_{Lt} = Lift coefficient of tail
δ_e = Elevator deflection
α_t = Angle of attack of h.tail
$C_{hot} = dC_h/d\alpha_t$
$C_{hoe} = dC_h/d\delta_e$
C_h = Hinge moment coefficient
η_t is assumed to be 0.95
$d\epsilon/d\alpha$ is estimated using the following approximate formula from ref[2]:
$\frac{d\epsilon}{d\alpha} = \frac{114.6 \times a_w}{\pi A} = 0.3523$
$\tau = 0.5$ from Ref.[2]
$(S_{ele}/S_h) = 0.35$
$C_{h\alpha} = 0.0044\ deg^{-1}$
$C_{hoe} = 0.0065\ deg^{-1}$
After putting all these value in above equation, RHS = -0.4207V_H
It was found from ref[12], $C_{m\alpha}$ = -1.4 per radian, for M = 0.778
Hence,
$\left(\frac{dC_m}{dC_L}\right) = \frac{dC_{m\alpha}}{a_w} = -0.25328$
After substituting all values in equation (8.4) and solve for V_H,
$V_H = 0.61419$
Noting that $V_H = \frac{S_h}{S}\frac{l_{hm}}{c}$
$\implies S_h = \frac{V_H c S}{l_{hm}} = \frac{0.615 \times 4.7 \times 185.11}{22.3} = 24.068\ m^2$

$$\boxed{S_h = 24.068\ m^2}$$

8.2.3 Remark

Cross-check 1-Adequacy of elevator with $|\delta_e| < 25^\circ$ in landing configuration with c.g. at the most forward location

$$C_{mcg} = (C_{mac})_{at} + (\Delta C_{mac})_{flap} + C_{Lawg}(i_w - \alpha_{oLW})\left(\frac{x_{cg}}{\bar{c}} - \frac{x_{ac}}{\bar{c}}\right) + (C_{m0})_{f,n,p} - V_H \eta C_{L\alpha tg}(i_t - \epsilon_{og} + \tau_{tab}\delta_t)$$
$$+ C_{L\alpha wg}\left(\frac{x_{cg}}{\bar{c}} - \frac{x_{ac}}{\bar{c}}\right)\alpha + (C_{ma})_{f,n,p}\alpha - V_H \eta C_{L\alpha tg}\left(\alpha(1 - \frac{d\epsilon_g}{d\alpha} + \tau\delta e\right) \tag{8.5}$$

To perform this cross-check, substitute $C_{mcg} = 0$ in above equation and obtain $(\delta_e)_{reqd}$.
The value of $(\delta_e)_{reqd}$ should be less than or equal to 25^o. if $(\delta_e)_{reqd}$ is more than 25 the elevator area needs to be increased or the forward shift of c.g. needs to be decreased by suitale rearrangement of items in fuselage.
Elevator required during landing with c.g. at the foremost location:
The foremost c.g. location is $0.198\bar{c}$.
The following additional quantities need to be obtained.
(a) $(\Delta C_{mac})_{flap}$
(b) C_{Lawg}, C_{Latg} under landing condition and with correction for proximity of ground.
(c) $(d\epsilon/d\alpha)$ in proximity of ground
(d) angle of attack of airplane during landing.

(e)$C_{m0}|_f$ and $C_{m\alpha}|_f$ which are calculated as specified in ref[12]
(A) $(\Delta C_{mac})_{flap}$

$$(\Delta C_{mac})_{flap} = (\Delta C_{mac})_{airfoil} \frac{S_f}{S} \frac{\bar{c_f}}{\bar{c}} \tag{8.6}$$

where,
S_f = area of wing which contains the flap
$\bar{c_f}$ = mean aerodynamic chord of the wing which contains the flap.
It is assumed that in landing configuration, the flap deflection is 40 degree. $(\Delta C_{mac})_{airfoil}$ for this case is -0.6.
The area of wing which contains the flap is estimated as 39.65 m^2.
The mean aerodynamic chord of wing which contains the flap is estimated as 2.691 m.
Consequently,: $(\Delta C_{mac})_{flap} = -0.6 \times \frac{39.65}{58.48} \times \frac{2.691}{2.295}$ = -0.477

(B) Angle of attack(α) at landing
The angle of attack at landing is calculated at $V = V_{TD}$, with landing taking place at sea level. A rough estimate is obtained below.
V_{TD} = Touch down velocity. $V_{TD} = 1.15V_s$
V_s is calculated assuming $C_{Lmax} = 2.7$ with slotted-flaps from ref[12]
C_L at V_{TD} is = $C_{LTD} = 2.7/1.15^2 = 2.042$
C_{Lmax} without flap is 1.5 from ref[12]. Hence, $(\Delta C_{Lmax})_{flap}$ = 2.7 - 1.5 = 1.2
Consequently, C_L due to angle of attack = $2.042 - 1.2 = 0.842$
At this stage, $C_{L\alpha w}$ is obtained at V = V_{TD} and correction applied for proximity of ground; W_{land} is taken as W_0 for simplicity.

$V_{TD} = \sqrt{\frac{2W}{\rho S C_{LTD}}}$ = 69.568 m/s

(c) Mach number at touch down (M_{TD})

Sonic velocity(a) = 330 m/s
$M_{TD} = V_{TD}/a = 0.2108$
Hence, $\beta^2 = (1 - 0.21^2) = 0.9555$

$(C_{L\alpha w})_{M=M_{TD}} = 0.09402\ deg^{-1}$

the height of wing above ground (d_g) = 4.7m
Hence, $d_g/(b/2) = 0.2186$
for A = 12 and $d_g/(b/2) = 0.2186$, $(C_{Lawg}/C_{L\alpha w}) = 1.08$
Hence, $C_{L\alpha wg} = 1.015\ rad^{-1}$
Hence, α_w at touchdown = 42.28°. Note $\alpha_{oLw} = -5.2$
Angle of attack of airplane = $\alpha = \alpha_{cr} - i_w = 41.72^o$

(D) Slope of lift curve for h.tail at M_{TD}:

$(C_{L\alpha t})_{MT} = 3.9575\ rad^{-1}$
The h.tail is 6.4m above the ground. The semi-span (b/2) of tail is 3.725m.
Hence, $(d_g/(b/2))_{tail}/ = 0.4183$
$C_{L\alpha tg}/C_{L\alpha t} = 1.1$
Hence, $C_{L\alpha tg} = 3.52\ rad^{-1}$

(E) Downwash in proximity of ground:

$\left(\frac{d\epsilon}{d\alpha}\right)_g = 0.5\left(\frac{d\epsilon}{d\alpha}\right)$, and $(\epsilon_o)_g = 0.5\epsilon$
Hence, $\left(\frac{d\epsilon}{d\alpha}\right)_g = 0.17615$ and $(\epsilon_o)_g = 1.0146$

(F) $C_{mo}|_f$ **and** $C_{m\alpha}|_f$
The formulas from ref[12] are as follows:

$$C_{m0}|_f = \frac{-(K_1 - K_2)}{0.365 S\bar{c}} \left(\sum_{i=1}^{9} 33 w_i^2 (\alpha_{\circ Lf} + i_f) \Delta x \right) \tag{8.7}$$

$$C_{m\alpha}|_f = \frac{-(K_1 - K_2)}{0.365 S\bar{c}} \left(\sum_{i=0}^{10} w_i^2 \frac{d\epsilon}{d\alpha} \Delta x \right) \tag{8.8}$$

The tables for this calculation as shown below:
$K_2 - K_1 = 0.92$ from ref[12]

Station	Δx	w_f	$\alpha_{\circ Lf} + i_f$	$w_f^2(\alpha_{\circ lf} + i_f)\Delta x$
1	4.96	2.00	-10	-198.40
2	4.96	4.00	1.1	87.30
3	4.96	4.00	1.1	87.30
4	4.96	4.00	1.1	87.30
5	4.96	4.00	1.1	87.30
6	4.96	4.00	1.1	87.30
7	4.96	3.48	-5.4	-324.36
8	4.96	2.15	-5.4	-123.94
9	4.96	0.82	-5.4	-18.10
			Sum	-228.33

$l_f/d_f = 11.15$

$$\implies C_{\circ m}|_f = -0.0066$$

Similary for the other,

Station	Δx	w_f	x_i	x_i/c	$\frac{d\epsilon}{d\alpha}$	$w_f^2 \times d\epsilon/d\alpha \times \Delta x$
1	3.60	2.00	14.39	2.17	1.00	14.39
2	3.60	4.00	10.79	1.63	1.00	57.56
3	3.60	4.00	7.19	1.09	1.30	74.82
4	3.60	4.00	3.60	0.54	2.50	143.89
5	6.62	4.00	0.00	0.00		0.00
6	4.72	4.00	4.72	0.71	0.14	10.34
7	4.72	3.96	9.44	1.42	0.27	20.28
8	4.72	2.70	14.15	2.14	0.41	14.10
9	4.72	1.43	18.87	2.85	0.55	5.31
10	4.72	0.17	23.59	3.56	0.69	0.09
					Sum	340.78

$$\implies C_{m\alpha}|_f = 0.009\ rad^{-1}$$

Also, i_w = wing incidence = 0.56°

$$C_{mcg} = (C_{mac})_{at} + (\Delta C_{mac})_{flap} + C_{Lawg}(i_w - \alpha_{oLW}) \left(\frac{x_{cg}}{\bar{c}} - \frac{x_{ac}}{\bar{c}} \right) + (C_{m0})_{f,n,p} - V_H \eta C_{L\alpha tg}(i_t - \epsilon_{og} + \tau_{tab}\delta_t)$$
$$+ C_{L\alpha wg} \left(\frac{x_{cg}}{\bar{c}} - \frac{x_{ac}}{\bar{c}} \right) \alpha + (C_{ma})_{f,n,p}\alpha - V_H \eta C_{L\alpha tg} \left(\alpha(1 - \frac{d\epsilon_g}{d\alpha} + \tau\delta e \right) \tag{8.9}$$

Putting $C_{mcg} = 0$ for trim in above equation, gives the required value of δ_e ,

$\delta_e = -27.608$

Keypoint: Our $|\delta_e| > 25^o$, we need to increase our elevator area. Keeping this mind, in the second iteration the elevator area was changed to 10.725 m^2 rectifying this.

8.3 Directional stability and control

8.3.1 Specifications

The directional static stability criterion, $dC_n/d\beta$, should be positive for any flight speed greater than 1.2 times the stalling speed.
The yawing moment control(rudder) must be powerful enough to counteract the yawing moment encountered (a) in roll(adverse yaw), (b) in cross-wind landing or takeoff, (c) when one engine is inoperative for multi-engine airplanes. The spin recovery is also effected primarily by the rudder.

8.3.2 Equations for directional stability

The equation for directional stability can be derived as:

$$\frac{dC_n}{d\beta} = (C_{n\beta})_{Fuselage} + (C_{n\beta})_{power} + (C_{n\beta})_{V.tail} \tag{8.10}$$

8.3.3 Revised estimate of area of vertical tail

In the preliminary analysis of directional static stability, the contributions of wing, power and interference effects are ignored. It is further assumed that the contributions to $C_{n\beta}$ due to wing sweep and low wing position cancel each other.

$(C_{n\beta})_{fuselage}$:

An approximate formula is:

$$(C_{n\beta})_{Fuselage} = \frac{-k_n V_n}{28.7Sb} \tag{8.11}$$

where,
k_n = a factor which depends on fineness ratio of fuselage = 37.31
V_n = volume of fuselage, which is approximated from the formula from ref[2] = $\frac{3.4\times A_{top}\times A_{side}}{4\times l_f} = \frac{3.4\times 144.68\times 144.68}{4\times 43} =$ 398.95 m^3
S, b = wing span, area

$(C_{n\beta})_{Fuselage} = -0.065\ rad^{-1} = 0.0011$ per deg

$(C_{n\beta})_{V.tail}$:
$(C_{n\beta})_{V.tail} = a_v \frac{S_v l_v}{Sb}$,
a_v = slope of lift curve of v.tail = 0.0416 deg^{-1}

$V_v = \frac{S_v l_v}{Sb}$

Hence, $(C_{n\beta})_{V.tail} = 0.0416 \times V_v$

The value of $C_{n\beta(desirable)} = 0.0005 \left(\frac{W}{b^2}\right)^{1/2}$
W = weight of airplane

b = span of wing
Hence , $C_{n\beta(desirable)} = 0.001709$per deg

$$C_{n\beta(desirable)} = C_{n\beta(fuse)} + C_{n\beta(V.tail)} \tag{8.12}$$

Substituting various values: $0.001709 = -0.0011 + 0.0416 \times \bar{V_v}$
Or $V_v = 0.07$

This value is almost the same as that obtained in the initial tail sizing.
Hence, the vertical tail area is:
$S_v = \frac{V_v \times SB}{l_v} = 72.425\ m^2$

$$\boxed{S_v = 74.425\ m^2}$$

8.3.4 Area of rudder

Rudder must provide adequate control during the following situations:

1. Cross wind take-off and landing
2. One engine inoperative condition for multi-engine airplane
3. Adverse yaw during roll

Cross wind take-off and landing

For an airplane, the critical condition during take-off, is with a cross wind equal to 20 % of V_{To}. The tendency of an airplane possessing directional static stability, is to align itself with the wing direction (weather cock effect). That is, the airplane must be able to counteract the yawing moment due to the side-slip produced by the cross wind $C_{n\beta} \times \Delta\beta$. And the moment due to rudder is given by: $(C_n)_{rudder} = -a_v \tau_r (S_V/S)(l_V/b)\delta_{r,max}$.
where,
a_v = slope of the lift curve for vertical tail = 5.713 per radian.
l_V is the vertical tail arm = 20.07 m
$\delta_{r,max}$ = maximum rudder deflection = 25^0

$$C_{n\beta} \times \Delta\beta = -a_v \tau_r (S_V/S)(l_V/b)\delta_{max} \tag{8.13}$$

The LHS evaluates to $C_{n\beta} \times \Delta\beta = 0.102 \times -0.2 = -0.0204$.
RHS gives,

$$-5.713 \times \tau_r \times (74.425/185.11) \times (20.07/43) \times 25 \times \pi/180 = -0.433\tau_r$$

$$\implies \tau_r = 0.0204/0.433 = 0.04712$$

From ref [2], we get $S_{rudder}/S_v = 0.15$ for this $\tau_r \implies S_{rudder} = 0.15 \times 72.425 = 10.864\ m^2$

One engine inoperative condition for multi-engine airplane

The yawing moment caused by the asymmetric thrust is countered by the yawing moment due to the rudder. The working formula for that would be:

$$T \times Y_p = \eta_v q S_v l_v \frac{dC_{Lv}}{d\delta_r}\delta_r$$

where
T = Operating thrust = 282.443 KN
Y_p is the distance of the FRL from the thrust line = 15.5 m
η_v is the tail efficiency assumed to be 95%
$q = (1/2)\rho v^2 = 0.1824 \times v^2\ N$
$\frac{dC_{Lv}}{d\delta_r}$ is assumed to be 0.2 per degree from ref[12]
and max rudder deflection(δ_r) = 25^0

l_v is the vertical tail arm = 20.05 m
Solving for v we get minimum control velocity as:

$$\boxed{V_{min,control} = 186.45\ m/s^2}$$

Adverse yaw during roll

When an airplane is rolled to the right, the rate of roll produces a yawing moment tending to turn the airplane to the left. Similarly, a roll to left produces yaw to right. Hence, the yawing moment produced as a result of the rate of roll is called adverse yaw. The $(C_n)_a dverse, yaw \approx \frac{C_L}{8}\frac{pb}{2v}$
where,
p = rate of roll in radians per second; b = wing span; v = flight velocity.
From ref[14] we get, $pb/2V = 0.07$ for our aircraft. This adverse yaw must be countered with the yawning moment of the rudder$(C_n)_{adverse,yaw}$.
The equation we get from ref[12] is:

$$-\frac{C_L}{8}\frac{pb}{2V} = -a_v\tau_r(S_V/S)(l_v/b)\eta_v\delta_{r,max} \tag{8.14}$$

Solving for τ_r we get, $\tau_r = 0.03 \implies S_r/S_{vt} \approx 0.15$ which is the same as we got in the cross wind case, so vertical tail area is the same as in that case.

8.4 Lateral Stability and control

8.4.1 Selection of dihedral angle

The levels of longitudinal and directional static stability ($C_{m\alpha}$ and $C_{n\beta}$) can be adjusted by changing the areas of the horizpntal tail (S_t) and the vertical tail respectively. The level of $C_{l\beta}^{'}$, can be adjusted by choosing an appropriate dihedral angle. To arrive at the dihedral angle needed for an airplane, the contributions due to wing sweep, fuselage, power plant and vertical tail are first calculated. Then, the difference between the sum of these contributions and the desirable level of $C_{l\beta}^{'}$ is provided by choosing an appropriate dihedral angle.

$$(C_{l\beta}^{'})_{desirable} = -(C_{n\beta}) \tag{8.15}$$

Criterion for stabilizing dihedral effect

A bank to right produces positive β. This β should produce a negative L to bring the airplane back to zero roll. Hence, for stabilizing effect, $C_{l\beta}^{'}$ should be negative.
The contribution to $C_{l\beta}^{'}$ can be expressed as:

$$C_{l\beta}^{'} = (C_{l\beta}^{'})_w + (C_{l\beta}^{'})_{vt} \tag{8.16}$$

Contribution of wing to $C_{l\beta}^{'}$

The contributions of wing to $C_{l\beta}^{'}$ are due to the dihedral angle and the sweep.

$$C_{l\beta}^{'}|_{wing} = (C_{l\beta}^{'})|_{dihedral} + (C_{l\beta}^{'})|_{sweep}$$

Remarks:
(1) It may be noted that the contribution of dihedral to $C_{l\beta}^{'}$ is negative. Since, $C_{l\beta}^{'}$ is called a stabilizing

contribution.
(2) For a wing with tape ratio λ:

$$(C_{l\beta}^{'})_{dihedral} = -0.25\Lambda \frac{dC_L}{d\alpha}\left[\frac{2(1+2\lambda)}{3(1+\lambda)}\right] per\ radian = -0.25(0.1)(5.52)(0.82) = -0.113\ rad^{-1} \tag{8.17}$$

$$(C_{l\beta w}^{'})_{sweep} = -C_L \frac{\bar{y}}{b} sin(2\Lambda) = -0.633 \times 0.205 \times \sin(2 \times 0.5) = -0.041\ per\ radian \tag{8.18}$$

$\frac{\bar{y}}{b} \approx 0.25 \times \left(\frac{2(1+2\lambda)}{3(1+\lambda)}\right)$ from ref[12]

$$C_{l\beta}^{'}|_{wing} = -0.567 - 0.118 = -0.154\ rad^{-1} \tag{8.19}$$

Contribution of fuselage of $C_{l\beta}^{'}$

The contribution of fuselage to $C_{l\beta}^{`}$ arises due to the interference effect. Consider an airplane having positive β or the sideward velocity component ($v = Vsin\beta$) from right to left. It is observed that for the high wing case the change in angle of attack, $\Delta\alpha$, is positive on the right wing and negative on the left wing. This would result in a negative rolling moment which is a stabilizing contribution.
$\Delta C_{l\beta}^{`} = -0.0006\ deg^{-1}$ from ref[15]

Contribution of vertical tail to $C_{l\beta}^{'}$

Its contribution is too small with respect to contribution of others, hence, its contribution is neglected from ref[12]

Contributions due propeller and flaps to $C_{l\beta}^{'}$

Its contribution is too small with respect to contribution of others, hence, its contribution is neglected from ref[12]

$$C_{l\beta}^{'} = (C_{l\beta}^{'})_w + (C_{l\beta}^{'})_{f,n,p} + (C_{l\beta}^{'})_{vt} \tag{8.20}$$

$(C_{l\beta}^{'})_{fuselage}$ = -0.034 rad^{-1}
$(C_{l\beta}^{`})_{wing}$ = -0.154 rad^{-1}
Because of small value, others contribution is neglected.

$$(C_{l\beta}^{`})_{final} = -0.189\ rad^{-1} \tag{8.21}$$

Value of $C_{l\beta}^{`}$ is negative which satisfied the stability criteria, hence it is stable.

Selection of dihedral angle

The levels of longitudinal and directional stability can be adjusted by changing the areas of the horizontal tail and vertical tail respectively. The level of $C_{l\beta}^{'}$, can be adjusted by choosing an appropriate dihedral angle. To arrive at the dihedral angle needed for an airplane, the contributions due to wing sweep, fuselage, power plant and vertical tail are first calculated. Then, the difference between the sum of these contributions and the desirable level of $C_{l\beta}^{'}$ is provided by choosing an appropriate dihedral angle.

$$(C_{l\beta}^{'})_{desirable} = -(C_{n\beta}/2) = -0.102/2 = 0.051\ rad^{-1} \tag{8.22}$$

$(C_{l\beta}^{`})_{desirable}$ = -0.051
Based on it, new dihedral chosen is 0.1^o

Chapter 9

Performance estimation

9.1 Level flight performance

In steady Level flight, the equations of motion, in standard notations, are

$$T - D = 0 \tag{9.1}$$

$$L - W = 0 \tag{9.2}$$

$$L = W = \frac{1}{2}\rho V^2 S C_L \tag{9.3}$$

$$T = D = \frac{1}{2}\rho V^2 S C_D \tag{9.4}$$

9.1.1 Stalling speed

In level flight,

$$V = \sqrt{\frac{2W}{\rho S C_L}} \tag{9.5}$$

Since, C_L cannot exceed C_{Lmax}, there is a flight speed below which the level flight is not possible. The flight speed at $C_L = C_{Lmax}$ is called the stalling speed and is denoted by V_s.

$$V_S = \sqrt{\frac{2W}{\rho S C_{Lmax}}} \tag{9.6}$$

Since, ρ decreases with altitude, V_S increases with height. It is noted that $W/S = 6189 N/m^2, C_{Lmax} = 2.7$ with landing flaps and $C_{Lmax} = 1.4$ without flaps. The values of stalling speed at different altitudes and flap

settings are tabulated below

h (m)	$\rho(kg/m_3)$	$V_S(_{Lmax}$= 1.4	$V_S(_{Lmax}$= 2.7
0	1.225	84.01	60.49
1000	1.112	88.17	63.49
2000	1.007	92.66	66.72
3000	0.909	97.51	70.21
4000	0.819	102.71	73.97
5000	0.736	108.35	78.02
6000	0.660	114.44	92.41
7000	0.590	121.05	87.17
8000	0.526	128.23	92.34
9000	0.467	136.05	97.97
10000	0.413	144.60	104.12
12000	0.311	166.78	120.09
15000	0.195	210.67	151.70

Table 9.1: Variation of stalling speed with altitude

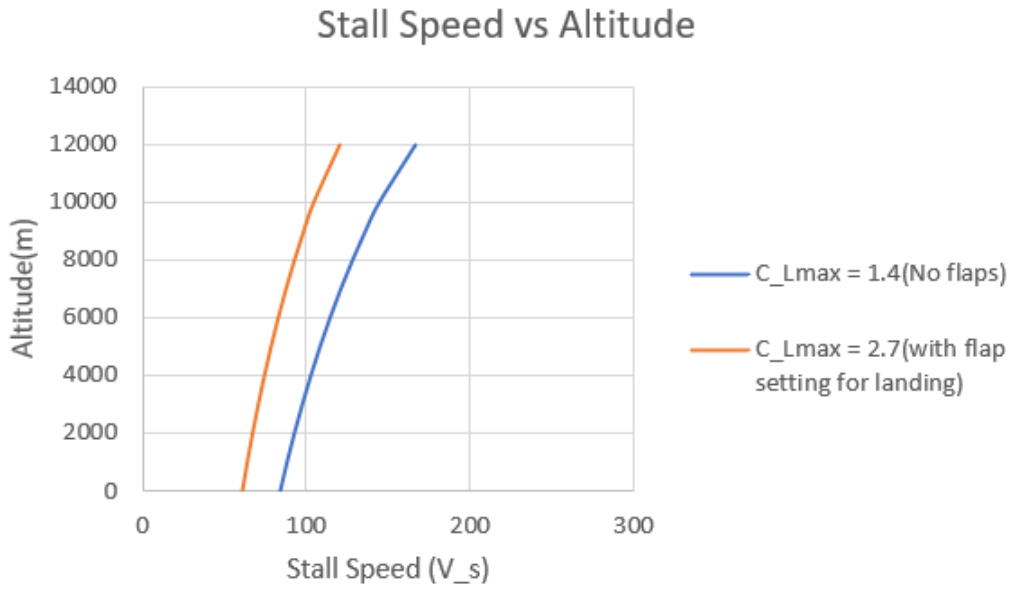

Figure 9.1: Stalling Speed Vs Altitude

9.1.2 Variations of V_{min} and V_{max} with altitude

To determine V_{min} and V_{max} at each altitude, the following procedure is adopted.
(1) The engine thrust (T_{avail}) assumed to be constant with velocity and values of T_a obtained for different altitude from the figure 9.4.
(2) The drag at each altitude is found as a function of velocity using the drag polar and the level flight formulae given below.

$$C_L = \frac{2 \times (W/S)}{\rho V^2} \tag{9.7}$$

$$C_D = C_{DO} + KC_L^2; \tag{9.8}$$

$$Drag = \frac{1}{2}\rho V^2 S C_D \tag{9.9}$$

The values of $C_{DO} = 0.016$ and $K = 0.0447$ are valid at subcritical Mach number. However, the cruise Mach number(M_{cruise}) for this airplance is 0.778. Hence, C_{DO} and K are expected to become functions of Mack number above M_{cruise}.
These polars are approximated by the parabolic polar expression namely $C_D = C_{DO} + KC_L^2$. The values of C_{DO} and K at various Mach numbers are given below.

M	C_{DO}	**K**
0.75	0.016	0.0447
0.778	0.016	0.0447
0.78	0.0159	0.0447
0.785	0.0159	0.0447
0.79	0.0160	0.0447
0.795	0.0160	0.0448
0.8	0.0160	0.0450
0.805	0.01605	0.04539
0.81	0.01608	0.04582
0.82	0.01615	0.04637
0.83	0.01624	0.04794
0.84	0.01636	0.05021
0.85	0.01649	0.05331
0.86	0.01665	0.05734
0.87	0.01683	0.06245
0.88	0.01704	0.06876
0.89	0.01726	0.07632

Table 9.2: Variations of C_{D0} and K with Mach number (Parabolic fit)

The variations in C_{DO} and K with Mach number are plotted in the Figs. 9.2 and 9.3. It is seen that there is no significant increase in C_{DO} and K upto M = 0.8. This is expected to be the cruise Mach number for the airplane.Following analytical expressions are found to closely represent the change in C_{DO} K from M = 0.70 to M = 0.9.

$$C_{DO} = 0.016 - 0.001(M - 0.8) + 0.11(M - 0.8)^2 \tag{9.10}$$

$$K = 0.0447 + (M - 0.8)^2 + 20.0(M - 0.8)^3 \tag{9.11}$$

In the case of the present airplane, the cruise Mach number is 0.778. The variations of C_{DO} and K above M_{cruise} and upto M = 0.9, are taken as follows.

$$C_{DO} = 0.016 - 0.0001(M - 0.778) + 0.11(M - 0.778) \tag{9.12}$$

$$K = 0.0447 + (M - 0.778)^2 + 20.0(M - 0.778)^3 \tag{9.13}$$

(3) $(V_{min})_e$ is the minimum speed from thrust available consideration. To arrive at V_{min}, the minimum speed of the airplane at an altitude, the stalling speed(V_s) also needs to be taken into account. V_{min} is higher of $(V_{min})_e$ and V_S. V_S is taken for C_{Lmax} withput flaps. The plots are presented only for climb thrust case. An analytical expression for Vmax can be deduced when it is assumed that the thrust available (Ta) ,C_{DO} and K remain constant with flight speed. The derivation is as follows.

$$T_a = 0.5 * \rho v^2 S C_{DO} + K\frac{2W^2}{\rho V^2 S} \tag{9.14}$$

or

$$AC^4 - BV^2 + C = 0 \tag{9.15}$$

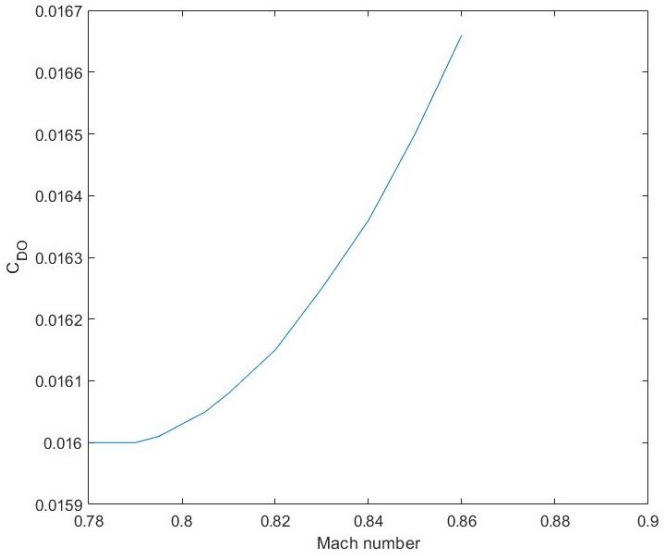

Figure 9.2: Variation of C_{D0} with Mach number

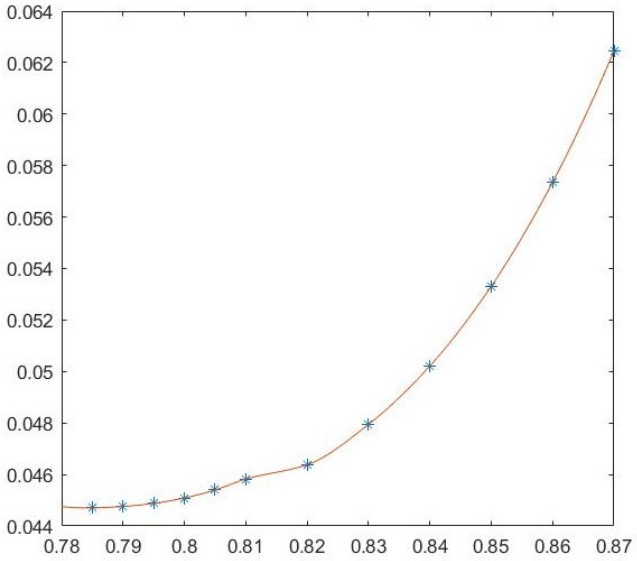

Figure 9.3: Variation of K with Mach number

where,

$$A = 0.5\rho S C_{DO}, B = T_a, C = \frac{2KW^2}{\rho S}$$

When Ta, C_{DO} and K have constant values,Eqs(9.16) gives,

$$V = \frac{B \pm \sqrt{B^2 - 4AC}}{2A} \tag{9.16}$$

Consequently, V_{max} being the larger of the two solutions, is :

$$V_{max} = V = \frac{B + \sqrt{B^2 - 4AC}}{2A} \tag{9.17}$$

Substituting for A, B and C yields :

$$V_{max} = \sqrt{\frac{T_a^2}{\rho S C_{DO}} + \sqrt{\frac{T_a^2}{\rho^2 S^2 C_{DO}^2} - \frac{4W^2}{S^2}\frac{K}{\rho^2 C_{DO}}}} \tag{9.18}$$

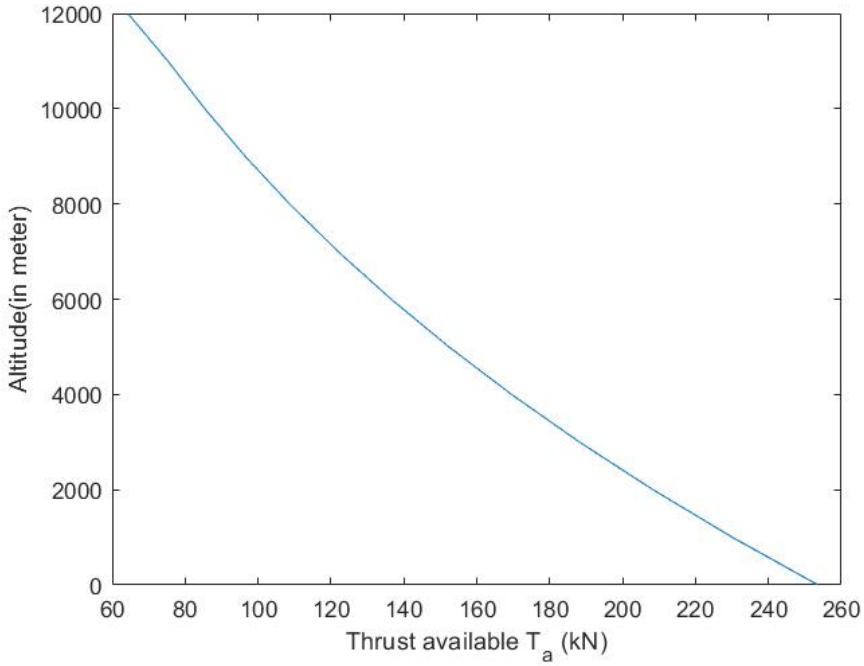

Figure 9.4: Variation of T_a with Altitude

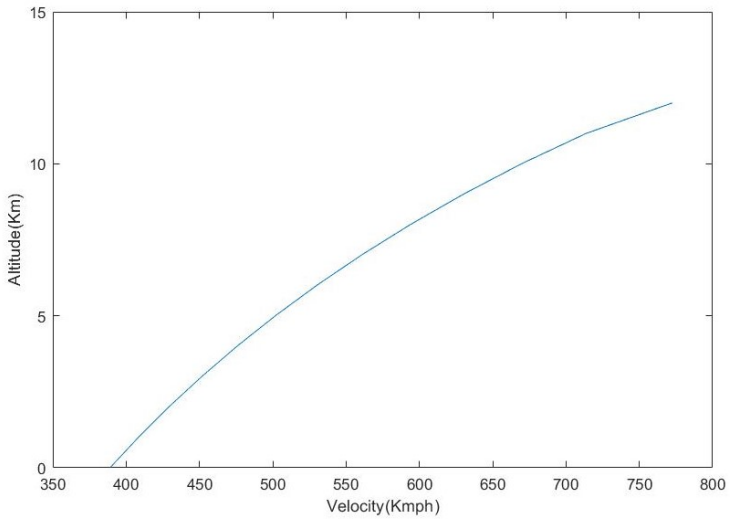

Figure 9.5: Variation of V_{min} with Altitude

The variations of V_s, V_{min} and V_{max} are tabulated in Table 9.3 and presented in Fig. 9.5,9.6 and 9.7.

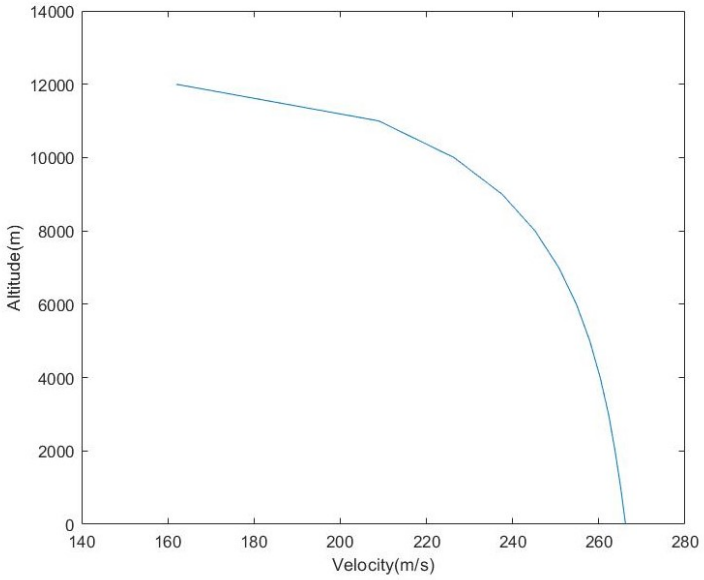

Figure 9.6: Variation of V_{max} with altitude

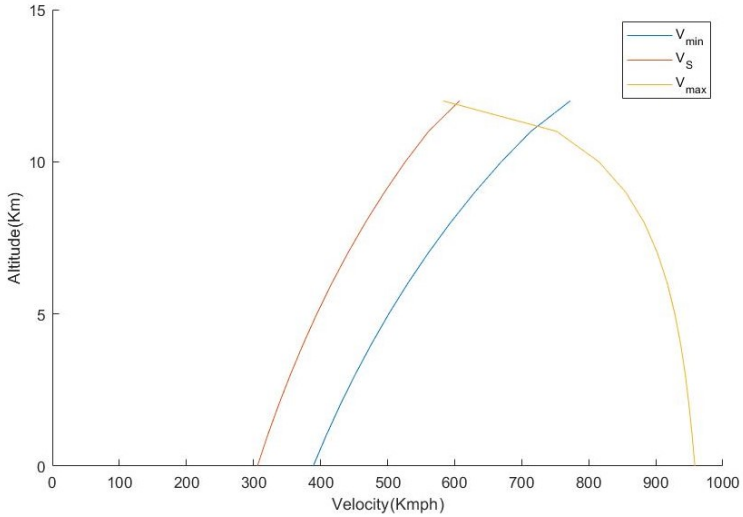

Figure 9.7: Variations of V_{min} and V_{max} with altitude

9.1.3 Steady climb

In this flight, the c.g. of the airplane moves along a straight line inclined to the horizontal at an angle γ. The velocity of flight is assumed to be constant during the climb. Since, the flight is steady, acceleration is zero and the equations of motion can be written as:

$$T - D - W sin\gamma = 0 \tag{9.19}$$

h(m)	$V_S(m/s)$	$(V_{min})(m/s)T = T_{climb}$	$(V_{max})(m/s)T = T_{climb}$	$(V_{max})(kmph)T = T_{climb}$
0	84.96	108.06	266.19	958.28
1000	89.17	113.42	265.07	954.25
2000	93.7	119.19	263.76	949.54
3000	98.61	125.43	262.25	944.1
4000	103.88	132.13	260.31	937.12
5000	109.57	139.38	257.9	928.44
6000	115.73	147.21	254.79	917.24
7000	122.42	155.71	250.7	902.52
8000	129.67	164.95	245.2	882.72
9000	137.58	175	237.55	855.18
10000	146.23	186	226.4	815.04
11000	155.87	198.27	208.92	752.11
12000	168.66	214.53	161.95	583.02

Table 9.3: Variation of V_{min} and V_{max}

$$L - Wcos\gamma = 0 \tag{9.20}$$

To calculate the variation of rate of climb with flight velocity at different altitudes, the following procedure is adopted.
(1)Choose an altitude.
(2)Choose a flight speed.

Noting that $C_L = 2Wcos\gamma/\rho SV^2$, gives:
$C_D = C_{DO} + K\left(\frac{2Wcos\gamma}{\rho SV^2}\right)$

Also
$V_c = Vsin\gamma$
$cos\gamma = \sqrt{1 - \frac{V_c^2}{V^2}}$
Using above equations yields the following equation for (V_c/V),

$$A\left(\frac{V_C}{V}\right)_2 + \left(\frac{V_C}{V}\right) + C = 0 \tag{9.21}$$

$$A = \frac{KW^2}{0.5\rho V^2 S}; B = -W : C = T_{avail} - 0.5\rho V^2 S C_{DO} - \frac{2kW^2}{\rho V^2 S} \tag{9.22}$$

Since, altitude and flight velocity have been chosen, the thrust available is read from the thrust-Altitude curve.

(3) Above equation gives 2 values of V_C/V. The value which is less than or equal to 1.0 is chosen as $sin\gamma$ cannot be greater than unity. Hence,

$$\gamma = sin^{-1}(V_c/V) \tag{9.23}$$

$$V_C = Vsin\gamma \tag{9.24}$$

(4) This procedure is repeated for various speeds between V_{min} and V_{max}. The entire procedure is then repeated for various altitudes.

A summary of results is presented below in table.

h(m)	R/C_{max}**(m/min)**	$V_{R/C(max)}$**(m/s)**	γ_{max} **(Degrees)**
0	1835.4	222.65	11.91
1000	1641.6	223.49	9.66
2000	1459.8	224.53	7.86
3000	1288.8	225.87	6.4
4000	1127.4	227.45	5.2
5000	975	229.39	4.19
6000	831.6	231.74	3.45
7000	694.8	234.6	2.87
8000	563.4	238.07	2.31
9000	436.8	242.26	1.78
10000	313.2	247.32	1.27
11000	190.8	253.68	0.77
12000	42	262.7	0.17

Table 9.4: Climb performance

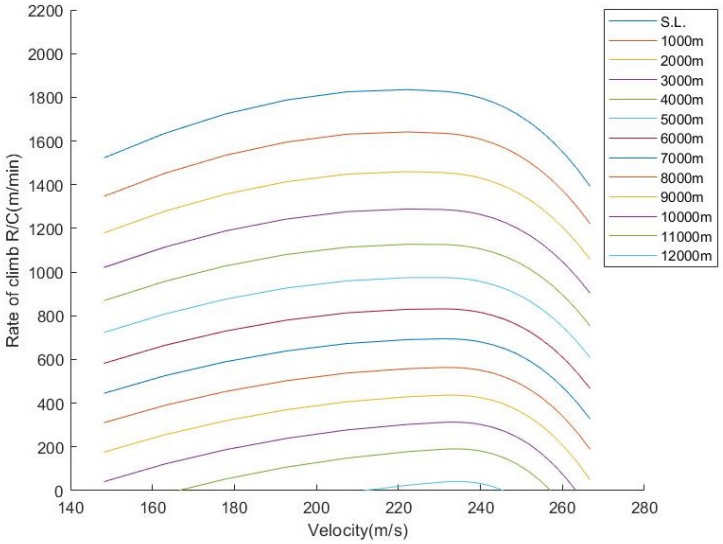

Figure 9.8: Rate of climb vs velocity for various altitudes

1. the absolute ceiling (at which (R/C)max is zero) is 12.24 km.
2. The service ceiling at which (R/C)max equals 30 m/min is 12.07 km

9.1.4 Range and endurance

In this section, the range of the aircraft in a constant altitude and constant velocity cruise is studied. Range is given by the formula:

$$R = \frac{3.6V}{TSFC\sqrt{KC_{DO}}}\left[tan^{-1}\frac{2W_1}{\rho V^2 S}\sqrt{\frac{K}{C_{DO}}} - tan^{-1}\frac{2W_2}{\rho V^2 S}\sqrt{\frac{K}{C_{DO}}}\right] \tag{9.25}$$

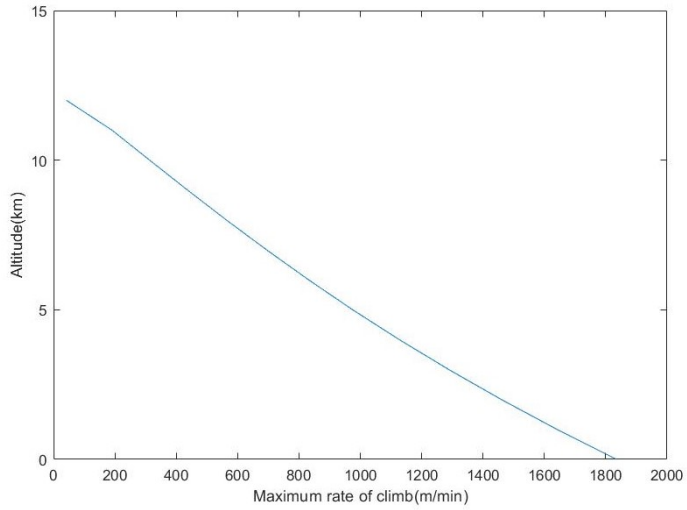

Figure 9.9: Maximum rate of climb vs altitude

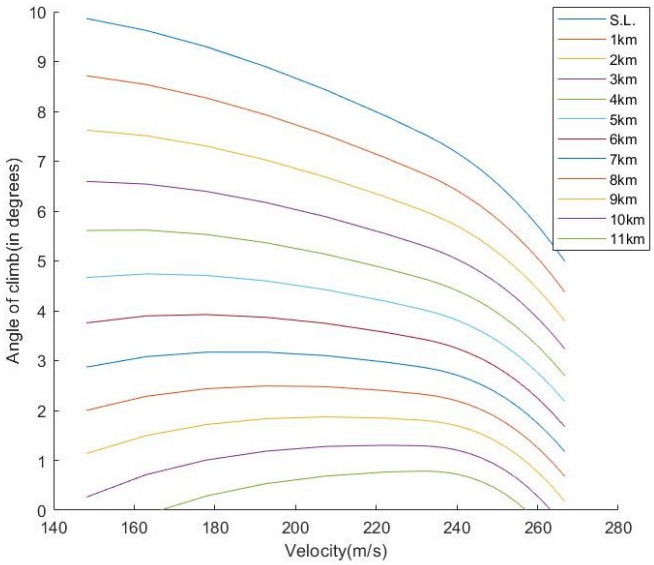

Figure 9.10: Angle of climb vs velocity for various altitudes

where, W_1 is the weight of the airplane at the start of the cruise and W_2 is the weight of the airplane at the end of the cruise.

The cruising altitude is taken as h = 10700 m. TSFC is taken to be constant as $0.549hr-1$. The variation of drag polar above M = 0.778 is given by Eqs 9.12 and 9.13
$W_1 = W_0 = 114196.45 \times 9.8N$
$W_f = 0.255 \times W_1$

Allowing 6% fuel as trapped fuel, W_2 becomes
$W_2 = W_1 - 0.94 \times W_f$
The values of endurance (in hours) are obtained by dividing the expression for range by 3.6V where V is in m/s. The values of range(R) and endurance(E) in flights at different velocities are presented below

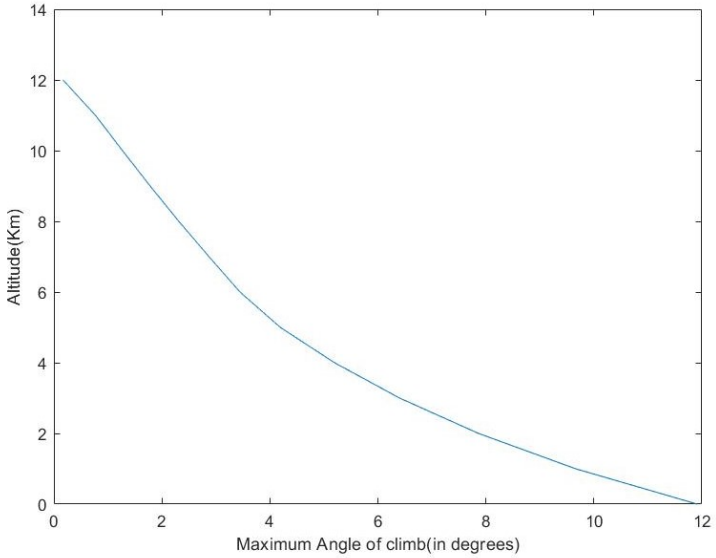

Figure 9.11: Maximum angle of climb vs Altitude

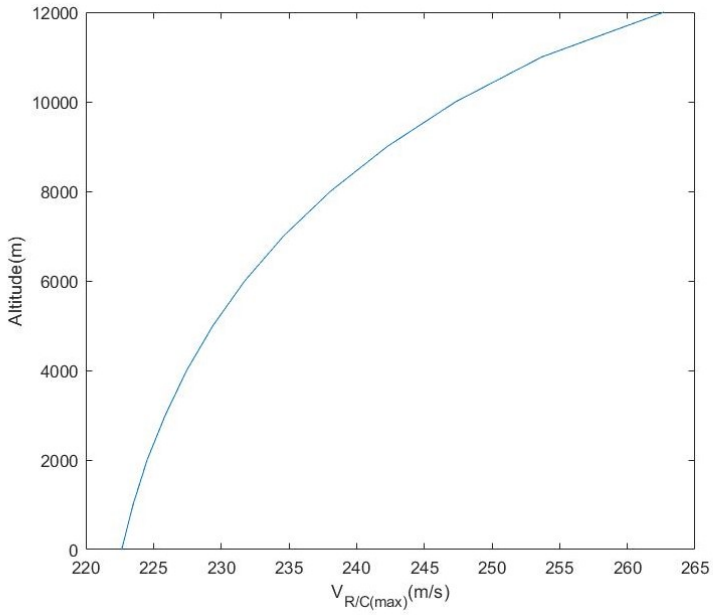

Figure 9.12: Velocity at maximum rate of climb vs Altitude

,

M	V(in m/s)	C_{DO}	K	R (in km)	E (in hours)
0.5	148.18	0.016	0.0447	3833.3	7.19
0.55	163	0.016	0.0447	4702.1	8.01
0.6	177.82	0.016	0.0447	5535.93	8.65
0.65	192.64	0.016	0.0447	6288.16	9.07
0.7	207.46	0.016	0.0447	6925.93	9.27
0.75	222.28	0.016	0.0447	7432.76	9.29
0.778	230.57	0.016	0.0447	7658.09	9.23
0.78	231.17	0.016	0.0447	7672.81	9.22
0.785	232.65	0.016	0.04476	7703.81	9.2
0.79	234.13	0.016	0.04488	7729.26	9.17
0.795	235.61	0.01601	0.045009	7744.37	9.13
0.8	237.09	0.01603	0.0454	7748.67	9.08
0.805	238.58	0.01605	0.04582	7744.83	9.02
0.81	240.06	0.01608	0.04638	7728.01	8.94
0.82	243.02	0.01615	0.04795	7662.45	8.76
0.83	245.98	0.01625	0.05022	7548.75	8.52
0.84	248.95	0.01636	0.05331	7393.92	8.25
0.85	251.91	0.0165	0.05735	7195.06	7.93
0.86	254.88	0.01666	0.06245	6961.29	7.59
0.87	257.84	0.01684	0.06874	6698.46	7.22
0.88	260.8	0.01704	0.07633	6414.45	6.83

Table 9.5: Range and endurance in constant velocity flights at h = 10700 m

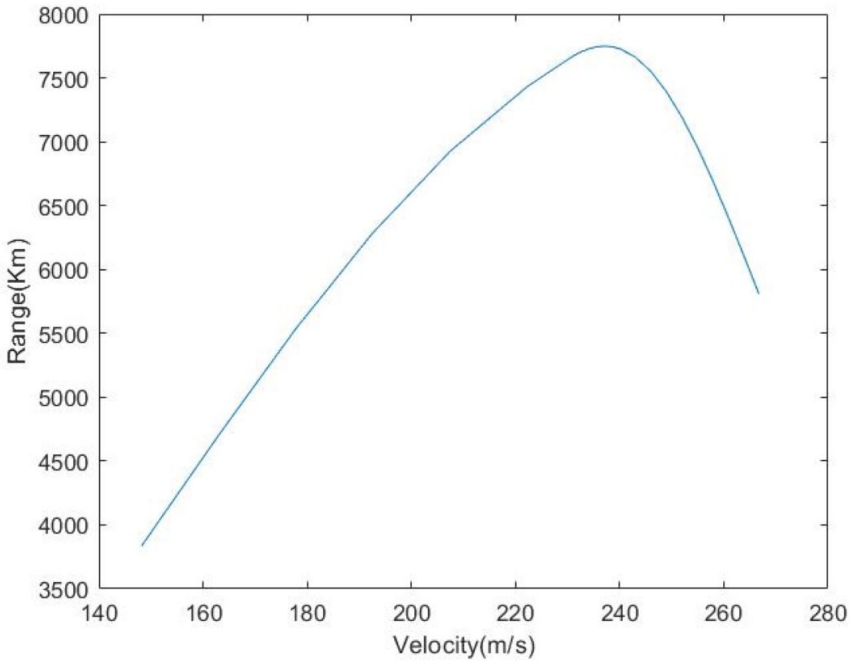

Figure 9.13: Range in constant velocity flights at different flight speeds (h = 10700 m)

1. It is observed that the maximum range of 7748.60 km is obtained at a velocity of 237.09 m/s.
2. The maximum endurance of 9.30 hours occurs in a flight at V = 215.5 m/s.

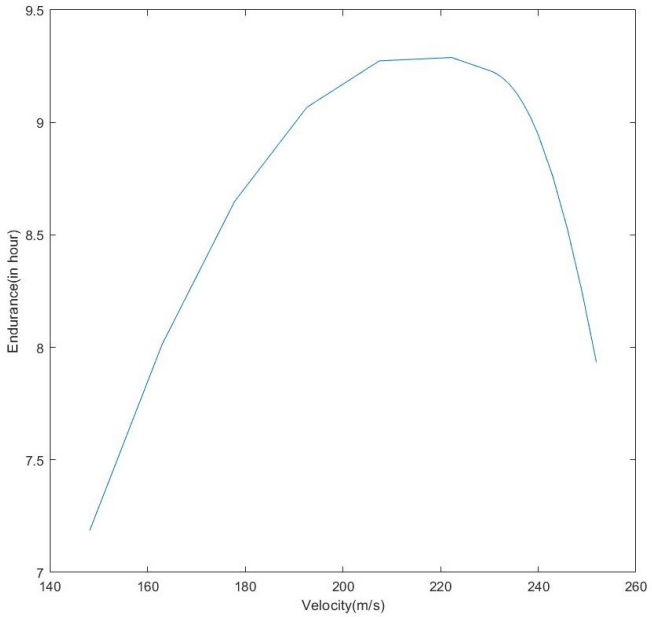

Figure 9.14: Endurance in constant velocity flights at different flight speeds (h = 10700 m)

9.1.5 Turning performance

In this section, the performance of the airplane in a steady, co-ordinated, level turn is studied. the equations of motion in this case are:
T-D = 0
$W - Lcos\phi = 0$ $Lsin\phi = \frac{W}{g}$
where, ϕ is the angle of bank.
These equations give:
$r = \frac{V^2}{gtan\phi}$

$\Psi` = \frac{V}{r} = \frac{gtan\phi}{V}$

Load factor(n) = $\frac{L}{W} = \frac{1}{cos}\phi$

where, $\Psi`$ is the rate of turn and r is the radius of turn.
The following procedure is used to obtain r_{min} and $\Psi`$
1. A flight speed and altitude are chosen and the level flight lift coefficient C_{LL} is obtained as:
$C_{LL} = \frac{2(W/S)}{\rho V^2}$

2. If $C_{Lmax}/C_{LL} < n_{max}$ is the maximum load factor for which the aircraft is designed, then the turn is limited by C_{Lmax} and $C_{LT1} = C_{Lmax}$. However, if $C_{Lmax}/C_{LL} > n_{max}$, then the turn is limited by n_{max}, and $C_{LT1} = n_{max}C_{LL}$.

3. From the drag polar, C_{DT1} is obtained corresponding to C_{LT1}. Then, $D_{T1} = 0.5\rho V^2 S C_{DT1}$

If $D_{T1} > T_a$, where, T_a is the available thrust at that speed and altitude, then the turn is limited by the engine output. In this case, the maximum permissible value of C_D in turning flight is obtained from:
$C_{DT} = \frac{T_a}{0.5\rho V^2 S}$

From the above relation, the value of C_{LT} is calculated as
$C_{LT} = \sqrt{\frac{C_{DT} - C_{DO}}{K}}$

However, if $D_{T1} < T_a$, then the turn is not limited by the engine output and the value of C_{LT} calculated is step(2) is retained.

4. Once C_{LT} is known, the load factor during the turn is determined as $n = \frac{C_{LT}}{C_{LL}}$
Once n is known, the values of ϕ, r and $\psi^{'}$ can be calculated using the equations given above.
The above steps are repeated for various speeds and altitudes. A typical turning flight performance estimation is presented in table below. In these calculations $C_{Lmax} = 1.5$ (considering the situation when flaps are not deployed) and $n_{max} = 3.5$ are assumed from references and remaining parameters like k,C_{Do} are taken from the values from previous chapters. The variation of turning flight performance with velocity is shown below in table. The code for the graphs and values are attached at the end of the report

V (m/s)	**n**	C_{LT}	ϕ**(degrees)**	**r (m)**	$\Psi^{'}$ **(rad/sec)**
80	1.0399	2.6325	515.919	2287.3	0.035
100	1.6248	2.0752	52.015	795.93	0.125
120	2.3397	1.6974	64.697	693.95	0.173
140	3.019	1.4219	70.654	701.44	0.199
160	3.355	1.2100	72.661	814.78	0.196
180	3.430	0.0997	73.396	984.69	0.183
220	3.500	0.6676	73.398	1471.0	0.149

Table 9.6: Typical Turning flight performance at sea level

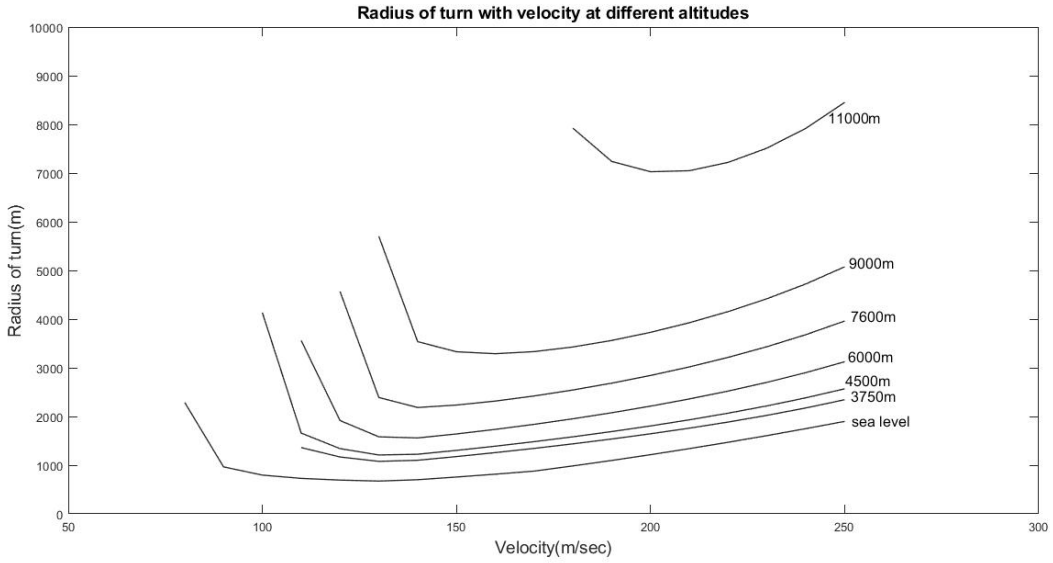

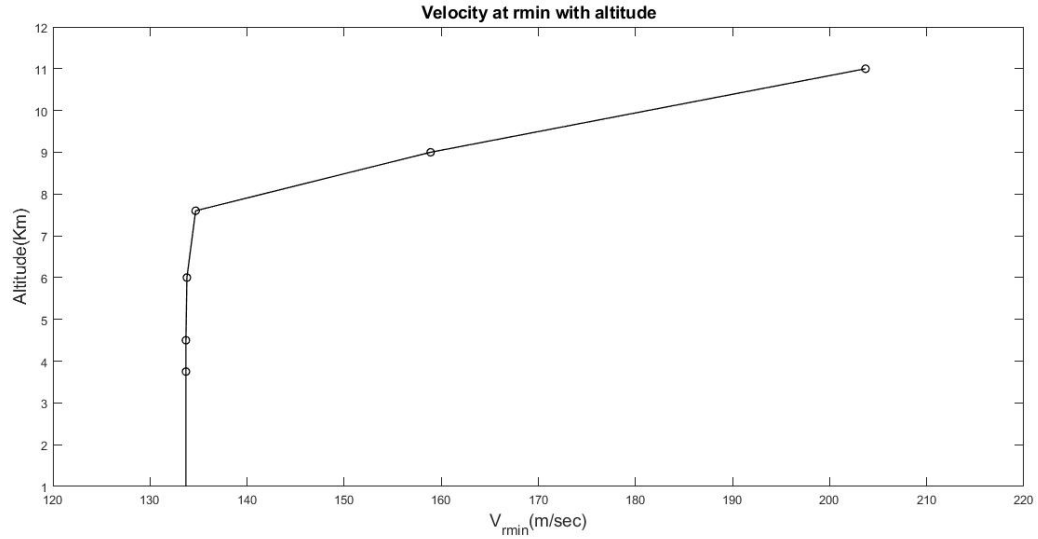

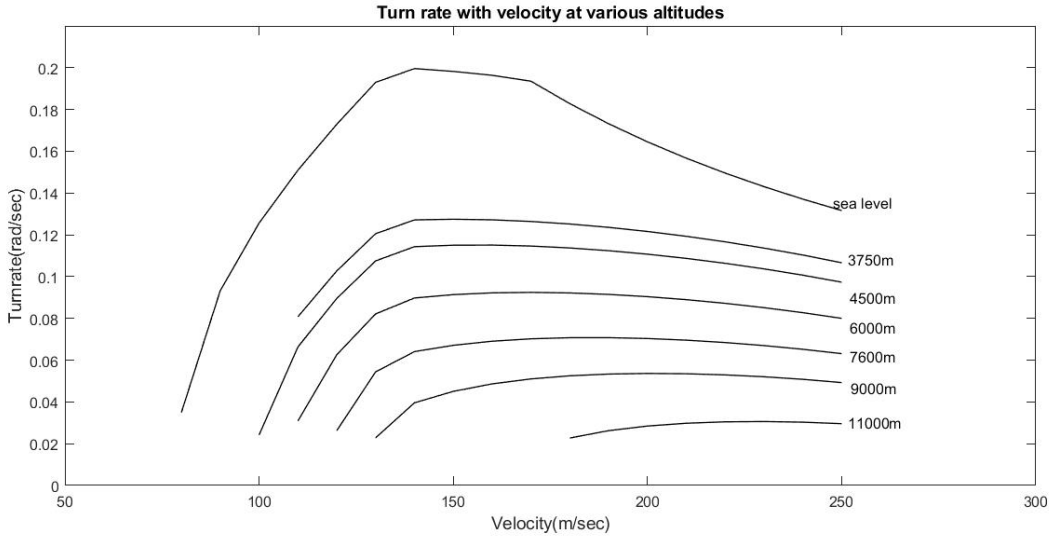

h (m)	r_{min}**(m)**	V_{min} **(m/s)**	$\dot{\Psi}_{max}$ **(rad/s)**	$V_{\dot{\Psi}_{max}}$ **(m/s)**
0.0	668.23	133.70	0.2001	133.8
3750	1056.7	133.73	0.1275	149.9
4500	1178.7	133.73	0.1151	1560
6000	1516.1	133.74	0.0924	169.3
7600	2176.0	134.66	0.0708	185.4
9000	3288.9	158.90	0.0536	201.4
11000	7014.0	203.66	0 .0306	228.0

Table 9.7: Turning Flight Performance

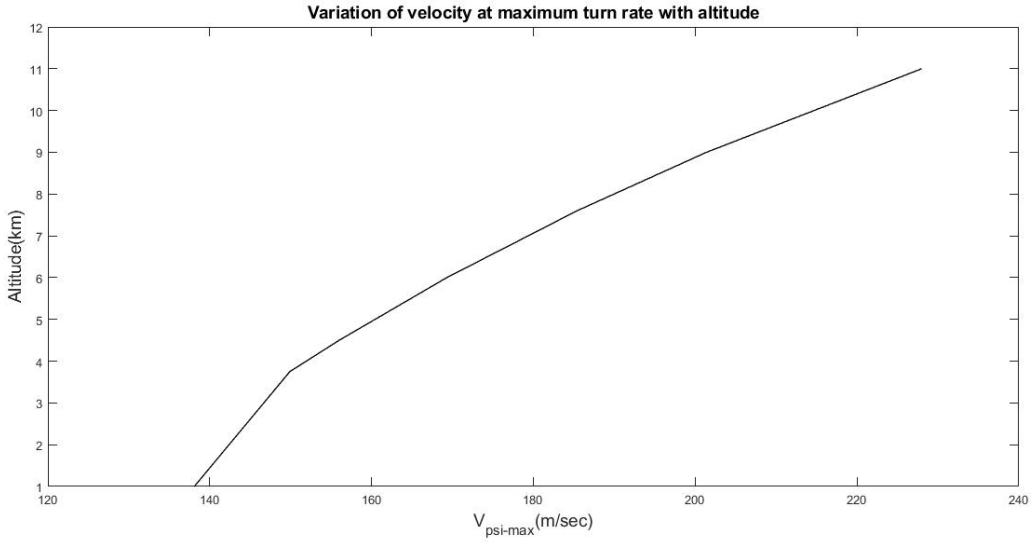

1. The maximum value of $\dot{\Psi}_{max}$ is 0.2001 rad/sec at sea level at a velocity of $133.8 m/sec$
2. The minimum radius of turn is 668.2m at sea level at a velocity of $133.7 m/sec$
3. The various graphs from turn performance show a discontinuity in slope when the criterion,which limits the turn, changes from n_{max} to thrust available

9.1.6 Take-off distance

In this section, the take off performance of the airplane is evaluated. The take-off distance consists of take-off run, transition and climb to screen height. Rough estimates of the distance covered in these phases can be obtained by writing down the appropriate equations of motion. The following formulae for take-off distance and balance field length based on the take-off parameter.
This parameter is defined as:

$$Take - offparameter = \frac{W/S}{\sigma C_{LTO}(T/W)} \tag{9.26}$$

where, W/S is wing loading in lb/ft^2, C_{LTO} is 0.8XC_{Lland} and σ is the density ratio at take-off altitude. In the present case:
$\frac{W}{S} = 6189 N/m^2 = 129.26 lb/ft^2; C_{LTO} = 0.8 \times 2.7 = 2.16; \sigma = 1.0$
and $\frac{T}{W} = \frac{279730.71 kN}{114196.45 \times 9.81} = 0.2497$
Hence,
Take-off parameter $= \frac{129.26}{1.0 \times 2.16 \times 0.2497} = 239.66$

the take off distance, over 50, is 5100 ft or 1554.48 m. For take off parameter 239.65 The balance field length of two engined airplane is 11000 ft or 3352.8 m. It may be noted that the balance field length is more than twice the take off distance.

9.1.7 Landing distance

In this section the landing distance of the airplane is calculated. The landing distance for commercial airliners is given by the formula

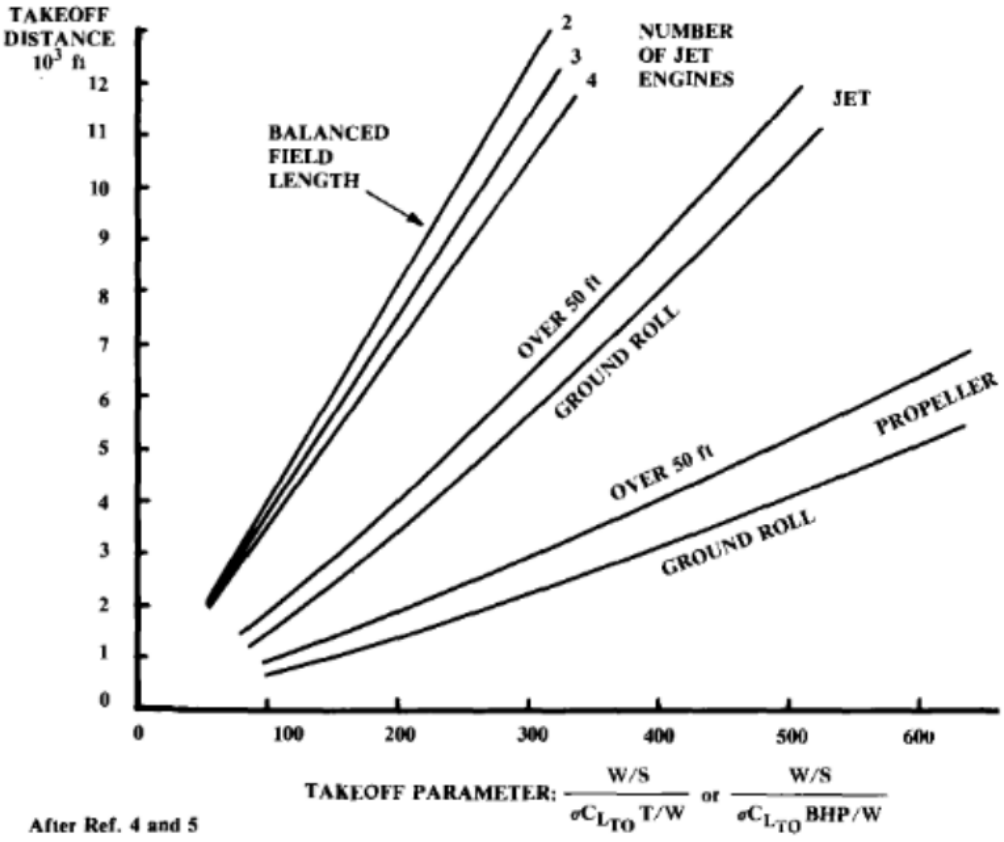

Fig. 5.4 Takeoff distance estimation.

Figure 9.15: Takeoff distance estimation

$$S_{land} = 80\left(\frac{W}{S}\right)\frac{1}{\sigma C_{Lmax}} + 1000ft \tag{9.27}$$

where, W/S is in lbs/ft^2. In the present case:
$(W/S)_{land} = 0.85 \times (W/S)_{takeoff} = 0.85 \times 129.26 = 109.87 lb/ft^2$

$C_{Lmax} = 2.7$
$\sigma = 1.0$
Hence,
$S_{land} = 80 \times 109.87 \frac{1}{1.0*2.7} + 1000 = 4255.43ft$=1297.06 m

Chapter 10

Final Specifications:

10.1 Specifications

The final specifications values determined through chapter 1 to 7 are :

1. **General description of airplane**
   Type of airplane: Modular commercial airplane

2. **Power plant**
   Type of power plant:Three shaft high bypass ratio turbofan
   Name: RR trent 1000
   Engine rating: 6.01
   Specific fuel consumption: 0.549 hr^{-1}
   Weight of power plant:12240 kg
   No. of engines: 2

3. **Wing**
   Span(m): 43
   Tip chord(m): 1.98
   Sweep(in degree):30
   Flap area(m^2): 34.43
   Taper ratio(λ):0.3
   Flap area/wing area(S_{flap}/S):0.17
   Flap chord/wing chord(c_{flap}/c_{wing}): 0.17
   Aileron chord/wing chord($c_{aileron}/c_{wing}$):0.025
   Location of wing on fuselage(high wing/mid wing/low wing):High wing configuration
   Root chord(m): 6.62
   Area (S in m^2): 185.11
   Mean aerodynamic chord(m): 4.72
   Aileron area(m^2): 4.69 Aspect ratio(A): 10
   Aileron area/wing area($S_{aileron/S}$): 0.025

4. **Horizontal tail**
   Airfoil: NACA 0012
   Span(m): 15.3
   Tip chord(m): 1.25
   Area(m^2): 26.8
   Sweep(in degree): 35
   Elevator area(m^2): 10.75
   Aspect ratio: 4.74

Taper ratio: 0.256
Elevator area/Tail area: 0.4
Tail area(S_{ht}/wing area(S): 0.145
Elevator chord/tail chord root: 0.4

5. **Vertical tail surface**
   Type of vertical tail: Conventional
   Airfoil: NACA 0012
   Height(m): 7.7
   Root chord(m): 6.49
   Tip chord(m): 1.966
   Area(m^2): 72.42
   Sweep: 35
   Rudder area(m_2): 10.86
   Aspect ratio(Av): 1.71
   Taper ratio: 0.303
   Rudder area/tail area: 0.15
   Tail area(S^{vt})/wing area(S): 0.39
   Rudder chord/Vertical tail chord: 0.15

6. **Fuselage**
   Length(m): 44.6
   Length of nose(l_{nose}): 1.3 m
   Length of cockpit($l_{cockpit}$): 4 m
   Length of tail cone($l_{tailcone}$): 14.3 m
   Length of payload compartment: 25
   Upsweep angle: 15°

   Number of seats in cockpit: 4
   Length/wingspan: 1.037

7. **Landing gear**
   Type of landing gear: Tricycle
   Number and size of wheels: 3 * 4
   Wheel base(m): 15.57
   Wheel tread(m): 9.82
   Location of landing gears: Refer 3-view diagram

8. **Overall dimensions of airplane**
   Length(m): 44.6
   Wing span(m): 43
   Height(m): 4.7
   Landing gear wheel tread(m): 9.82
   Landing gear wheel base(m): 15.57
   Length/span: = 1.037
   Height/span: 0.11
   Tread/span: = 0.23

9. **Weights**
   Pay load(kgf): 30000
   Empty weight(kgf): 58782.33
   Fuel weight(kgf): 29120
   Landing weight(kgf): 84941.6

Normal gross weight(kgf): 114,196.45
Payload/gross weight: 0.26
Empty weight/gross weight: 0.51
Fuel weight/gross weight: 0.25
Wing loading: 630.94
Thrust loading: 0.25

10. **Performance**
Maximum speed(ms^{-1}) at sea level:266.19 m/s
Maximum speed(ms^{-1}) at altitude: 216
Cruise speed(ms^{-1}) and altitude(km): 216, 10.7
Maximum sea level rate of climb(m/min): 1835.4
Range or radius of action(km): 7.75
Endurance(hours): 9.3

Chapter 11

Conclusions

- For an opted payload of 30,000 kg, Maximum Take-Off Weight $W_0 = 159.97$ tonnes and $S = 252.92m^2$ are obtained from data collected for similar aircraft.
- From the weight estimation calculations, we get $W_0 = 114.20$ tonnes, $W_f = 29.12$ tonnes and $W_e = 59.78$ tonnes
- Final Thrust Loading from graph(maximum from the 4 considerations is for t_{hmax1}) is 0.0537 N/kg and the final Thrust at sea level is found to be 253.61 kN
- Thrust to Weight ratio is 6.01 and the Thrust Loading for the Rolls Royce Trent 1000(twin jet engine) is 0.579
- Final Wing loading range is from 601.81 to 630.94 kg/m^2 and the wing loading calculated using aircraft data and weight estimation is 625 kg/m^2
- Final Optimum Wing Loading from graph(maximum from the 4 considerations) turns out to be 618.95 kg/m^2
- This weight estimation is not accurate design weight as it is calculated using best linear fit of data of similar air crafts and some crude assumptions. Also as we are including a new deployment mechanism without considering the mechanics, its only an approximate weight and could be possibly higher.
- Super-critical airfoil NASA SC(2) - 0714 is chosen for our aircraft based on design lift coefficient(0.63) and mach divergence number.
- The detachable fuselage has been fitted with both parachute and an auto rotation based rotors for safe landing of the capsule.
- The terminal velocity of airplane in pod deployed situation is 6 m^2. The plane will also contain airbags underneath the passenger carriage which will function during landing. This reduces the impact much further during touchdown phase.
- The total fuselage length is 44.6 m with a passenger capacity of 140 passengers.
- Conventional tail layout has been chosen for the aircraft.
- NASA 0012 airfoil is chosen for the aircraft.
- Nose wheel landing gear are chosen for the aircraft.
- C.G. shift estimation and aircraft weight estimation has been presented.
- After cross checking the tail surfaces with stability analysis,the revised estimates of the horizontal tail surface area and vertical tail surface area are $24.068m^2$ and $74.425m^2$ respectively
- The absolute ceiling and the Service ceiling values obtained are 12.24km and 12.07km respectively

- The thrust available values at different heights for turn and climb performance are taken as density ratio because for high bypass turbofans the thrust available is almost constant with velocity at a particular altitude
- The minimum turn radius is 668.2m and maximum turn rate is 0.2001 rad/sec both occurring at sea level
- The Take off distance is 1554.48m and the landing distance is 1297.06m.Also the Maximum Range is 7748.6Km.

Chapter 12

Bibliography

[1] Data of reference aircrafts https://booksite.elsevier.com/9780340741528/appendices/data-a/default.htm

[2] Aircraft Design: A Conceptual Approach https://soaneemrana.org/onewebmedia/AIRCRAFT%20DESIGN%20%3B%20A%20Conceptual%20Approach%20BY%20DANIEL%20P%20RAYMER.pdf

[3] https://en.wikipedia.org/wiki/Boeing_737

[4] https://en.wikipedia.org/wiki/Airbus_A310

[5] https://en.wikipedia.org/wiki/Airbus_A320_family

[6] https://en.wikipedia.org/wiki/Rolls-Royce_Trent_1000#Specifications

[7] https://science.howstuffworks.com/transport/flight/modern/airplanes12.htm

[8] https://www.google.com/url?sa=t&rct=j&q=&esrc=s&source=web&cd=1&cad=rja&uact=8&ved=2ahUKEwiEzqzo7rXnAhUMzDgGHdw7DSgQwqsBMAB6BAgLEAQ&url=https%3A%2F%2Fwww.youtube.com%2Fwatch%3Fv%3DZPkr3A9DTOc&usg=AOvVaw0K0_sqWSU2OVNPAoC32UiT

[9] https://www.youtube.com/watch?v=-kVhurg5b9U&feature=youtu.be

[10] https://www.bbc.com/future/article/20131223-should-planes-have-parachutes

[11] https://www.researchgate.net/publication/329944773_Performance_Analysis_of_High_Bypass_Turbofan_Engine_Trent_1000-A

[12] NPTEL Airplane Design by Dr. E. G. Tulapurkara https://nptel.ac.in/courses/101/106/101106035/

[13] https://soaneemrana.org/onewebmedia/AIRCRAFT%20DESIGN%20%3B%20A%20Conceptual%20Approach%20BY%20DANIEL%20P%20RAYMER.pdf

[14] McCormick, B.W. *Aerodynamics, aeronautics and flight mechanics*

[15] Pamadi, B.*Performance,stability, dynamics and control of airplanes*

Appendix A

Matlab code for weight estimation

```
w0=102500:115000;
w1=30000./(0.759-(0.97.*(w0.^(-0.06))));
for j=1:length(w0)
if abs(w0(j)-w1(j))<=1
    wfinal=w0(j);
    break
end
end
```

Appendix B

Matlab code for wing loading

```
clear all;
close all;
rho=0.3648;vp=229.5;%Mach=0.778 at 11km
p=1000:0.5:15000;
q=0.5*rho*vp*vp;
F1=0.00914;
F2=1.12/1000000;%m^2/N
F3=0.0447;
t_vp=(q*(F1+(F2.*p)+(F3.*p.*p./(q^2)))./(p);
p_opt=q*sqrt(F1/F3);
B=min(t_vp);m=1;
for a1=1:length(p)
if abs(t_vp(a1)-(1.05*B))<=0.000005
    plu(m)=p(a1);
    m=m+1;

end

end

frame=lines,
framesep=2mm,
baselinestretch=1.2,
%bgcolor=LightGray,
fontsize=\large,
linenos
]
{python}
rhosl=1.225;v=10:1:300;
```

```
for j=1:291

maxrateofclimbatsealevel=10.16;
vc=10.16;

q1(j)=0.5*rhosl*v(j).*v(j);
p1v(j)=sqrt(F1*q1(j).*q1(j)./F3);
trc_minv(j)=(vc./v(j))+((q1(j).*(F1+(F2.*p1v(j))+(F3.*p1v(j).*p1v(j)./(q1(j).^2)))).(p
end
C=min(trc_minv);
n=1;
for a2=1:length(p1v)
if abs(trc_minv(a2)-(1.05*C))<=0.00013
    p1vlu(n)=p1v(a2);
    n=n+1;
end
end
A=min(trc_minv);
j=find(trc_minv==A);
p1v_opt=p1v(j);

u=ones(1,length(p));
y=1.05*B*u;
u1=ones(1,length(p1v));
y1=1.05*C*u1;
y2=0.0507825*u;
y3=0.056175*u;
qhmax=10239;
t_hmax1 = sqrt(4*F3*(F1+(F2.*p)));
hold on;

t_hmax2 =(qhmax*2*(F1+(F2.*p))./p);
for a=1:28001
if abs(t_hmax1(a)-t_hmax2(a))<=0.000005
    p_opthmax=p(a);
    t_hmaxopt=t_hmax1(a);
    break;
end
end
rho = 0.3648;
```

```
TSFC = 0.00015333; % in Sec inverse
R = 5000000; %in meter
sigma=rho/rhosl;
Wfbywmean = ((R/3.6)((rho/2)^(0.5))*TSFC((sigma*q)^(0.5))((F1(p.^(-1)))+F2+(F3*p./(q^2)))
D=min(Wfbywmean);
y4=1.05*D*u;
plot(p,Wfbywmean);
n1=1;
for a3=1:28001
if abs(Wfbywmean(a3)-(1*D))<=0.000005
    p_optrange(n1)=p(a3);
  n1=n1+1;
end
end

plot(p,t_hmax2);
hold on;
hold on;
plot(p,t_vp);

hold on
plot(p,y2);
plot(p,y);
hold on;
ylim([0 0.175]);
xlim([0 21000]);
plot(p1v,trc_minv);
hold on;
plot(p1v,y1);
hold on;
plot(p,y3);
hold on;
plot(p,y4);
```

Appendix C

Matlab code for Turn Performance

```
g=9.81;W=114196.45*g;Cd0=0.016;R=287;
h=[0 3.75 4.5  6 7.6 9  11];
k=0.0447;
C_lmax=1.5 ;nmax=3.5;j=1;m=0;b=1;
 for i=1:7

 if h(i)<=11
    T(i)=288.15-(h(i)*6.5);
    rho(i)=1.225*(T(i)/288.15)^4.2588;
end
if h(i)>11
    rho(i)=0.3636*(exp(-g*(h(i)-11)*1000/(R*216.65)));
end
Tsl=253;
Tdash(i)=(Tsl*1000*((rho(i)/1.225)));S=198.12;
end
for i=1:7
    m=m+1;j=1;b=1;
for v=80:20:240
s=1;
C_ll=(2*W)/(rho(m)*S*v*v);
a=C_lmax/C_ll;
if a<nmax
    C_lt1=C_lmax;
end
if a>nmax
    C_lt1=nmax*C_ll;
end
C_dt1=Cd0+(((C_lt1)^2)*k);
```

```
Dt1=0.5*rho(m)*v*v*C_dt1*S;
if Dt1>Tdash(m)
    C_dt=2*Tdash(m)/(rho(m)*v*v*S);
    C_lt=sqrt((C_dt-Cd0)/k);
end
if Dt1<Tdash(m)
    C_lt=C_lt1;
    C_dt=C_dt1;
end
n(m,j)=C_lt/C_ll;
z(m,j)=C_ll;
x(m,j)=C_lt;
if n(m,j)>1
    t(m,b)=v;
    tanphi(m,b)=sqrt((n(m,j)^2)-1);
    phi(m,b)=(180/pi)*atan(tanphi(m,b));
r(m,b)=(v*v)/(g*tanphi(m,b));
turnrate(m,b)=g*tanphi(m,b)/v;
b=b+1;
end

j=j+1;
end
rdash=turnrate(m,1:b-1);
rmin(m)=min(rdash);
index=find(rdash==rmin(m),1,'first');
vrmin(m)=((index+18001-b)*0.01) +70;
%psimax=max(turnrate(m,:));
end
h=[0 3.75 4.5 6 7.6 9 11];
plot(vrmin,h);
ylim([1,12]);
xlim([120,240]);
```